TARO VEIN CHLOROSIS NUCLEORHABDOVIRUS AND OTHER VIRUSES OF TARO IN THE PACIFIC

A THESIS SUBMITTED TO THE GRADUATE DIVISION OF THE
UNIVERSITY OF HAWAI'I AT MANOA IN PARTIAL FULFILLMENT
OF THE REQUIREMENTS FOR THE DEGREE OF

MASTER OF SCIENCE
IN
MOLECULAR BIOSCIENCES AND BIOENGINEERING

NOVEMBER 2019

By
Jarin Loristo

Thesis Committee:
Michael Melzer, Chairperson
John S. Hu
Michael Shintaku

Keywords: *Taro vein chlorosis nucleorhabdovirus*, *Taro-associated totivirus*

DEDICATION

I dedicate this thesis to my family members who have been supportive of my journey, including my mom, dad, aunty, and uncle. Their influence and support are always an important reminder of what I should strive to achieve in my life, and my journey would be very different if they did not serve as role models that I needed to improve myself both professionally and scholastically. I am grateful for all the love, happiness, and memories that they have given to me over the years, and words cannot express how meaningful it is to be able to experience new things and learn more about myself, my family, and the many exploits that they achieved in their lives that allowed them to get to where they are and shape their perspective of the world as well as mine. I can never truly repay them for everything, but I can always work to live up to their expectations and prepare myself to be a good role model for my peers and my family-to-be.

ACKNOWLEDGMENTS

This would not be possible without the gracious support from many of the people that I've met over the years. I would like to express my gratitude to the teachers and professors who were willing to give me a chance to constantly strive for more and improve myself professionally and academically. I am thankful to Dr. Jon-Paul Bingham for allowing me to be a part of a rigorous graduate program that allowed me to explore more of the biological sciences and gave me confidence in my abilities.

I would also like to thank Dr. Michael Melzer for his support and guidance through the course of my project. He gave me a place in academia when I struggled to find a project that was suitable for me, and for that, I am very grateful and appreciative for everything. I also thank Drs. John Hu and Michael Shintaku for providing useful insight. Thanks to Dr. Melzer and Nelson Masang, Jr. for providing me with samples of taro leaves from different locations. I also thank the Agrosecurity Laboratory for their input with topics related to laboratory work and otherwise, as well as my family for always being there to give me a nudge in the right direction. You're all wonderful!

ABSTRACT

The taro virome has been documented to include a few currently known viral species. Among these, *Taro vein chlorosis nucleorhabdovirus* (TaVCV) is a virus that has been discovered in several different countries across the South Pacific, and, as of 2013, has started to infect taro in Hawaii. Efforts to detect TaVCV in infected taro across regional variants has remained a challenge, as the regional genomic diversity of this virus has been noted to reach as high as 21%. A previous study conducted on Hawaiian TaVCV isolates has determined a very low diversity among local variants, so a sampling method to take infected taro samples from Hawaii, Samoa, Guam, Palau and Vanuatu was conducted to determine the genomic sequences from each of these regions and perform a phylogenetic analysis of these variants. Next-generation sequencing (NGS) performed on double-stranded (ds)RNA found TaVCV genomes that diversified by up to 20% compared to the TaVCV sequence available from GenBank, derived from a Fijian isolate. Additionally, NGS also contributed to the discovery of a unique taro-associated totivirus, which has been fully sequenced and characterized.

TABLE OF CONTENTS

LIST OF TABLES AND FIGURES

List of tables

List of figures

CHAPTER 1: INTRODUCTION AND LITERATURE REVIEW

Taro, *Colocasia esculenta* (L.) Schott

1.0 Botany and Ecology

1.1 History of Classification

Colocasia esculenta, commonly referred to as taro, is a member of the genus *Colocasia*, under the family *Araceae*. Over many generations, this plant has been cultivated in many different locations globally and has therefore resulted in several different varieties and agronomical cultivars. This has resulted in many different taxonomic synonyms for *Colocasia esculenta*, which arose from many different attempts and disagreements between botanists regarding the classification of taro (Lim, 2014; Onwueme, 1999).

Originally, two unique species, *Arum colocasia*, and *Arum esculentum* were described by Linnaeus in 1753, though the genus *Colocasia* was later described by Schott and the species described by Linnaeus were both moved under that genus and renamed *Colocasia antiquorum* and *Colocasia esculenta*, respectively (Hill, 1939). Later, *C. acris* (formerly described as *Calladium acre*) was added to the genus in 1810 by Schott, followed by *C. nymphaeifolia* in 1841 by Kunth, then *C. fontanesii* in 1854 by Schott and *C. euchlora* in the same year by C. Koch and Sello. By then, the number of described species in the genus *Colocasia* rose to six.

Schott would then re-organize the classification in 1856, recognizing *Colocasia antiquorum* as the only species, while the others were then ranked as varieties of that species. The varieties ‘typica’ and ‘illustris’ in 1879 by Engler and ‘aquatilis’ and ‘globulifera’ in 1920 by Engler and Krause were subsequently described. The changes that Schott made in re-organizing the genus back in 1856 were considered unlawful by the *International Rules of*

Botanical Nomenclature (also referred to as the "Vienna Rules" of 1906), as an older species could not be changed to being considered a variety of a species that would be described at a later date. Accordingly, future literature would describe *C. esculenta* as the main species, while *C. antiquorum* would then be considered as a variety of that species (Hill, 1939). Of the varieties of the taro that are cultivated, the common varieties used include *Colocasia esculenta* (L.) Schott var. 'antiquorum' and *Colocasia esculenta* (L.) Schott var. 'esculenta' (Purseglove, 1973).

The 'esculenta' variety of *C. esculenta* has corms, which are the edible underground stems, and cormels, which are smaller bud-like structures. Additionally, the leaves and petioles (above the ground) may also be consumed (Alercia, 2013). The 'antiquorum' variety, by comparison, has a small globular central corm, from which several cormels that are relatively large arise. Agronomically, the 'esculenta' variety is referred to as the dasheen type of taro, whereas the 'antiquorum' variety is referred to as the eddoe type. The dasheen type comprises the majority of the taro that is cultivated in the Asia-Pacific region (Onwueme, 1999).

As taro has widespread cultivation, several different cultivars are grown around the world, and as such, these different cultivars can have varying physiological characteristics, which can include the size and/or shape of the corm and leaves, as well as the texture and color of the leaves and petioles. Some additional contributing factors to distinguishing cultivars include agronomic or culinary preference (Onwueme, 1999). Historical records establish that Hawaiian agriculture, even before European contact in 1778, involved approximately 300 cultivars of taro, which included both wetland and dryland types. Based on their morphology and ability to grow in certain environmental conditions, these cultivars were separated accordingly (Cho, Yamakawa, & Hollyer, 2007; Jacobs, 2011), though it was stated by Whitney et al. (1939) that approximately half of those were duplicates.

1.2 Origin and Distribution

The origin of taro was speculated to be in South Central Asia; specifically, a high likelihood that its origin is from India or the Malay Peninsula (Hill, 1939; Whitney et al., 1939). A karyotypic study would later reveal that the origin of taro is in northeastern India (Kuruvilla & Singh, 1981). Taro would then spread to the rest of Southeast Asia, as well as China and Japan. Seafaring voyagers would contribute to the spread of taro to the Pacific Islands. A westward spread would also occur simultaneously to Egypt and the Eastern Mediterranean, as well as Africa and, from there, to the Caribbean and the Americas (Lee, 1999; Matthews, 1995, 2004; Onwueme, 1999; Plucknett, 1983). The primary origin of the introduction of *C. esculenta* into Hawaii is considered to be the Polynesian migration to Hawaii (Greenwell, 1947).

A high degree of genetic diversity was observed in Asian taro as well as a characteristic gene pool in the Pacific that was observed during an isozyme variation study of Asian and Oceanian taro cultivars. Further, the results of the study indicated that the Indonesian cultivars have the highest genetic variation and that a narrow base within that gene pool could be the origin of many Pacific cultivars (Lebot & Aradhya, 1991). Further studies seem to support these findings, including a study done by Kreike et al. (2004) using amplified fragment length polymorphism (AFLP-)PCR. These research efforts, which yielded enough data to perform a phylogenetic analysis, helped to conclusively separate 255 taro accessions and assort them into Asian and Pacific gene pools.

Though the variety ‘Lehua Maoli’ had been the preferred variety for cultivation in Hawaii, modern production of taro primarily consists of the varieties ‘Maui lehua,’ ‘Moi,’ and ‘Bun Long,’ and hybrids between Hawaiian and Palauan varieties (Cho et al., 2007). Despite

records indicating the availability of many different varieties, there is a clear preference for some varieties which may have been reinforced due to factors which include large-scale commercial farming, palatability, and research studies promoting or utilizing certain varieties in preference over others. Thus, there is an idea that the cultivation of taro that had once been considered a sacred commodity has transformed into a crop that is raised procedurally in a way that deviates from tradition (Jacobs, 2011).

1.3 Morphology and Anatomy

Taro is a herbaceous perennial plant that can grow up to 1-2 meters tall and the spread of its canopy can span a comparable area. The main stem structure of taro is represented by the central corm grown underground. The corm is large in the dasheen type of taro and its shape resembles that of a cylindrical top, with features of rough ridges, lumps, and fibrous gangling roots. The dimensions of a corm can measure up to 30 cm in length and 15 cm in diameter, and typically weigh 1-2 lbs, but can range up to eight pounds in weight (Moore & Lawrence, 2003; Onwueme, 1999).

Most parts of taro contain idioblasts, which are cells that contain raphides (needle-shaped crystals composed of calcium oxalate). Consumption of plants that contain raphides can result in edema, vesicle formation, and dysphagia, as well as an onset of burning and painful stinging to the throat and mouth for a duration of up to two weeks (Watson et al., 2005); due to these health risks, it is not recommended to eat any such plants uncooked. The skin that covers the corm is brown with some patches of pink or white and the woodiness and density of the corm both increase with age. Smaller cormels (which are also edible) or tubers can be produced off the side of the main corm in certain varieties of *C. esculenta*. Some taro plants can produce runners as

well, which grow horizontally with interspersed intervals of rooting down to induce new standing plants (Moore & Lawrence, 2003; Onwueme, 1999). These morphological characteristics are also supplemented with a detailed passage by Whitney et al. (1939):

> "Extremely variable, succulent, glabrous herb, 4 to 18 dm. tall. Stem a subterranean corm with scaly outer bark and thin, usually highly colored cortex, single or branching from the apex, with conspicuous leaf-scar rings, producing cormels (oha) or rhizomes as offshoots. Petioles 4 to 18 dm. long, erect or spreading, sheathing at base with sinus to about midway, uniformly light or dark green to variously highly colored, striped, or flecked. Blades 25 to 85 cm. long, 20 to 60 cm. wide, usually peltate, ovate to more or less sagittate, the apex acuminate, a dark-colored spot known as piko on the upper surface at the point of junction with petiole. Inflorescences 2 to 5 together in the leaf axils, the peduncles 15 to 50 cm. long, each spadix enclosed within a spathe. Spathes oblong-lanceolate, divided by a transverse constriction into two unequal parts, the lower part 3 to 5 cm. long, loosely or tightly convolute, more or less fleshy, tubular, the upper part 15 to 35 cm. long, usually tightly but sometimes loosely convolute, lanceolate. Spadix 6 to 14 cm. long, with female flowers at the base, consisting of a few obovoid or ellipsoid ovaries 0.5 to 1.5 mm. in diameter, the stigma sessile, capitate; constricted above the female flowers and beset over a length of 2 to 5 cm. with light yellow sterile flowers; above the sterile flowers and over a length of 2 to 4 cm. beset with male flowers consisting of 2 to 6 sessile anthers which are fused into an obconical synandrium; with yellow constricted, obtuse or acute sterile appendage at apex.

Fruit a berry, 3 to 5 mm. across, ellipsoid. Seed 1.2 to 1.5 mm. long, 0.7 to 1 mm. wide, hard, ovoid."

2.0 Ethnobotany of Taro

2.1 Food Security, Nutritional and Economic Importance of Taro

Throughout the Pacific Island Countries (PICs) and some West African countries, taro is widely considered a staple crop and therefore plays a significant role in food security, nutrition, and economy in countries that depend on it. Taro had historically been considered the most important crop in the Hawaiian Islands (Moore & Lawrence, 2003), though it no longer holds that status in modern Hawaiian agriculture, especially when compared to coffee, nuts, and seed corn (Gomes, 2012). Despite this, taro still plays a significant role in many of the PICs.

The corm of the taro is often included with many vegetable and meat preparations, with one popular method being taro baked in a dug-out earth oven together with other staple crops and meat, done during celebrations, festivities, and traditional ceremonies; this method is referred to as "imu" in Hawaii, "umu" in Samoa and "lovo" in Fiji (Deo et al., 2009). Palusami, or young taro leaves cooked together with coconut cream, meat or tuna, is a delicacy prepared with the aforementioned method. Additionally, the inflorescence of taro can be a delicacy itself in certain Pacific or Asian cultures (Rao et al. 2010).

Poi, a traditional dish of fermented or unfermented paste made from mashing cooked corm together with water until the paste has the desired consistency, is a staple of Hawaiian food culture (Lee, 1999; Potgieter, 1940). Lu'au, another traditional Hawaiian dish, is made by cooking meat with young taro leaves and tops and coconut cream (Uchida et al., 2008). Some additional applications of taro include processing corm starch into flour (Payne, Ley, & Akau,

1941), which has had some use in the baking industry (Ammar, Hegazy, & Bedeir, 2009), and also into taro chips (Hollyer, Paull, & Huang, 2000). Despite these applications, taro cultivation has steadily decreased over the years and is now often considered an underutilized commodity (Alercia, 2013), but its importance and role in culture and commercial use places pressure on researchers to maintain and uphold the food security of taro.

Due to the abundance of complex carbohydrates in taro corm, it is considered a primary source of starch comparable to that of potatoes. In contrast, taro starch has a high digestibility value of 98.8% which is due to the miniature size of its starch granules which are approximately ten times smaller than that of starch in potatoes (Jane et al., 1992). This property makes it an ideal ingredient for both infant formula and canned baby foods. For individuals that may have allergies to cereals and milk, taro can be a sufficient substitute (Lee, 1999; Moore & Lawrence, 2003). The leaves are high in protein while the corm contains some dietary fiber and a low amount of fat. Both contain the essential vitamins B1, B2, B6, B9, C and E, and some minerals, including calcium, copper, magnesium, iron, potassium, phosphorus, and manganese (Alcantara, Hurtada, & Dizon, 2013; Alercia, 2013; Payne et al., 1941; Potgieter, 1940; Temesgen & Retta, 2015). The strong nutritional benefit has also motivated researchers to recommend the use of taro as a key ingredient in animal feed (Adejumo, Babalola, & Alabi, 2013; Moore & Lawrence, 2003).

Besides the nutritional benefit of taro, it also plays a role in traditional and herbal medicine in several cultures. In Africa, leaves are used as a demulcent for wounds, sores, and boils, as well as to clot blood to prevent excessive bleeding; in Indonesia, the stem is used for neutralizing poisons from snakes, and rheumatism and acne are treated using the extract from roots (Abbas, 2011). Leaves and corms were prepared in the Philippines with a unique

preparation method to help alleviate pain for women undergoing childbirth, while some tribes also used morning dew on the leaves as an eyewash or had a woman suffering from dysmenorrhea sit on a leaf to help reduce the pain; reduction of bleeding was also treated using styptic petiole extracts. In Hawaii, one approach to an anti-inflammatory treatment to treat conditions such as fever was to drink raw taro juice mixed with sugar. Poi has some additional utility as a probiotic (Brown & Valiere, 2004).

As one of the few plants that have both the parts above-ground and underground consumed, taro is a very important fresh crop in domestic markets across most of the PICs (McGregor et al., 2011). Export markets were recently opened in a few countries, including Fiji, Samoa, Tonga, and Vanuatu, due to a recent revamp in taro production (Sami, 2011). FAO statistics show that, in 2017, worldwide production of taro is approximately 10 million tonnes, where 4% (approximately 409,000 tonnes) of that production originates from Oceania. Fiji was the most active country in terms of exports, in which a value of 20 million FJD per annum was attributed to nearly 95% of total exports (McGregor et al., 2011). Papua New Guinea (PNG), which is the largest taro producer in Oceania and produces more than half the amount of taro associated with Oceania, prefers the domestic sale of taro, which accounts for the low export figures. Additionally, a high shipping cost to trading partners causes export prices to be high, which prevents prices from being competitive compared to Fiji. In Hawaii, production of taro was approximately 1,350 tonnes in 2018 valued at around 1.97 million USD ("USDA Crop Production 2018 Summary," 2019, "USDA Crop Values 2018 Summary," 2019).

2.2 Socio-Cultural Importance of Taro in Hawaii and Oceania

Though its origins can be traced back to Asia, taro remains a critical component in the culture of the Hawaiian Islands and the PICs, starting with the early cultivation of taro in lo'i, flooded taro patches, as daily routine and the foundation of civilization for native Hawaiians (Greenwell, 1947). Agriculture and medicine were not the only roles that taro played a part in, as taro would also have a central role in beliefs about creation.

"Kumulipo" is a Hawaiian chant that depicts a narrative in which taro was the plant that was the progenitor of Hawaiians and features the legend of the Earth Mother, Papa, and the Sky Father, Wakea, and their child Ho'ohokukalani, who was to be the most beautiful and charming woman ever. Later in life, Ho'ohokukalani had a child, Haloa-naka, but the child was stillborn and was buried. From the burial site arose a kalo (the Hawaiian nomenclature for taro) plant, which provided nourishment for the second child, Haloa. Haloa-naka would live on through the vegetative propagation of taro, which made it a holy plant to be respected and treated as an elder sibling. Hawaiians would then base their lineage on the younger brother, Haloa (Cho et al., 2007; Jacobs, 2011; Uchida et al., 2008).

Prayers were regularly performed to seek blessings from the Gods for each new activity performed during a farming cycle, which would honor and signify the work and effort put into farming to produce taro. Rather than being focused on profit (which the early Hawaiians did not utilize), the early agricultural system played a role in feeding people, maintaining religious practices and beliefs, reinforcing tradition, and sustaining customary obligations (Uchida et al., 2008). Despite the commercialization of taro, the spiritual connection and symbolism of the taro plant continue to persist even today, and this idea is illustrated and reinforced through taro as a core art theme present throughout the state of Hawaii (Deo et al., 2009).

Eduardo Trujillo, a plant pathologist associated with the College of Tropical Agriculture and Human Resources (CTAHR) at the University of Hawaii at Manoa (UHM), introduced three improved taro varieties in 2002 that came as a result of a breeding experiment that had started in the early 1990s ("CTAHR and Taro," 2009), and an effort to patent these varieties to UHM was undertaken. These varieties contained a desirable phenotype correlated with that of the 'Maui Lehua' variety (one of the cultivars of the royal Lehua family of Hawaiian cultivars), as well as a notable resistance to taro leaf blight (TLB) (Trujillo, Menezes, Cavaletto, Shimabuku, & Fukuda, 2002). The cultural attachments and sentiments about taro caused a discordance with certain communities regarding the patents, which led to protests in 2006. Suitably, UHM relinquished its patent rights and made the three varieties available to the public ("CTAHR and Taro," 2009). In 2007, an announcement was made in which kalo was declared as the state plant.

Controversy surrounded the use of genetically modified taro in cultivation, and many pushed for the Legislature of the State of Hawaii to pass bills HB704 and SB958, which would start a ten-year moratorium prohibiting the use of genetically modified taro. Accordingly, a ban on genetically engineered taro and coffee on the Big Island was issued by the Hawaii County Council by passing a bill in 2008 which forbade the experimentation, release, and propagation of genetically engineered taro and coffee within the county. Maui County Council would soon emulate this notion in 2009 (Jacobs, 2011).

Palauans also have a strong cultural attachment to taro, which is demonstrated through its use as an emblem of exchange and gratitude during many different events, which include birth ceremonies and funerals (Bishop, 2013). Likewise, in Fiji (Vilsoni, 1993), Micronesia (Primo, 1993), Samoa (Taotua, 1993), the Solomon Islands (Liloqula, Saelea, & Levela, 1993), Tonga (Pole, 1993), and several other countries in the South Pacific (Sivan & Liyanage, 1993), taro is

considered superior to other root crops and is also the favored commodity for royalty, gift-giving, feasting, and social obligations. Overall, many Pacific cultures have integrated taro into folklore, myths, and legends (Deo et al., 2009), and taro itself is often the core to the cultural identity of those cultures (Onwueme, 1999). This proves that the socio-economic role of taro across the PICs is unmatched by other root crops, and that role will continue to persist for further generations.

3.0 Known Pests and Diseases of Taro

3.1 Pests

Throughout much of the South Pacific, the taro beetle, *Papuana* spp. (family *Scarabaeidae*, order *Coleoptera*), is arguably the most important pest of taro, which has been documented to cause critical damage to the corm. The size of these shiny black beetles can range from 15 to 25 mm in the adult stage. As the beetles burrow into the corm, the tunnels that result expose inner flesh and allow other pathogens to infect, causing a secondary rotting which plays a factor in corm spoilage in the field and post-harvest storage (Lal et al., 2008). While these beetles are not present in Hawaii, an accidental introduction via globalized trading routes may pose a risk in the foreseeable future, which necessitates quarantine efforts to prevent such an event from occurring.

The taro root aphid, *Patchella reaumuri*, has been a concern since its initial discovery in 1971 on the Big Island and later in 1995 on Oahu, since it is responsible for disrupting dryland taro production (though it has not yet produced any problems for wetland taro production). It is believed to be a pest that specifically targets taro and a few other closely related plants. Colonies of the taro root aphid are typically covered with a white, fine, cotton-like, and waxy substance,

though the aphids themselves are yellow-gray. The reproduction of the aphid occurs without male fertilization. Between 75% to 100% of losses in taro varieties are attributed to the taro root aphid, and drought conditions exacerbate the damage, especially on young plants (Sato et al. 1997).

Some additional pests of concern to taro include the taro planthopper (*Tarophagus* spp.) by causing wilting and death in heavy infestations, hawk-moth (*Hippotion celerio*) and armyworm caterpillars (*Spodoptera litura*) both by causing defoliation via feeding on leaves, spiraling whitefly (*Aleurodicus dispersus*), the aphid *Aphis gossypii* and mealybugs. The growth of sooty molds promoted by exuded honeydew can interfere with photosynthesis. Spider mites (*Tetranychus* spp.) can cause some yellow-white speckling and premature leaf death (Carmichael et al., 2008). Most notably, mealybugs have often been associated with the infection of taro by the transmission of the *Taro bacilliform virus* (TaBV) (Gollifer et al., 1977; Macanawai et al., 2005).

Snails are also pests of taro, with the giant African snail (GAS) reported to be feeding on taro leaves across many PICs. Taro does not appear to be the plant that GAS prioritizes feeding on, as with low populations, they can be seen feeding on green cabbage instead (Carmichael et al., 2008). The apple snails *Pomacea canaliculata* (in all Hawaiian islands with the exception of Molokai and Lanai) and *Pila conica* (Molokai only) were originally introduced to Hawaii for the purpose of the Hawaiian aquaculture industry but escaped and pose a major threat to taro by causing significant damage to the foliage of taro, playing a role in reduced yield in leaves and corm (Levin, 2006; Martin, 2004), and can even cause injury or annoyance to workers maintaining taro crops.

3.2 Nematodes

From the Solomon Islands in 1983 came a report of a nematode *Hirschmanniella miticausa* which caused a unique "miti miti" disease (Bridge, Mortimer, & Jackson, 1983), though it can also be found in PNG. Dry, brown rot of the corm about the size of 1 to 10 mm can result from an infestation of this nematode. Chlorosis and wilting of the leaves may be indicators of infestation, but it is difficult to ascertain that infestation is the cause until corms are harvested (Carmichael et al., 2008). Other nematodes that affect taro include root knot nematodes (*Meloidogyne* spp.), which, like their namesake, can cause root knots and decay; and lesion nematodes (*Pratylenchus coffeae*) can cause stunting and death. Yield loss of corms due to nematodes has been documented (Arakaki, 1993; Sipes & Arakaki, 1997; Torigoe, Fukunaga, & Muta, 2002).

3.3 Fungal Diseases

The soil-borne fungus *Athelia rolfsii* is responsible for the most common fungal disease of taro in the Pacific, characterized by the rotting of the taro corm, and in some cases, a pinkish rot that occurs post-harvest. *Neojohnstonia colocasiae*, causing orange leaf spot, and *Cladosporium colocasiae*, causing brown leaf spot, are also common throughout the PICs. *Lasiodiplodia theobromae*, causing spongy black rot, has been found infecting taro in Guam, PNG, Samoa, and the Solomon Islands. *Leptosphaerulina trifolii*, causing white spot disease of taro, has been found infecting taro in American Samoa, PNG, Samoa, Solomon Islands, and Tuvalu. The fungi causing spongy black rot and white spot diseases of taro have also been positively identified in other hosts in the Pacific. *Marasmiellus stenophyllus*, causing corm and leaf spot in taro, has been identified in American Samoa, Tahiti, Wallis, and Futuna, though

another host was found with that fungus in Fiji. Other notable fungal pathogens of taro in the Pacific include *Ceratocystis fimbriata* (causing black rot), *Fusarium* spp. (causing fusarium dry rot), *Phoma* spp. (causing symptoms of "shot hole"), *Phyllosticta colocasiophila* (causing phyllosticta leaf spot), *Pseudocercospora colocasiae* (causing leaf blotch), and *Rhizopus stolonifera* (causing rhizopus rot) (Carmichael et al., 2008; Ooka, 1990; Parris, 1941).

3.4 Oomycete Diseases

Taro leaf blight (TLB) is a very important disease in the history of taro, which caused a range of corm yield losses from 25% to 50% in the Pacific and 25% to 35% in the Philippines. This disease is triggered by *Phytophthora colocasiae* and was first reported in Java, Indonesia in 1900 by Marian Raciborski. The most common site of infection is the leaves, though the petioles and corms may also be affected. Infection can also cause losses of up to 95% of leaf yield in susceptible taro in Hawaii (Brooks, 2005; Nelson, Brooks, & Teves, 2011). Later epidemics were believed to have been in 1918 in Guam, to the first report of TLB in 1920 in Hawaii (Hunter, Pouono, & Semisi, 1998).

An outbreak of TLB in 1993-1994 caused critical damage to the Samoan and American Samoan taro industries. The severity of the damage can be noted in profits in the Samoan market made after the outbreaks, which was reduced heavily from their usual profits of 10 million USD annually to as little as 60 thousand USD, a mere 0.6% of what was earned before. Additionally, an annual yield of approximately 400,000 kg in American Samoa before the outbreak was reduced to 5,000 kg in 1995, about 1.25% of the typical annual yield (Brooks, 2008; Singh et al., 2012). Recently, TLB occurs in many places globally, including much of the Pacific, Asia, Africa, the Caribbean and the Americas (Nelson et al., 2011)

Pythium rot is another disease caused by oomycetes in the genus *Pythium*, which was first reported by Sedgwick in Hawaii in 1902. Rotting may start from a part of the corm and spread upward to infect the whole of the tuber, and the color of the rotting tissue is highly variable, including whitish-yellow, gray, blue or purple (Parris, 1941). The appearance of the aboveground parts of the plant can make it seem as though it were stunted while dying away (Carmichael et al., 2008). Some *Pythium* species have been found in Hawaii, New Caledonia, Palau, Samoa, and the Solomon Islands, and infections can cause losses of up to 80%.

3.5 Bacterial Diseases

Erwinia chrysanthemi infection has been reported in the Solomon Islands, leading to bacterial soft rot which is characterized by an aqueous soft rotting that is whitish to dark blue and a pungent odor (Carmichael et al., 2008). Infection by *Xanthomonas axonopodis* pv dieffenbachiae has also been observed in Hawaii, causing bacterial leaf spot, though the symptoms are not severe in taro (Ooka, 1990).

3.6 Viral Diseases

Many viral diseases of taro are important, and one such viral disease is “alomae,” noted to be a critically destructive disease to taro. The prevalence of this disease is limited to the Solomon Islands and PNG, and plants affected by the disease develop symptoms of a feathery mosaic, crinkled emerging leaves that do not open, stunting with twisted, dark green leaves; in some cases, this causes plant death and consequently causes significant yield losses (Gollifer et al., 1978). The causative agent of this disease is believed to be a co-infection of *Colocasia bobone disease-associated cytorhabdovirus* (CBDaV) and *Taro bacilliform virus* (TaBV)

(James, Kenten, & Woods, 1973; Ooka, 1990), though it has been speculated that *Taro vein chlorosis nucleorhabdovirus* (TaVCV) may also play a role in the onset of the disease (Carmichael et al., 2008). The delphacid *Tarophagus proserpina* is a pest associated with the transmission of CBDaV, while the mealybugs *Planococcus citri* and *Pseudococcus longispinus* are associated with the transmission of TaBV (Gollifer et al., 1977; Macanawai et al., 2005).

CBDaV is destructive even when it doesn't co-infect taro together with TaBV, and is a putative rhabdovirus that is, like alomae disease, limited to the Solomon Islands and PNG. By itself, it causes the bobone disease, which is characterized by symptoms of severe stunting and leaves that are distorted, stiff, and thickened, and in some cases, galls may emerge on the petioles and larger leaf veins. CBDaV is speculated by some researchers to be the common factor in both alomae and bobone diseases and is therefore believed to be the causative agent that contributes to the Alomae/Bobone virus complex (ABVC) (Ivancic et al., 1993). The full genomic sequence of CBDaV (sampled from taro in the Solomon Islands affected by the bobone disease) was published as a 12,193 base pair (bp) negative single-stranded RNA viral genome, with a phylogenetic analysis placing it as a putative member of the *Cytorhabdovirus* genus (Higgins et al., 2016a, 2016b). A virus with milder effects, though with the most expansive prevalence across the Pacific, is *Dasheen mosaic virus* (DsMV), a member of the *Potyvirus* genus. Infection by DsMV causes mild to moderate distortions with an array of mosaic patterns, and, as a stylet-borne and nonpersistent virus, is caused by transmission via aphids, including *Aphis craccivora*, *A. gossypii*, and *Myzus persicae* (Ooka, 1990).

TaBV (genus *Badnavirus*) also has a widespread prevalence across the Pacific, initially reported by James et al. (1973) and sequenced about 30 years later (Yang et al., 2003). Symptoms of TaBV include latent and erratic yellowing of the veins, proximal to the margin of

the leaf, as well as creasing or bending of the leaf blades (Carmichael et al., 2008). A recent attempt to perform deep sequencing of small RNAs (sRNAs) from a sample of taro plants (displaying symptoms that resembled those of a plant infected with TaBV) yielded the discovery of another virus within the genus *Badnavirus*, tentatively named *Taro bacilliform CH virus* (TaBCHV) (Kazmi et al., 2015).

An important yet understudied viral pathogen of taro is *Taro vein chlorosis nucleorhabdovirus* (TaVCV), which was first reported in 1999 by Pearson et al. and later fully sequenced by Revill et al. in 2005 using a Fijian isolate, which allowed it to be officially recognized as a member of the genus *Nucleorhabdovirus*. Reports of TaVCV to date have confirmed that TaVCV-infected taro in nine countries in the Pacific, namely Fiji, the Federated States of Micronesia, New Caledonia, Palau, PNG, the Solomon Islands, Tuvalu, Vanuatu, and a recent discovery was made in Hawaii as a part of the United States of America (Long et al., 2014). A feather-like chlorotic symptom can be seen on leaves of infected taro, which gradually broadens with age and eventually fuses into a network with the possibility of necrosis in later stages. Chlorosis is more evident in TaVCV infections compared to TaBV infections. Additional symptoms include petiole streaking and stunting, and, in severe cases, plant death.

Another virus of taro is *Taro reovirus* (TaRV), found in PNG, the Solomon Islands, and Vanuatu, though its effects on taro are currently unclear (Revill et al., 2005). In India, an isolated case of *Groundnut bud necrosis virus* (GBDV) infecting taro was reported, causing symptoms of chlorotic spotting, mosaic patterns, necrotic flecking on leaves, and overall stunting (Sivaprasad et al., 2011). *Cucumber mosaic virus* (CMV) has also been reported in taro plants in China (Wang et al., 2014), and *Konjac mosaic virus* (KoMV) has been found to infect three aroid species including *C. esculenta* in India (Manikonda et al., 2011).

4.0 Taro vein chlorosis nucleorhabdovirus (TaVCV) (genus *Nucleorhabdovirus*, family *Rhabdoviridae*, order *Mononegavirales*)

4.1 Family *Rhabdoviridae*

The order *Mononegavirales*, established in 1991 (Pringle, 1991), encompasses many viral families that contain members that are monopartite, single-stranded, negative-sense RNA viruses. One of the families that are included in that order is the *Rhabdoviridae* family, which contains 20 assigned genera, including *Cytorhabdovirus* (with 11 species), *Dichoravirus* (with 5 species), and *Nucleorhabdovirus* (with 10 species), along with one unassigned species that has not yet been assigned to a genus ("International Committee on Taxonomy of Viruses," 2019). Members of families belonging to this order are often separated based on their hosts, the vector of transmission, as well as serological assays and properties of the viral genome (Jackson et al., 2005). From the 20 genera in the family, only three (*Cytorhabdovirus*, *Dichoravirus*, *Nucleorhabdovirus*) contain members that have been documented to infect plants (Walker et al., 2000). Typical morphological features of *Rhabdoviridae* family members include enveloped virions with a bacilliform shape, ranging from a width of 45 to 100 nm to a length of 130 to 350 nm (Brown, 1987), though members of the genus *Dichoravirus* are exceptions, with unenveloped particles and bipartite genomes (Kondo et al., 2006).

The organization of a rhabdovirus, from the 3'-end to 5'-end (in negative polarity), is the leader sequence; the open reading frames (ORFs) coding for nucleoprotein (N), phosphoprotein (P), matrix protein (M), glycoprotein (G), RNA-dependent RNA polymerase (RdRp, or L); then trailer sequence. The nucleoprotein (N) is a protein that makes up a significant portion of the nucleocapsid, part of the virion. The phosphoprotein (P) is a regulatory protein and non-catalytic

cofactor of the RdRp coded downstream. The matrix (M) protein is a structural component of the rhabdovirus virion and is usually involved in interactions with cellular membranes and the budding process. The glycoprotein (G) aids in binding to surface receptors on host cells, causing the virus to be taken into the cell. Lastly, the RdRp (L) is the polymerase responsible for replication of the viral RNA genome. Though these five genes are common features of all rhabdoviruses, those that have been fully sequenced may carry up to four additional ORFs, positioned between either the P and M ORFs or the G and L ORFs (Healy, Banyard, & Fooks, 2013; "International Committee on Taxonomy of Viruses," 2019; Jackson et al., 1987; Redinbaugh & Hogenhout, 2005; Walker et al., 2000, 2015).

4.2 Genus *Nucleorhabdovirus*

The genus *Nucleorhabdovirus* is one of the three viral genera that have plant hosts in family *Rhabdoviridae*. The morphology of the virion is typically either bacilliform or bullet-shaped, with dimensions of 170 to 380 nm in length and 55 to 100 nm in diameter, encapsulating an unsegmented negative-sense single-stranded (ss)RNA genome (Fig. 1.1). The virion is arranged in a symmetrical helix, with glycoproteins spread across the surface, and its composition is roughly 1% nucleic acid, 70% protein, and 25% lipid (Adams & Antoniw, n.d.). Once the virus has entered the cell via effraction or plasmodesmata transport, the virus is moved to the nucleus of the host cell, where its replication and maturation site is located.

Nucleorhabdovirus, as per most genera of the family *Rhabdoviridae*, typically have monopartite, linear, and negative-sense ssRNA genomes 11 to 15 kb in length (Brunt et al., 1996). The type member of the genus *Nucleorhabdovirus* is *Potato yellow dwarf nucleorhabdovirus* (PYDV), and other members include *Sonchus yellow net nucleorhabdovirus*

(SYNV), *Rice yellow stunt nucleorhabdovirus* (RYSV), *Sowthistle yellow vein nucleorhabdovirus* (SYVV), *Eggplant mottled dwarf nucleorhabdovirus* (EMDV), *Maize fine streak nucleorhabdovirus* (MFSV), *Maize mosaic nucleorhabdovirus* (MMV), *Maize Iranian mosaic nucleorhabdovirus* (MIMV), and *Taro vein chlorosis nucleorhabdovirus* (TaVCV) ("International Committee on Taxonomy of Viruses," 2019). The genome organization of most members of the genus *Nucleorhabdovirus* follows the family *Rhabdoviridae* in that there are N, P, M, G, and L ORFs, but this genus contains members that contain an additional ORF, gene 3, between the P and M ORFs (Fig 1.2). The function of this gene 3 ORF is currently unclear.

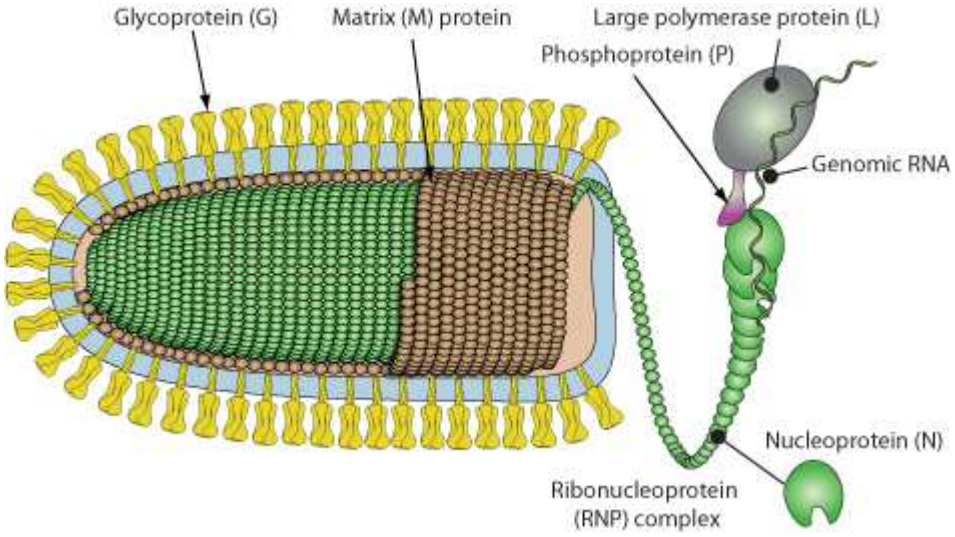

Fig. 1.1. Diagram of the putative *Nucleorhabdovirus* structure.

Adopted from: http://viralzone.expasy.org/all_by_species/78.html

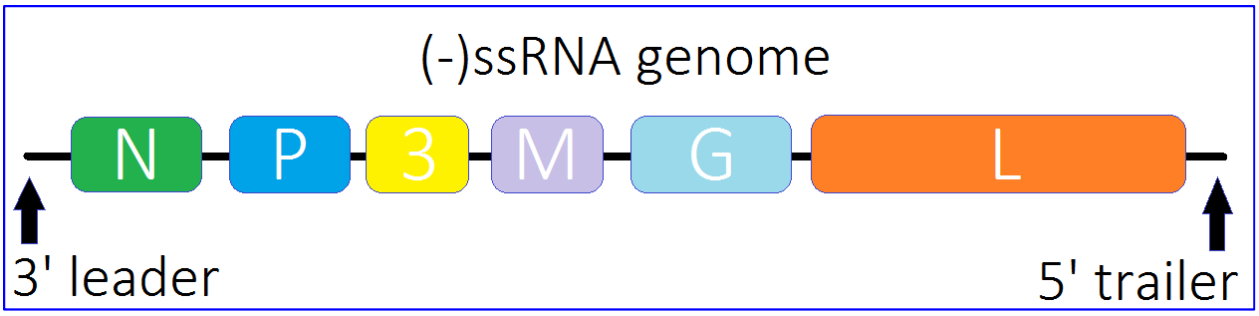

Fig. 1.2. Genomic arrangement of typical members of the genus *Nucleorhabdovirus*, including *Taro vein chlorosis nucleorhabdovirus*. The following ORFs in coding orientation are nucleoprotein (N), phosphoprotein (P), gene 3, matrix protein (M), glycoprotein (G), RNA-dependent RNA polymerase (L). Based on: http://viralzone.expasy.org/all_by_species/78.html

4.3 Known Distribution and History of TaVCV

TaVCV has been reported across several countries in the South Pacific, including the Federated States of Micronesia, Fiji, New Caledonia, Palau, PNG, the Solomon Islands, Tuvalu, Vanuatu (Carmichael et al., 2008), and recently in Hawaii. The earliest reports of TaVCV originated from Fiji, PNG, Tuvalu, and Vanuatu. The original demarcation of TaVCV was done by comparison of the viral morphology (in terms of particle size), symptoms, and serological activity to distinguish TaVCV from CBDaV (Pearson et al., 1999). The effects of the virus on taro resulted in the nomenclature of "*Taro vein chlorosis virus*."

A viral survey done in 2002 by inspection of taro plants in Fiji found that TaVCV was widespread based on a visual inspection of symptoms alone (Harding, Williams, & Jackson, 2002). The purpose of this survey was to collect taro leaf tissues from symptomatic plants to purify and index the virus. The publication by Revill et al. (2005a) was the first publication detailing the complete sequence (and electron microscopy) of TaVCV, which was sampled from an isolate in Fiji, and allowed TaVCV to be officially recognized as a member of the genus

Nucleorhabdovirus. The basis of this recognition was the six ORFs which were analogous to the six ORFs (N, P, 3, M, G, L) found in other members of the genus.

Another element of their publication claimed that high nucleotide diversity existed between TaVCV isolates from Fiji, the Federated States of Micronesia, New Caledonia, PNG, the Solomon Islands, and Vanuatu. They also showed that the most closely related species was *Maize mosaic virus* (MMV), another member of the *Nucleorhabdovirus* genus. The identity of each of the ORFs with MMV were: 63.1% (N), 46.1% (P), 43.4% (gene 3), 46.4% (M), 49.9% (G), and 67.9% (L). A phylogenetic analysis using the L gene grouped TaVCV in a clade with other *Nucleorhabdovirus* members, apart from other clades in the family *Rhabdoviridae*.

4.4 The Symptomatology of TaVCV

Symptoms related to TaVCV typically emerge when a taro plant has matured. These symptoms include a yellowing of the leaf veins, close to the margin, gradually spreading through the leaf into a network. This chlorotic effect is often more visibly pronounced than in the chlorosis produced by TaBV infection. Necrosis may be seen in the later stages of viral infection, and the leaves may appear tattered or bent downward. Only a few leaves can appear diseased while other leaves appear healthy (Carmichael et al., 2008). Depending on the cultivar, taro may exhibit petiole streaking and stunting (Fig. 1.3a-g). Currently, it is unknown if TaVCV affects corm yield. Visual examination may suffice for a preliminary diagnosis of TaVCV, but the emergence of symptoms can vary between varieties and cultivars of taro, so further analysis regarding this issue is necessary.

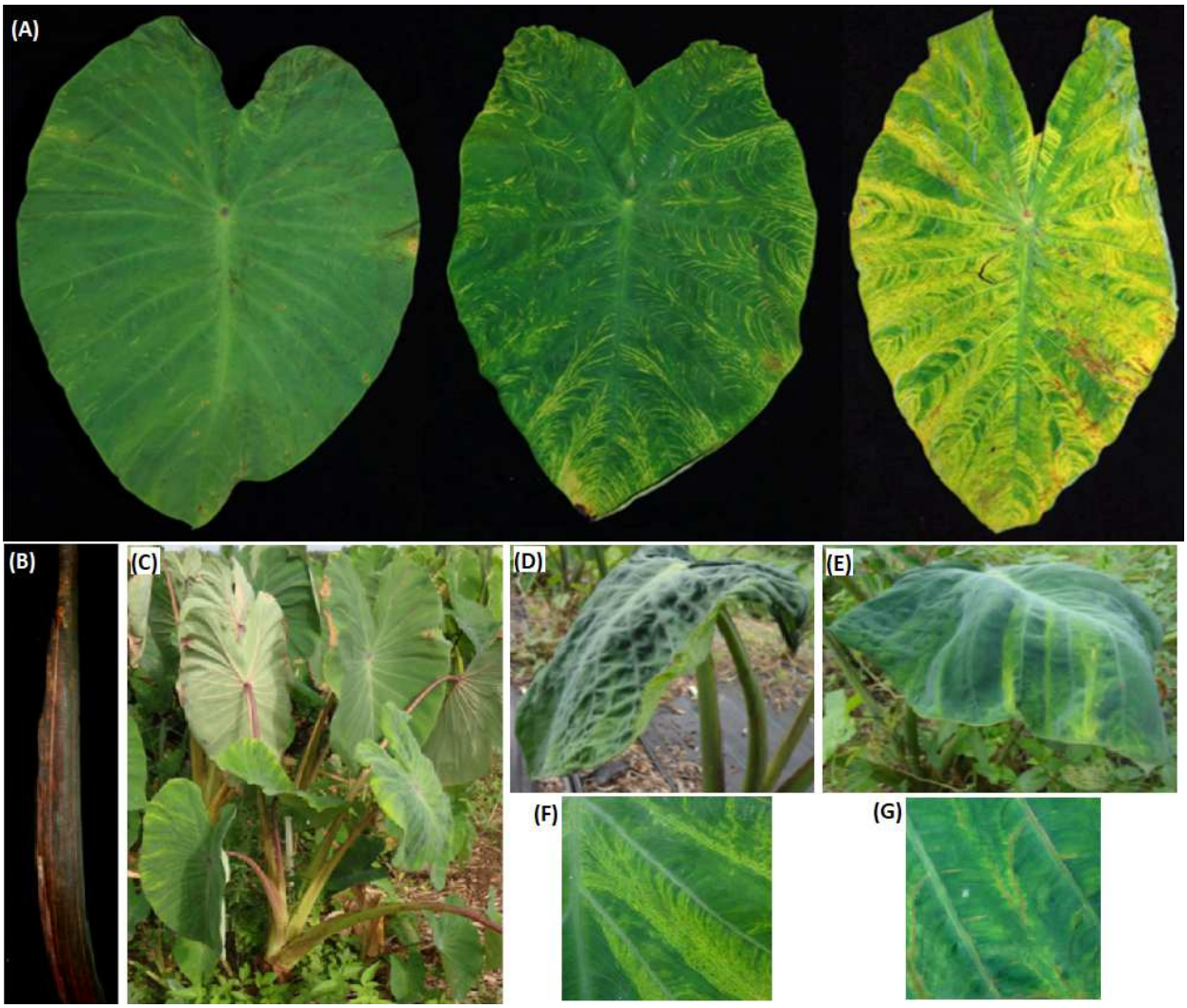

Fig. 1.3. Visual foliar symptoms of TaVCV in increasing severity from left to right (a); other symptoms that can be seen include petiole streaking (b), stunting (c), downward bending (d, e), veinal chlorosis (f), and necrosis (g). Adopted from https://www.ctahr.hawaii.edu/oc/freepubs/pdf/PD-111.pdf

4.5 Description of TaVCV

4.5.1 Particle Morphology

The electron microscopy data submitted by Revill et al. (2005a) confirms TaVCV to be bullet-shaped, with dimensions of 200 nm in length and 70 nm in diameter (Fig. 1.4).

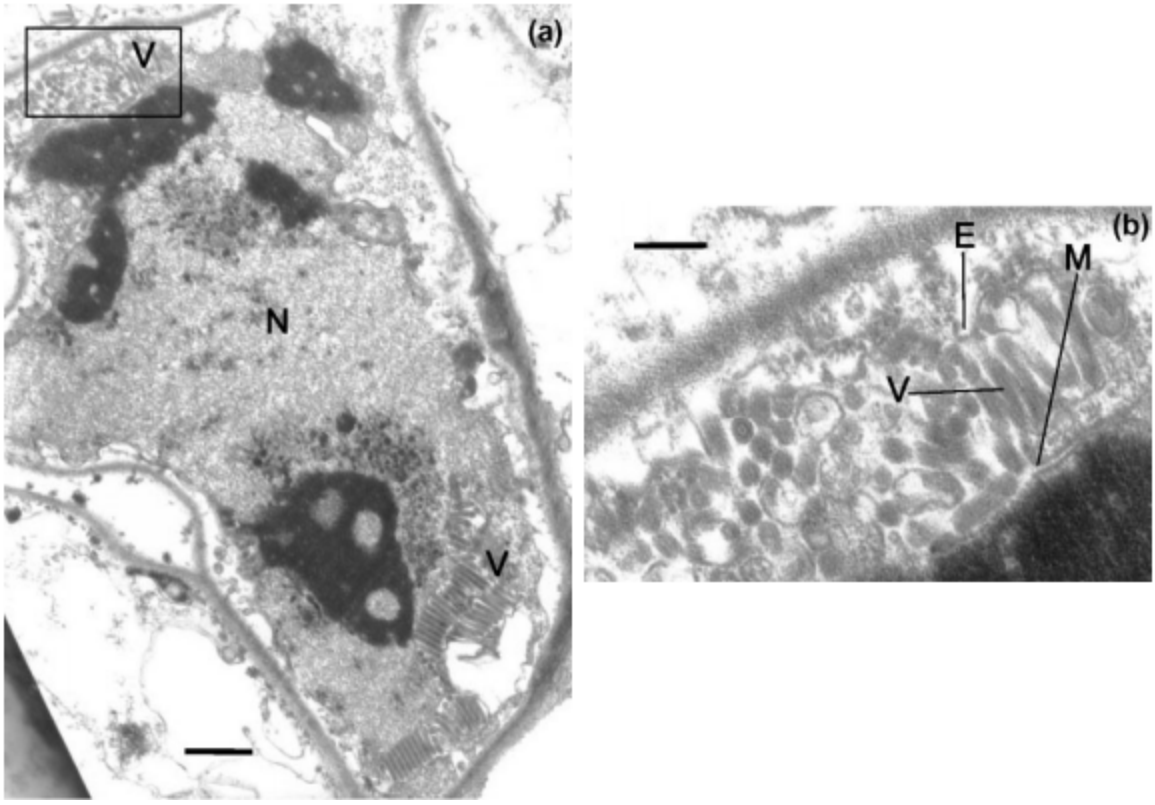

Fig. 1.4. Electron micrographs depicting cross-sections of a cell infected with TaVCV (a), focusing on the nucleus (N) of the cell, containing TaVCV virions (V). At the nuclear envelope seen more closely in the boxed area (b), the perinuclear space, between the inner membrane (M) and outer membrane (E), contains virions. Bar: 200 nm. Adopted from Revill et al. (2005a).

4.5.2 Genome Organization

The Fijian isolate of the negative-sense ssRNA genome of TaVCV (GenBank accession number NC_006942.1) is 12,020 base pairs (bp) in length, coding for six major ORFs. These ORFs are organized similarly to other *Nucleorhabdovirus* genus members, which is, in coding orientation, N, P, gene 3, M, G, L. The length of each gene in this isolate is 1506 (N), 813 (P), 861 (3), 705 (M), 1764 (G) and 5784 (L) nucleotides (Revill et al., 2005a). Though the function of the gene 3 protein has yet to be confirmed, it has been shown to serve as a putative movement

protein (MP) in RYSV (Huang et al., 2005) as well as SYNV, though gene 3 is referred to as the sc4 gene (Goodin et al., 2002; Scholthof et al., 1994).

4.5.3 Transmission

The vector of transmission for TaVCV has not yet been determined; however, it is useful to discuss possible modes of transmission by an analysis of transmission for other closely related viruses. It has been found that planthoppers are the vectors of transmission for other *Nucleorhabdovirus* genus members such as MMV via the corn planthopper *Peregrinus maidis* and MIMV via the planthopper *Ribautodelphax notabilis* (ICTV, online). Notably, CBDaV (a *Cytorhabdovirus*) is transmitted through *Tarophagus proserpina*, the taro planthopper (Gollifer et al., 1977).

Leafhoppers are also associated with the transmission of other *Nucleorhabdovirus* members, such as EMDV via the Agallinae leafhoppers *Anaceratogallia laevis*, *A. ribauti* and *Agallia vorobjevi* (Babaie & Izadpanah, 2003), MFSV via the blackfaced leafhopper *Graminella nigrifrons* (Redinbaugh et al., 2002; Todd et al., 2010), PYDV via the clover leafhopper *Aceratagallia sanguinolenta* (Black, 1943), and RYSV via the green rice leafhoppers *Nephotettix nigropictus*, *N. cincticeps*, and *N. virescens* (Chiu et al., 1965; Hiraguri et al., 2014).

Only two of the *Nucleorhabdovirus* members are transmitted through aphids: SYNV via *Aphis coreopsidis* (Christie, Christie, & Edwardson, 1974) and SYVV via the blackcurrant-sowthistle aphid *Hyperomyzus lactucae* (Duffus, 1963; Richardson & Sylvester, 1968) and, to a lesser degree of efficiency, the potato aphid *Macrosiphum euphorbiae* (Behncken, 1973).

TaVCV has been spread with the use of contaminated planting material (Long et al., 2014). Considering the transmission modes currently determined for the members of the genus

Nucleorhabdovirus, there is a high likelihood that a planthopper or leafhopper is the vector for TaVCV transmission. The insects that interact with taro are the taro planthoppers, *Tarophagus colocasiae*, *T. persephone*, and *T. proserpina*, which are each distributed in varying degrees across Asia and the Pacific (Asche & Wilson, 1989), and are likely vectors for TaVCV.

CHAPTER 2: GENOMIC ANALYSES OF PACIFIC TARO VEIN CHLOROSIS NUCLEORHABDOVIRUS (TAVCV) ISOLATES

Introduction

Many viral genomes are small compared to prokaryotic and eukaryotic genomes, with the latter often consisting of several megabases of genomic DNA. Additionally, prokaryotic and eukaryotic genomes encode DNA polymerases that have proofreading ability and thus minimize the probability of random mutations that can result when duplicating their genomes, while viruses often code for polymerases that lack proofreading ability. As a result, despite the small size of many viral genomes, viruses often evolve at a much faster rate due to a higher incidence of random mutations, contributing to their survival and adaptability when infecting hosts. The same concept applies to many viruses.

The study by Revill et al. reported a widespread prevalence of TaVCV across several different countries across the South Pacific (2005). This prevalence, combined with the concept of error-prone replication, could eventually yield a high genetic diversity of TaVCV among regional isolates. Therefore, a study utilizing next-generation sequencing to elucidate the full genomes of TaVCV, especially the protein-coding sequences, may help to shed light on a possible pathway through which the virus had spread historically, as well as to contribute genomic data of TaVCV isolates, which has not been further explored since the first submission of a Fijian TaVCV isolate in part of Revill's study.

The *Nucleorhabdovirus* genus is unique compared to other genera in the *Rhabdoviridae* family in that it contains members that can replicate and assemble in the nucleus, while the other genera contain members that replicate and assemble in the cytoplasm. Some proteins contain domains that interact with the nucleus, allowing migration to and from the nucleus. These

domains are the nuclear localization signals (NLSs) and nuclear export signals (NESs). A typical NLS consists of lysine and arginine amino acids, while a typical NES consists of leucine-rich segments that are usually hydrophobic. The cNLS Mapper (Kosugi et al., 2009) and NetNES 1.1 (la Cour et al., 2004) programs can detect NLSs or NESs, respectively, based on literature describing proteins with such motifs. cNLS Mapper scores detected NLSs, and a score of 8 through 10 suggests the protein is exclusively localized to the nucleus, while a lower score of 3 through 5 suggests the protein is distributed between the nucleus and cytoplasm. A score below 3 suggests exclusively cytoplasmic distribution and is therefore implied to not interact with the nucleus. NetNES 1.1 uses a score system which needs to meet a threshold to detect the presence of NESs in proteins of interest. While Revill's study was able to provide electron microscopy data, it would be useful to look at other isolates for these traits as some proteins from different isolates may have some differences in their sequences worth investigating. Additionally, the original publication does not reference the use of cNLS Mapper and NetNES 1.1, the latter of which was unavailable at the time of publication.

Materials and Methods

Sample Source

The Hawaii sample was collected on November 2017 at Waimanalo Research Station (21.335678, -157.712063). The Guam samples were collected on June 2018 by Nelson Masang, Jr. at Hagatña, Guam (approx. 13.471291, 144.760277) and imported under USDA-APHIS permit P526P-16-03581. The Palau samples were collected on June 2018 by Nelson Masang, Jr. at Koror, Palau (approx. 7.350186, 134.495277) and imported under USDA-APHIS permit P526P-17-03915. The Samoa samples were collected on November 2017 by the Ministry of

Agriculture and Fisheries Samoa and imported under USDA-APHIS permit P526P-17-03915. The variety of the Samoan sample was ‘Talo mumu’. The Vanuatu samples were collected on March 2019 at the Vanuatu Agricultural Research & Technology Centre, Espiritu Santo (-15.451257, 167.189511) and imported under USDA-APHIS permit P526P-17-03915.

All Fiji samples came from Viti Levu island. The Navua samples came from the fields located between Pacific Harbour and Navua town (approx. -18.226804, 178.132221). The Nais sample came from the roadside between Wainisikia and Naimasimasi villages (approx. -17.922106, 178.556247). The Nadi samples came from a residential garden near the airport (-17.743295, 177.450381). All were collected in March 2019 and imported under USDA-APHIS permit P526P-17-03915.

All samples were suspended in RNAlater and subsequently stored at -20 °C upon arrival prior to use.

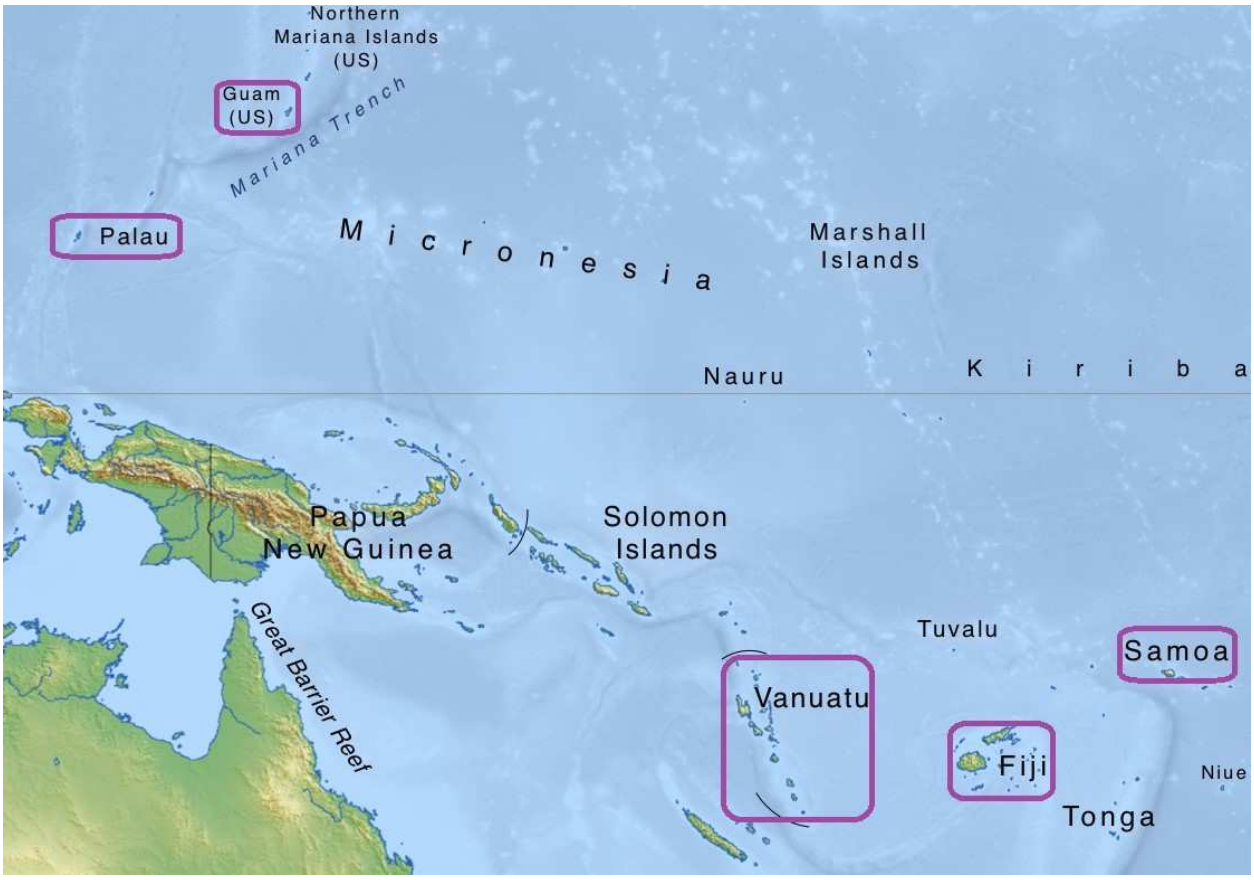

Fig. 2.1. Pacific-centric map featuring the sampling locations circled with a purple outline, except for Hawaii.

Detection of TaVCV

RNA was extracted from taro leaves using the plant RNA isolation protocol for the NucleoSpin RNA Plus kit. The reverse transcription polymerase chain reaction (RT-PCR) was performed using SuperScript III One-Step RT-PCR System as follows. 1 µL RNA, 1 µL 10 µM DCGF3 (5'-GTCTGGTAAAGAGGGGTTGA-3'), 1 µL 10 µM DCGR3 (5'-GTCGAGGGTCATGATAGAGT-3'), 6.2 µL nuclease-free H_2O were mixed, incubated at 95 °C for 8-10 min, then immediately chilled on ice for at least 1 min and centrifuged. To this reaction, 10 µL 2x Reaction Mix and 0.8 µL SuperScript III RT/Platinum Taq Mix were added. The

reaction was then incubated at 55 °C for 30 min, then 94 °C for 2 min, followed by 40 cycles of 94 °C for 15 sec, 55 °C for 30 sec, 68 °C for 1 min, then 68 °C for 5 min. This procedure was repeated for DCGF5 (5'-AGGGGYTGAGRCAAAAGGGGT-3') and DCGR5 (5'-CGCTCYTTCATACATGCSGCCTT-3') primers, replacing DCGF3 and DCGR3. These reactions were run on an agarose gel and a band corresponding to the expected size was cut from the gel, extracted by a centrifugation step through filter paper at maximum speed (21,130 g) for 2 min.

0.3 µL of pGEM T-Easy vector, 3.7 µL gel eluate, 5 µL 2x Rapid Ligation Buffer and 1 µL T4 DNA Ligase (3 U/µL) were mixed and incubated overnight at RT. The following day, a tube containing chemically competent *E. coli* DH5α cells was thawed on ice for 10 min, then 2-5 µL of the ligation reaction was added to the tube of cells, flicked gently 4-6 times and incubated on ice for 60 min. The tube was then added to a water bath at exactly 42 °C and incubated for 30-45 sec before immediately placing the tubes back on ice for 2 min. Super Optimal Broth (450 µL) was then added to the tube and incubated at 37 °C for 45 min with shaking (200-300 rpm). 250 µL was then plated on MacConkey Agar containing ampicillin antibiotics at a concentration of at least 100 µg/mL, then incubated overnight at 37 °C.

Bacteria colony PCR using T7 and SP6 primers was then performed for each white colony that grew on the agar, and colonies that amplified products at roughly the expected size were then grown in Luria-Bertani medium (LB) containing ampicillin at a concentration of at least 100 µg/mL overnight. The QIAgen Spin Miniprep Kit was used to purify the plasmid containing the insert of interest and the plasmid that was eluted from the kit was then sequenced.

Double-Stranded (ds)RNA Extraction (Large-Scale)

The following method is based on the plant viral double-stranded RNA (dsRNA) protocol by Morris and Dodds (1979), Bar-Joseph et al. (1983) and Dodds et al. (1984). About 5 g of symptomatic leaf tissue from Hawaii or Samoa was ground into a powder in liquid nitrogen using a mortar and pestle, which was pre-cooled overnight in a -20 °C freezer. The powdered leaf tissue was then added to 200 mL of dsRNA extraction buffer (10X STE 18 mL, 10% SDS 30 mL, β-Mercaptoethanol 2 mL, dH_2O 72 mL, saturated phenol 40 mL, chloroform 40 mL; 10X STE = Tris-HCl 61.0 g, NaCl 58.0 g, EDTA 3.7 g, dH_2O to 1000 mL, pH 8.0), then stirred with a magnetic stir bar for 45-60 minutes at 4 °C. The solution was then transferred to a 250 mL bottle and centrifuged at 8,000 rpm for 10 minutes. The aqueous phase was transferred to a new bottle, then 0.2 volumes (with respect to the aqueous phase volume) of EtOH was added. 2 g of CF-11 cellulose powder was added to the solution, which was then gently shaken on an orbital shaker for 30 minutes at room temperature (RT). This solution with cellulose powder was added to a column and the liquid was allowed to flow through, then the column was washed with at least 100 mL of 1X STE containing 16.5% (v/v) EtOH. The liquid was then purged from the cellulose and the dsRNA was then eluted into a 50 mL centrifuge tube with three 10 mL aliquots of 1X STE, each of which was purged after each elution. 6 mL EtOH (0.2 volumes with respect to elution volume), then 1.5 g of CF-11 cellulose powder was added to the eluate and gently shaken on an orbital shaker overnight at RT. The solution with powder was then added to a column, the liquid was allowed to flow through and the column was then washed with at least 100 mL of 1X STE containing 16.5% (v/v) EtOH. The liquid was then purged from the cellulose, and the dsRNA was then eluted into a 15 mL centrifuge tube with three aliquots of 3 mL 1X STE, each of which was purged after each elution. The tubes were then spun in a centrifuge for 1 minute to pellet the cellulose, and the supernatant was then transferred to a 30 mL Corex centrifuge tube.

0.9 mL of 3 M sodium acetate (pH 5.2) was then added to the transferred solution, and the tube was filled as close to the top as possible with 95% EtOH (about 20 mL). The tube was sealed with Parafilm, inverted to mix the solution well and incubated overnight at -20 °C.

The next day, the tubes were centrifuged at 12,000 rpm for 30 minutes. The supernatant was then decanted, and the pellet was then resuspended in 500 µL of molecular-grade (nuclease-free) water. The dsRNA solution was then concentrated using an Amicon Ultra centrifugal filter (50 kDa molecular weight cutoff).

Double-Stranded (ds)RNA Extraction (Small-Scale)

About 100 mg of symptomatic leaf sample from Guam, Palau and Vanuatu was homogenized in 1 mL CTAB extraction buffer (CTAB 10 g, PVP-40 10 g, 1 M Tris-Cl (pH 8) 50 mL, NaCl 41 g, 0.5 M EDTA (pH 8) 20 mL, 2-mercaptoethanol 2 mL, dH_2O to 500 mL) using a mortar and pestle after cooling in -20 °C for 5-15 min. The homogenized sample was then incubated at 65 °C for 15 min, followed by centrifugation at 10,000 g for 5 min. Up to 1 mL of supernatant was transferred to another clean microcentrifuge tube, then an equal volume of chloroform:isoamyl alcohol (24:1) solution was added to the supernatant, then mixed by vortexing before centrifuging at 5,000 g for 5 min. The aqueous upper phase was transferred to another clean microcentrifuge tube, and a volume of isopropanol equal to the volume of the aqueous phase was added, mixed gently, then incubated at room temperature for 5 min before centrifuging at 15,000 for 10 min. The supernatant was poured off and the pelleted nucleic acids left to dry at room temperature. The pellet was then resuspended in 100 µL of DNase/RNase-free dH_2O. About 20 µL of 95% EtOH was added to the solution, then about 40 mg of CF-11 cellulose powder was added, followed by incubation at 30 min at RT with gentle shaking in an

orbital shaker. The suspension was added to a makeshift spin column made from a 0.6-mL microcentrifuge tube with a small opening on the bottom and a small piece of filter paper made to prevent the passage of solid material. This was centrifuged in a 1.5-mL microcentrifuge tube at 1,000 g for 2 min to let the liquid flow through. The powder left in the column was washed at least three times with 250 µL aliquots of 1X STE containing 16.5% (v/v) EtOH. The liquid was then purged from the cellulose, and the dsRNA was eluted with three 100 µL aliquots of 1X STE, each of which was purged after elution. The eluate was centrifuged for 1 min to pellet any cellulose that may have passed through the filter, and the supernatant was transferred to an Amicon Ultra centrifugal filter (50 kDa molecular weight cutoff) to concentrate nucleic acids.

Preparation of cDNA Library for Next-Generation Sequencing

The dsRNA eluate was used as a template for reverse transcription. 1 µL dsRNA, 1 µL 10 µM Up-dN6 primer (5'-GCCGGAGCTCTGCAGAATTCNNNNNN-3'), 10 µL nuclease-free H_2O were mixed, incubated at 95 °C for 8-10 min, then immediately chilled on ice for at least 1 min and spun down by centrifugation. To this reaction, 4 µL 5x First-Strand Buffer, 2 µL 0.1 M dithiothreitol, 1 µL (40 U/µL) rRNAsin Ribonuclease Inhibitor and 1 µL SuperScript III Reverse Transcriptase (200 U/µL) were added. The reaction was incubated at 25 °C for 5-10 min, then 50 °C for 60 min, then inactivated by incubating at 98 °C for 2 min, followed by chilling on ice and a brief centrifugation step. 0.5 µL RNAse H (1.5 U/µL) was added and incubated at 37 °C for 30 min. 480 µL of nuclease-free water was then added to the reaction and purified and concentrated using an Amicon Ultra centrifugal filter (50 kDa molecular weight cutoff).

The eluate was mixed with an equal volume of 2x GoTaq Green Master Mix and incubated in a thermocycler with the following cycling conditions: 95 °C for 7 min, then 10

cycles of 95 °C for 1 min, 55 °C for 1 min and 72 °C for 1 min, followed by 72 °C for 7 min. 1 µL of the previous reaction, 2 µL 10 µM Up primer (5'-GCCGGAGCTCTGCAGAATTC-3'), 7 µL nuclease-free H_2O, 10 µL 2x GoTaq Green Master Mix were mixed and incubated in a thermocycler with the following cycling conditions: 95 °C for 7 min, then 35 cycles of 95 °C for 1 min, 55 °C for 1 min and 72 °C for 1 min, followed by 72 °C for 7 min. This reaction was then purified using an Amicon Ultra centrifugal filter (50 kDa molecular weight cutoff). Polymerase chain reaction (PCR) products which ranged from 300-1000 base pairs (bp) of length were then sequenced on the MiSeq platform for high-throughput sequencing. Sequencing data was then used to construct the genomes of viral sequences with the help of Galaxy version 19.05 and Geneious version 10.2.6.

Rapid Amplification of cDNA Ends (RACE)

Primers were designed based on the tentatively assembled viral genomes such that the terminal sequences can be generated by reverse transcription.

In a sterile microcentrifuge tube, 1 µL dsRNA, 1 µL 10 µM NeoTaVCV_N primer (5'-CTCGGGATTTCACCTGCCTT-3') or NeoTaVCV_C primer (5'-CATTGGAGGAAGGGCTGTCA-3') for 5'-RACE or 3'-RACE respectively, 10 µL nuclease-free H_2O were mixed, incubated at 95 °C for 8-10 min, then immediately chilled on ice for at least 1 min and spun down by centrifugation. To this reaction, 4 µL 5x First-Strand Buffer, 2 µL 0.1 M dithiothreitol, 1 µL (40 U/µL) rRNAsin Ribonuclease Inhibitor and 1 µL SuperScript III Reverse Transcriptase (200 U/µL) were added. The reaction was incubated at 50 °C for 60 min, then inactivated by incubating at 98 °C for 2 min, followed by chilling on ice and a brief centrifugation step, which was then purified by the QIAgen PCR Purification Kit.

The eluate was then used as a template for terminal deoxynucleotidyl transferase (TdT) tailing. 10 µL of the eluate containing cDNA, 5 µL 5x TdT buffer, 1.25 µL 100 µM dGTP (for 5'-RACE) or dATP (for 3'-RACE), 8.25 µL nuclease-free dH_2O and 0.5 µL TdT (15 U/µL) were mixed and incubated at 37 °C for 30 min, then inactivated by heating to 75 °C for 10 min. This reaction was also purified by the QIAgen PCR Purification Kit.

1 µL dGTP or dATP-tailed cDNA, 1 µL 10 µM Poly-dC_5_RACE primer for 5'-terminal dGTP-tailed cDNA (5'-TTACTAATATCCCCCCCCCCCC-3') or Poly-dT_3_RACE primer for 3'-terminal dATP-tailed cDNA (5'-GACCACGCGACGTGTCGAVTTTTTTTTTTTTTT-3') respectively, 7 µL nuclease-free dH_2O, 10 µL 2x GoTaq Green Master Mix was mixed, then incubated in a thermocycler at 95 °C for 5 min, then 52 °C (for 5'-terminus) or 37 °C (for 3'-terminus) for 2 min, then 72 °C for 40 min. 1 µL 10 µM terminal primer that was used for cDNA synthesis was then added to the reaction, then the reaction was incubated in a thermocycler for 30 cycles of 95 °C for 1 min, 60 °C for 1 min, 72 °C for 3 min with a final extension step of 72 °C for 15 min. Each reaction was diluted at a 1:100 ratio in nuclease-free dH_2O for a half-nested PCR. This half-nested PCR used another primer designed to anneal further down the terminal sequence.

1 µL dGTP or dATP-tailed cDNA, 1 µL 10 µM Poly-dC_5_RACE primer for 5'-terminal dGTP-tailed cDNA (5'-TTACTAATATCCCCCCCCCCCC-3') or Poly-dT_3_RACE primer for 3'-terminal dATP-tailed cDNA (5'-GACCACGCGACGTGTCGAVTTTTTTTTTTTTTT-3'), 1 µL 10 µM TaVCV_N primer (5'-GGGATRKTGATGTAYGACAT-3') or TaVCV_C primer (5'-TKCACGAYCTHCTGGA-3') for 5'-RACE or 3'-RACE respectively, 7 µL nuclease-free dH_2O, 10 µL 2x GoTaq Green Master Mix was mixed, then incubated in a thermocycler at 95 °C for 5 min, then 30 cycles of 95 °C for 1 min, 55 °C for 1 min, 72 °C for 3 min with a final

extension step of 72 °C for 15 min. This reaction was run on an agarose gel and a band corresponding to the expected size was cut from the gel, extracted by a centrifugation step through filter paper at maximum speed (21,130 g) for 2 min.

0.3 µL of pGEM T-Easy vector, 3.7 µL gel eluate, 5 µL 2x Rapid Ligation Buffer and 1 µL T4 DNA Ligase (3 U/µL) were mixed and incubated overnight at RT. The following day, a tube containing chemically competent *E. coli* DH5α cells was thawed on ice for 10 min, then 2-5 µL of the ligation reaction was added to the tube of cells, flicked gently 4-6 times and continued incubation on ice for 60 min. The tube was then added to a water bath at exactly 42 °C and incubated for 30-45 sec before immediately placing the tubes back on the ice for 2 min. 450 µL of Super Optimal Broth (SOB) was then added to the tube and incubated at 37 °C for 45 min with shaking (200-300 rpm). 250 µL was then plated on MacConkey Agar containing ampicillin antibiotics at a concentration of at least 100 µg/mL, then incubated overnight at 37 °C.

Bacteria colony PCR using T7 and SP6 primers was then performed for each white colony that grew on the agar, and colonies that amplified products at roughly the expected size were then grown in Luria-Bertani medium (LB) containing ampicillin at a concentration of at least 100 µg/mL overnight. The QIAgen Spin Miniprep Kit was used to purify the plasmid containing the insert of interest and the plasmid that was eluted from the kit was then sequenced.

Sequence Analysis and Phylogeny

MEGA-X (Kumar et al., 2018) was used for protein sequence alignment of L genes using the ClustalW algorithm. This alignment was then used for the generation of a phylogram with the neighbor-joining and maximum likelihood methods, which were each performed with 1,000 bootstrap replicates. To analyze the potential nuclear localization signals (NLSs) and nuclear

export signals (NESs), cNLS Mapper (cutoff score = 3) (Kosugi et al., 2009) and NetNES 1.1 (la Cour et al., 2004) were used for each of the putative protein sequences, respectively.

Primer name	Primer sequence (5'-3')
DCGF3	GTCTGGTAAAGAGGGGTTGA
DCGR3	GTCGAGGGTCATGATAGAGT
DCGF5	AGGGGYTGAGRCAAAAGGGGT
DCGR5	CGCTCYTTCATACATGCSGCCTT
Up-dN6	GCCGGAGCTCTGCAGAATTCNNNNNN
Up	GCCGGAGCTCTGCAGAATTC
Poly-dC_5_RACE	TTACTAATATCCCCCCCCCCCC
Poly-dT_3_RACE	GACCACGCGACGTGTCGAVTTTTTTTTTTTTTT
NeoTaVCV_N	CTCGGGATTTCACCTGCCTT
NeoTaVCV_C	CATTGGAGGAAGGGCTGTCA
TaVCV_N	GGGATRKTGATGTAYGACAT
TaVCV_C	TKCACGAYCTHCTGGA

Table 1. List of primers used in this study. NeoTaVCV_N and NeoTaVCV_C are both primers used for the reverse transcription reaction and the first round of PCRs for their respective terminal RACE procedure. TaVCV_N and TaVCV_C are both primers used for the half-nested PCRs following the first round of PCRs to improve specificity that may have been an issue if only one set of primers was used.

Results and Discussion

The spread of a destructive plant virus is a major concern for crop cultivation. As TaVCV is regarded as a taro pathogen with a dire impact on the production of taro by reducing plant yield as a result of infection, its regional prevalence across the Pacific is a concern for taro cultivation internationally. Though TaVCV was officially acknowledged as a unique virus separate from CBDaV due to electron microscopy in 1999 (Pearson et al.), the existence of several unique *Nucleorhabdovirus* species poses the possibility of the virus infecting taro many years before its initial report, though it is unclear as to how long TaVCV has been infecting taro. Due to its relative isolation in different Pacific Island Countries, the virus has been able to propagate and evolve independently of other isolates. As a result, high nucleotide sequence diversity among several different isolates of TaVCV has emerged, though this diversity is too low to be considered a separate species from the common ancestor of the virus. Nonetheless, with better tools readily available for the analysis of these isolates, more information regarding the viral sequences as well as putative protein products can be gleaned based on considerations of functions that were established in other related species of the *Nucleorhabdovirus* genus. Thus, sampling alternate isolates from different Pacific Island Countries both contributes to the current breadth of knowledge regarding both *Nucleorhabdovirus* species and TaVCV, and provides more genomic data of TaVCV, supporting the initial observation of high nucleotide diversity by Revill et al. (2005a).

All samples except those from Fiji were positive for TaVCV in RT-PCR. Any mention of the Fijian isolate in this chapter is based on the GenBank accession number NC_006942.1, the submission of the *Taro vein chlorosis nucleorhabdovirus* genome from Revill et al. (2005a). The number of reads obtained from high-throughput sequencing and the number of TaVCV-specific

reads are listed together with their respective isolate in Table 2. The complete sequence of the Hawaiian TaVCV isolate is 12,037 bp in length with a G/C content of 47.1%, the Samoan TaVCV isolate is 12,086 bp in length with a G/C content of 47.7%, the Palauan TaVCV isolate is 12,072 bp in length with a G/C content of 46.8%. All isolates (including from Fiji, Guam, and Vanuatu) contained six major open reading frames (ORFs) on the same strand. Each of the ORFs correspond to the respective protein that is encoded, including the putative proteins for a nucleorhabdovirus: nucleocapsid protein (N), phosphoprotein (P), gene 3, matrix protein (M), glycoprotein (G) and RNA-dependent RNA polymerase (L). The lengths of the putative amino acid products from the six major ORFs are organized together with their respective isolate (Table 3). The amino acid lengths of gene 3 and G in all isolates are the same, with other genes having some level of variability in this aspect. Hawaii and Guam isolates have longer putative N and M products with a product size of 487 amino acids and 249 amino acids, respectively, compared to the Palau, Samoa, and Vanuatu isolates. The M product is also shorter in the Fiji isolate. Only the Palau isolate exhibited a different length for P at 259 amino acids while other isolates had a length of 271 amino acids. The N protein varied widely between the isolates, especially for Fiji with a length of 502 amino acids.

A putative polyadenylation site (3'-AAUUCUUUUUGGG-5' in virion-sense orientation) is observed in all isolates in the 3'-leader sequence and downstream of each putative ORF. For each polyadenylation site except for the one downstream of the L gene, at least an additional two uracils follow immediately after the guanines in the site. This site is conserved in all isolates, having no nucleotide variability.

A table was compiled for all protein sequences for the results of the cNLS Mapper and NetNES 1.1, together with the scores of all predicted NLSs (Table 4). NLSs were predicted for

all putative protein products in TaVCV for all isolates, and for most isolates, the scores for all predicted NLSs ranged between 3-5. A notable exception is the Fiji isolate, where a monopartite NLS was predicted with a score of 9 for the N protein. The Hawaii, Guam, and Palau isolates had a putative N protein with a predicted monopartite NLS with a score of 4. This monopartite NLS was not predicted for the Samoa and Vanuatu isolates, though there were still predicted bipartite NLSs. A score of 3-5 corresponds to a distribution of the protein between the nucleus and cytoplasm, while a score of 8-10 corresponds to an exclusive localization of the protein in the nucleus. The monopartite NLS in particular corresponds to the RGTKRPNPAAT sequence in Hawaii, Guam, and Palau isolates, whereas this corresponds to the RGTKRPNPAVF sequence in Fiji. NESs were predicted for all proteins except for the phosphoprotein (P), which was a consistent property in all isolates.

At the gene junction, the 3'-leader site, and the 5'-trailer site, there is a short 13-16 nucleotide sequence 3'-AAUUCUUUUUGGG(UUG)-5' which follows after each ORF (with the exception of the 3'-leader site, which lacks any ORF to precede it). This site downstream of the L gene in all isolates contains the 13 nucleotide sequence 3'-AAUUCUUUUUGGG-5' though the other nucleotide sequences following other genes are at least 15 nucleotides, with 3'-AAUUCUUUUUGGGUU-5'. This sequence is well-conserved between all isolates of TaVCV. This site is important for viral mRNA, as the poly-U region of the sequence contributes to polymerase stuttering, which is a random event that causes RdRp, together with its nascent (positive-sense) RNA, to move back one nucleotide and either continue or release the RNA. Presumably, the polymerase stuttering process may repeat several times, creating long poly(A) tails on the nascent mRNA despite a short run of uracil nucleotides on the virion-sense strand. This feature of polyadenylation was observed by Hunt et al. (1984) in a mutant of *Indiana*

vesiculovirus, which is a member of the genus *Vesiculovirus* in the family *Rhabdoviridae*. As this site is conserved in all isolates despite the high nucleotide diversity, it is clear that this particular sequence is crucial for the virus and expression of viral proteins. Another conserved genetic feature in all TaVCV isolates is the 3'-UGUU-5' in the 3'-leader sequence, characteristic of all rhabdoviruses.

Most of the proteins in the isolates have a similar length, but, notably, there is an extra segment in the Hawaii and Guam isolates at the N-terminal region of the nucleoprotein. In these isolates, the additional fragment is 34 amino acids in length but is not conserved across the other isolates, implying that this fragment of the nucleoprotein is not critical to its functionality. Interestingly, the aforementioned polymerase stuttering site (3'-AAUUCUUUUUGGGUUG-5') was present within the part of the coding sequence that codes for this particular 34 amino acid fragment.

Considering the lengths of the ORF products, it is clear that the nucleoprotein is the most varied, with Palau, Samoa, and Vanuatu isolates sharing a length of 453 aa, while Hawaii and Guam isolates share a length of 487 aa, which is the length of the 453 aa in the aforementioned isolates with the 34 aa fragment discussed previously. Fiji stands out from these isolates with a length of 502 aa. Comparing the amino acid sequence of the Fijian nucleoprotein to the other isolates examined in this study, the sequence diverges completely starting at Val-411. In Revill et al. (2005a), the amino acid sequence of the nucleoprotein contained three groups of basic amino acids resembling the nuclear localization signal of other nucleoproteins belonging to different rhabdoviruses. These groups are ^{402}RGTKR^{406}, ^{421}HPTKKRTWK^{429}, and ^{462}RGKHHR^{467}. The latter two groups are not seen in Hawaii, Guam, Samoa, Palau, or Vanuatu isolates, though the RGTKR motif is present and conserved in all examined isolates. This implies that there is a key

role of the RGTKR motif as the nuclear localization signal for the nucleoprotein, though it appears that the other motifs are not as necessary for viral replication in the nucleus. The cNLS Mapper results for the nucleoprotein were mostly consistent with this observation, though it failed to predict a NLS containing the RGTKR motif in Samoa and Vanuatu isolates. The monopartite NLS predicted for Hawaii, Guam, Palau, and Fiji all contained the RGTKR motif, but the score for the Fiji isolate was drastically different for Fiji, which scored 9 as opposed to 4 in the other isolates. As a score of 9 indicates that the protein of interest would be exclusively localized to the nucleus, this would be consistent with the electron microscopy data by Revill et al. (2005a) in which the virus was observed to be distributed exclusively in the nucleus. For the other isolates, this exclusivity may not necessarily be observed, as a score of 4 indicates a distribution between the nucleus and cytoplasm. This implies that this distribution could be observed in other TaVCV isolates but an electron microscopy experiment was not performed with these isolates. Despite having a score of 4, these predictions may still be consistent with the trend of *Nucleorhabdovirus* genus members having the unique ability to replicate and assemble in the nucleus, as other viruses that replicate and assemble in the cytoplasm typically lack these signals and do not depend on them for their functions. With the current sequence data, the important part of the nucleoprotein sequence is the domain spanning amino acids 1-410 in the Fijian isolate and the corresponding domain in the other TaVCV isolates. Notably, if a nucleotide was added to the part of the gene coding for the nucleoprotein in the Fijian genome, the length of the resulting protein product is 453 aa, comparable to the other isolates. The rest of the sequence becomes more similar to the sequences of the other isolates established in this study, raising the possibility that the Fijian genome may be missing a nucleotide due to a potential sequencing error.

There is a higher degree of sequence conservation with regard to the other five main functional proteins, especially with genes 3 and the ORF coding for glycoprotein (G), which have a uniform amino acid sequence length across all studied isolates, which implies that the domain that is necessary for the function of these proteins is within the full length of each respective protein (1-287 for gene 3, 1-588 for G). For P, the only isolate with a shorter length is the Palau isolate with a length of 259 aa, due to a frameshift which causes the sequence to diverge starting at the 217th aa. Thus, the functional domain of P is contained within amino acids 1-216. There is a hydrophilic pocket noted in residues 108-200 of the Fijian isolate and this domain is mostly conserved between isolates. Notably, the frameshift in the P gene of the Palau isolate could be due to a sequencing error, as adding an A where the frameshift occurs results in a protein sequence very similar to the other isolates.

P is the only major protein in the genome which does not have a predicted NES. Curiously, cNLS Mapper did not predict a monopartite NLS with a high score in the P protein of TaVCV. In MMV, there is a predicted monopartite NLS with a score of 10 which corresponds to the motif ^{154}PSIKRKAEAM^{163}, while in the more closely related putative nucleorhabdovirus Morogoro maize-associated virus (MMaV), there is a predicted monopartite NLS with a score of 9 which corresponds to the motif ^{169}PNPKRKKEAM^{178} (Read et al., 2019). The corresponding amino acid sequence in TaVCV is ^{157}PDSAKRQEAL^{166} (Hawaii; for Guam and Palau, 159-T replaces 159-S), ^{157}PDATKKQEAL^{166} (Samoa and Vanuatu), or ^{157}PDQAKKQEAL^{166} (Fiji). A typical marker of NLSs is the presence of lysine and arginine residues; this fragment in TaVCV has less of these residues compared to the corresponding motifs in MMV and MMaV. As P is a co-factor of RdRp, a high scoring predicted monopartite NLS would support solely nuclear replication with this genus, but TaVCV seems to have an exception with its deviated motif.

The 3 protein seems to be relatively well-conserved, as all isolates have the same length of the putative protein product, despite a lack of definitive evidence concerning the function of this protein. It is believed to be a putative movement protein in other *Nucleorhabdovirus* genus members (Huang et al., 2005; Min et al., 2010), but when this virus was first characterized, there was a low protein sequence identity to the analogous protein product in MMV. There are both predicted bipartite NLS (scoring in the range of 3-5 across different isolates) and predicted NES. The sequence of the predicted NES is the conserved motif ^{55}LQFTSLTI^{62} found in all isolates, visualized in Fig. 2.2. While the NetNES score is lower for the Fiji isolate, some residues still surpass the threshold score for a prediction.

The Hawaii and Guam isolates have an additional 14 amino acid fragment at the N-terminus of M, similar to the nucleoprotein in those isolates. This fragment is absent in the other isolates, and thus the functional domain of M is contained in amino acids 1-235 in the Fiji, Palau, Samoa, and Vanuatu isolates and the analogous domain in the Hawaii and Guam isolates. Similar to other M gene products in other rhabdoviruses that infect plants and animals, there is a ^{69}HHIIRNK^{75} cluster of basic residues upstream of a YXG motif shared by the Fiji, Samoa, and Vanuatu isolates. This is mostly conserved in the Hawaii, Guam, and Palau isolates but instead contains the cluster ^{69}HHIVRSK^{75} upstream. Isoleucine and valine are both amino acids with nonpolar side chains, and, notably, the codons that code for isoleucine (ATT, ATC, ATA) can be mutated into the codons that code for valine (GTT, GTC, GTA) and vice-versa by an A/G missense mutation. Asparagine and serine are both amino acids with polar side chains, and like isoleucine and valine contain similar codons that can interchange the amino acid with an A/G nonsense mutation (AGT or AGC for serine and AAT or AAC for asparagine). Notably, the amide functional group in the side chain of asparagine is a more polar functional group than the

alcohol functional group of serine. These modifications presumably have an overall minor effect on the protein.

The glycoprotein (G) was a consistent length in all isolates and all shared the six conserved glycosylation signals (N-X-S/T). Interestingly, before residue 35, some of the amino acids showed relatively little similarity; many of the amino acid differences between sequences are attributable to a hypervariable segment of the coding region. This might imply that some of the residues in this fragment may not contribute as much to the functionality of the glycoprotein; this segment is also void of any glycosylation signals. Interestingly, Revill et al. (2005a) noted that the 70 kDa virion-associated polypeptide has an N-terminal sequence of VVDLNRN. This N-terminal sequence is associated with a protein that starts at residue 25 of the Fijian isolate, lending credence to the earlier assertion that the early protein fragment is not as critical to the overall function of the glycoprotein. Some of the first few amino acids in the fragment are leucine and other hydrophobic residues (such as valine and isoleucine), associated with an NES. When all G protein sequences were analyzed with NetNES, many of the residues in the first 12-17 amino acids had high NES scores, corresponding to predicted NESs (Fig. 2.3). Therefore, it could be speculated that the protein is first expressed fully, which allows the glycoprotein in the assembled virus to be exported out of the nucleus, after which the fragment containing the nuclear export signal is later removed from the glycoprotein.

A conserved domain search of each protein reveals only a few results: pfam17055, or viral matrix protein M2 domain (the hit spans the entirety of the matrix protein M with the exception of the 14 amino acid fragment in the Hawaii and Guam isolates); pfam00946, or Mononegavirales RNA-dependent RNA polymerase domain (the search hit spans residues 143-1075 in Hawaii, Guam, Palau, and Fiji, but 41-1075 in Samoa and Vanuatu); and TIGR04198, or

paramyxovirus family mRNA capping enzyme or mRNA (guanine-7-)methyltransferase domain (the search hit spans residues 1176-1922 in Hawaii, Guam, and Palau, and 1176-1924 in Fiji, Samoa, and Vanuatu). The family *Paramyxoviridae* is a family which belongs to the order *Mononegavirales*, the same order that the family *Rhabdoviridae* is classified under ("ICTV", 2019). While the functional domain of each protein is implied with the differences between the isolates, especially in the case of the nucleoprotein as discussed earlier, information regarding protein domains relevant to the genus *Nucleorhabdovirus* is lacking except for the earlier conserved domain search results.

From a comparison of the complete predicted protein and nucleotide sequences of the L gene, minimum nucleotide identity of 78% is observed from the genomic sequences of TaVCV, though the protein identity is higher, by comparison, having high degrees of identity by at least 90% (Table 5). A similar observation is found when comparing the full genome as nucleotide sequences and the whole viral proteome as protein sequences, though the minimum protein identity decreases very slightly to 89% (Table 6). A significant portion of the nucleotide diversity between the isolates is thus due to silent mutations, which do not change the resulting amino acid, and the rest of the mutations are missense mutations, changing the coded amino acid to a different one. This can have varied effects on a protein, as changing an amino acid to a similar one might not affect the function of the protein as much as a change to a dissimilar amino acid. A missense mutation can occur such that a critical function of a viral protein is impaired, though viruses impaired in this way have decreased fitness.

Phylograms generated using the L genes (Fig. 2.4a, b) of all the isolates together with MMaV and all other officially recognized nucleorhabdoviruses grouped Hawaii and Guam isolates together, as was the case with Samoa and Vanuatu isolates. The inclusion of the Palau

isolate into a clade together with Hawaii and Guam had high bootstrap support (100%). The Fiji isolate grouped with the Samoa and Vanuatu isolates in a clade when the maximum likelihood method was used, but it grouped with Hawaii, Guam, and Palau in a clade when the neighbor-joining method was used. A low bootstrap support (60% for maximum likelihood and 63% for neighbor-joining) was observed for the Fiji isolate. Samoa and Vanuatu isolates grouped separately from the other isolates in the maximum likelihood phylogram. TaVCV isolates grouped together in a clade separate from the other members of the *Nucleorhabdovirus* genus. Additionally, the putative nucleorhabdovirus MMaV grouped together with the TaVCV isolates one node further with a relatively high bootstrap support (76% for maximum likelihood, 100% for neighbor-joining). Phylograms generated by the whole viral proteomes (Fig. 2.5a, b) showed a slightly different result, as Fiji grouped together in a clade with Hawaii, Guam, and Palau in both maximum likelihood and neighbor-joining methods with a relatively low bootstrap support (62% for maximum likelihood and 78% for neighbor-joining). Notably, small terminal branch length was observed for all isolates of TaVCV compared to the terminal branch length observed for the other nucleorhabdoviruses, supporting their close relationship as TaVCV isolates. The longest terminal branch among TaVCV isolates belonged to the Fiji isolate, though the total branch length from the TaVCV ancestral node was similar when the neighbor-joining method was used for both the L gene and the whole viral proteome.

A high protein identity was noted for Hawaii and Guam isolates with 99% identity, and the Samoa and Vanuatu isolates were very close to having 100% identity, with a difference of only three amino acids in the L gene and only eight amino acids in the whole viral proteome. This would imply that the movement of TaVCV between Hawaii and Guam was a recent occurrence, with the same applying to the movement of TaVCV between Samoa and Vanuatu.

This is further supported by the branches observed in the phylogenetic trees. This is also the first known observation of TaVCV prevalence in Guam, which has not been reported to date.

The Palau isolate was observed to be more distantly related with an 88% nucleotide identity compared to the Hawaii and Guam isolates, but a high protein identity of 97% was still observed when comparing the Palau isolate to Hawaii and Guam isolates each. As discussed previously, a high nucleotide diversity may not correspond with high protein diversity. This would indicate that a common ancestor to Palau, Hawaii, and Guam TaVCV isolates was first spread to one of the three locations, then later distributed to the other two locations, with Hawaii and Guam isolates having a closer period of incidence. Interestingly, a taro cross-breeding project was conducted by Trujillo et al. in 2002 in response to the TLB epidemic devastating taro crops; the "Ngeruuch" variety from Palau was crossed with "Maui Lehua" to yield a hybrid that had preferable agronomic characteristics in addition to the TLB resistance from the "Ngeruuch" variant. The spread of TaVCV could have happened between Palau and Hawaii in this way, as TaVCV was not seen in Hawaii taro until a first report detailed its presence in 2013 (Long et al., 2014) and import of taro from elsewhere to Hawaii is usually restricted.

In a similar fashion, Fiji, Samoa, Tonga, and Vanuatu all participate in taro exports (Sami, 2011). A nearly identical genome of TaVCV found in Samoa and Vanuatu samples would suggest a very recent infection of taro from one country to the other. As TaVCV symptoms do not emerge until taro is mature and are difficult to spot when the virus does not cause severe symptoms, the virus could have been infecting taro that appeared healthy before its movement between countries. The nearly identical genomes suggest recent movement, as both countries have been documented to have some prevalence of TaVCV years prior to this study. Currently, having only one genome sequenced for each location limits our knowledge of the movement

paths of TaVCV and if other genomes were found, that could completely alter the conclusion of the movement of TaVCV across the Pacific.

Isolate	Number of Total Reads	TaVCV-Specific Reads
Hawaii	3625424	1573238
Samoa	3556006	241630
Guam	12090920	27098
Palau	6349336	31994
Vanuatu	10410134	415500

Table 2. Table for the number of reads obtained for each TaVCV-positive isolate and number of TaVCV-specific reads from each set of data.

	Length (aa)					
Isolate	N	P	3	M	G	L
Hawaii	487	271	287	249	588	1926
Guam	487	271	287	249	588	1926
Palau	453	259	287	235	588	1926
Samoa	453	271	287	235	588	1928
Vanuatu	453	271	287	235	588	1928
Fiji	502	271	287	235	588	1928

Table 3. A table detailing the amino acid length of the six major ORFs in TaVCV (N, P, 3, M, G, L). The Fijian isolate of TaVCV used in this chart is based on GenBank accession number NC_006942.1.

		NLS (cNLS Mapper)		NES (NetNES 1.1)
Protein	Length (aa)	Predicted	Score	Predicted
N	453-502	Yes	4^{M} (H/G/P) or 9^{M} (F), 3.1-4.3^{B}	Yes
P	259-271	Yes	3-3.3^{B}	No
3	287	Yes	3-5^{B}	Yes
M	235-249	Yes	3-4.8^{B}	Yes
G	588	Yes	3-3.7^{B}	Yes
L	1926-1928	Yes	3-5^{M} (all except F), 3-4.5^{B}	Yes

Table 4. A table depicting each putative protein paired with their range of predicted amino acid lengths, NLSs and NESs using cNLS Mapper and NetNES 1.1, respectively. All ORFs in all putative protein products of all isolates have a predicted NLS. A monopartite NLS is predicted in all putative N except for Samoa and Vanuatu, and in all putative L except for Fiji. Additionally, all isolates contain ORFs that code for proteins with a predicted NES except for the phosphoprotein (P). If isolate(s) is/are not specified for the score, assume that this value applies to all isolates. H = Hawaii, G = Guam, P = Palau, F = Fiji. ^{M}Monopartite NLS. ^{B}Bipartite NLS.

Protein Identity

Nucleotide Identity	Fiji	Guam	Hawaii	Palau	Samoa	Vanuatu
Fiji		91%	91%	91%	91%	91%
Guam	80%		99%	96%	90%	90%
Hawaii	80%	97%		97%	90%	90%
Palau	80%	88%	88%		90%	90%
Samoa	78%	78%	79%	79%		100%
Vanuatu	78%	78%	79%	79%	99%	

Table 5. Comparison table of the isolates studied here, including the Fijian isolate (GenBank accession number NC_006942.1). This table was compiled by a comparison of the RdRp gene as both protein and nucleotide sequences. Values in the table are rounded to the nearest whole number. Minimum nucleotide identity of 78% can be observed when comparing isolates, but protein identity between all isolates of TaVCV is high with at least 90% identity.

Protein Identity

Nucleotide Identity	Fiji	Guam	Hawaii	Palau	Samoa	Vanuatu
Fiji		89%	89%	89%	89%	89%
Guam	80%		99%	96%	90%	89%
Hawaii	80%	97%		96%	90%	90%
Palau	80%	89%	89%		89%	89%
Samoa	78%	78%	79%	78%		100%
Vanuatu	78%	78%	79%	78%	100%	

Table 6. Comparison table of the isolates studied here, including the Fijian isolate (GenBank accession number NC_006942.1). This table was compiled by a comparison of the whole viral proteome as compiled protein sequences, as well as the whole genomes of the isolates as nucleotide sequences. Values in the table are rounded to the nearest whole number. Minimum nucleotide identity of 78% can be observed when comparing isolates, but protein identity between all isolates of TaVCV is high with at least 89% identity.

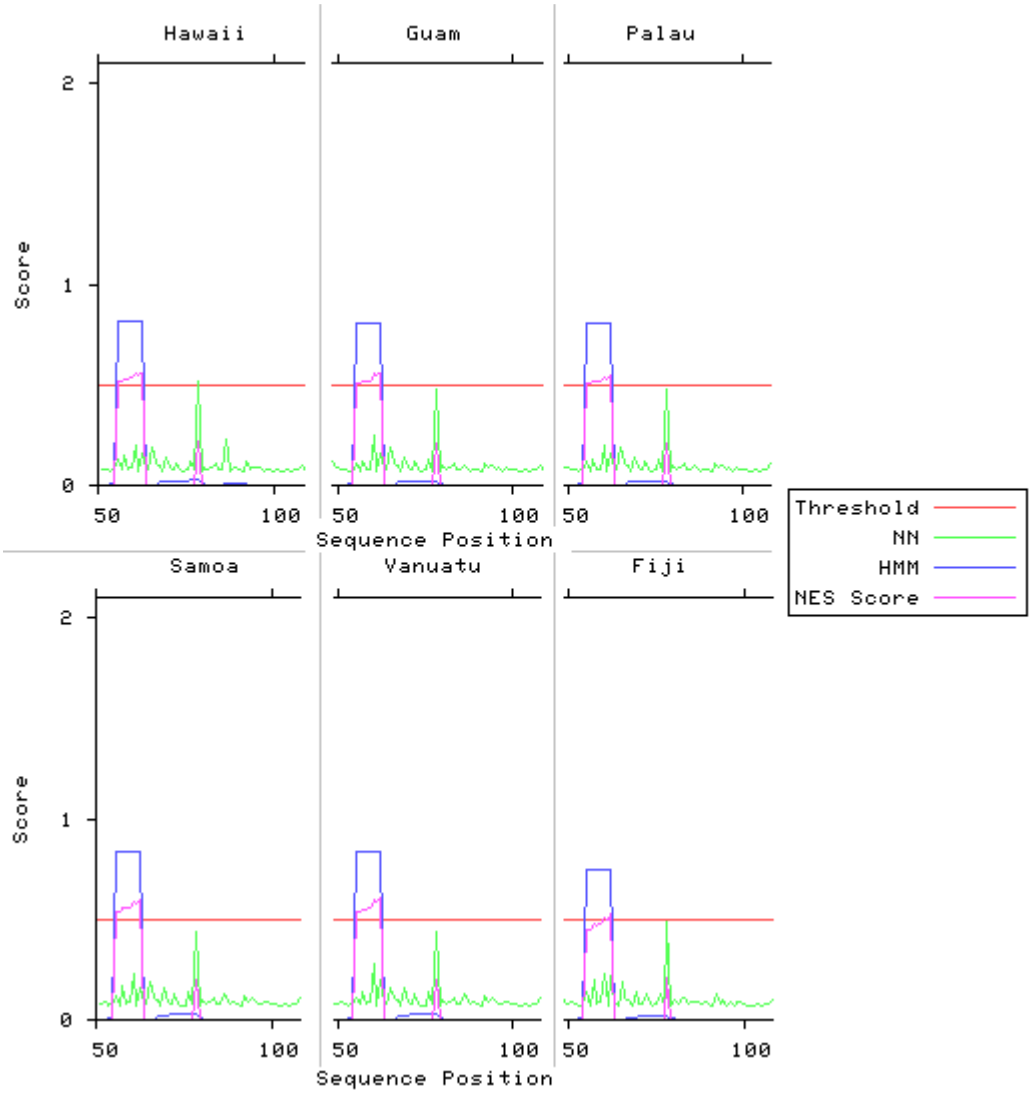

Fig. 2.2. Partial graphic of NetNES 1.1 results for gene 3 sequences in all isolates studied, together with the Fiji isolate. The NES score exhibited for each amino acid is calculated based on a post-processing algorithm which takes into account both the neural network (NN) and hidden Markov model (HMM) scoring; if this score exceeds 0.5 for a particular residue, NetNES marks the amino acid as a predicted NES. All isolates exhibit a predicted (leucine-rich) nuclear export sequence (NES) in the motif ^{55}LQFTSLTI^{62}.

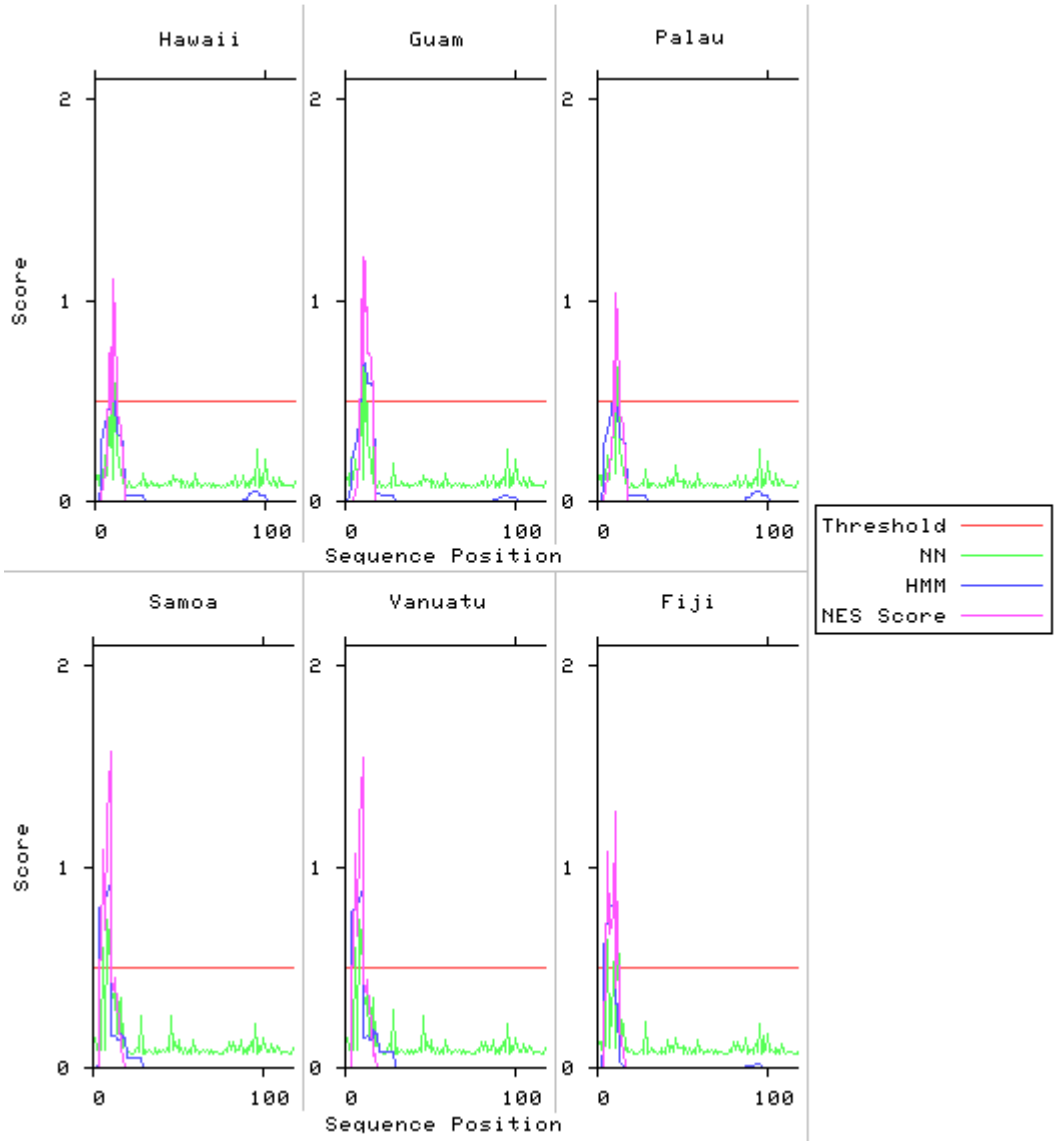

Fig. 2.3. Partial graphic of NetNES 1.1 results for glycoprotein (G) sequences in all isolates studied, together with the Fiji isolate. The NES score exhibited for each amino acid is calculated

based on a post-processing algorithm which takes into account both the neural network (NN) and hidden Markov model (HMM) scoring; if this score exceeds 0.5 for a particular residue, NetNES marks the amino acid as a predicted NES. All isolates exhibit a predicted (leucine-rich) nuclear export sequence (NES) in the first few amino acids of the protein sequence.

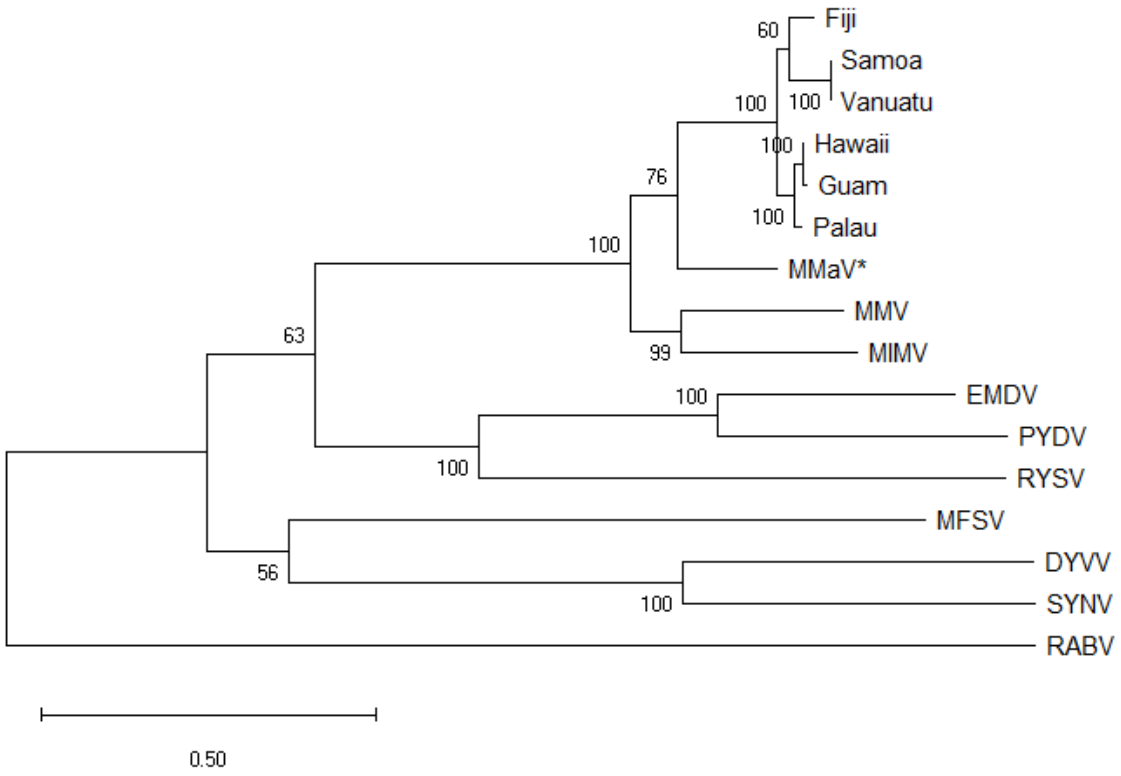

Fig. 2.4a. Phylogenetic tree generated using the maximum likelihood method for the L genes (as amino acid sequences) of the TaVCV isolates and other members of the genus *Nucleorhabdovirus*. Morogoro maize-associated virus (MMaV, GenBank accession number MK063878.2) is a putative nucleorhabdovirus that is the most closely related viral species to TaVCV, but is not yet formally recognized by the ICTV. 1,000 bootstraps were performed. *Rabies lyssavirus* (RABV) is used as the outgroup.

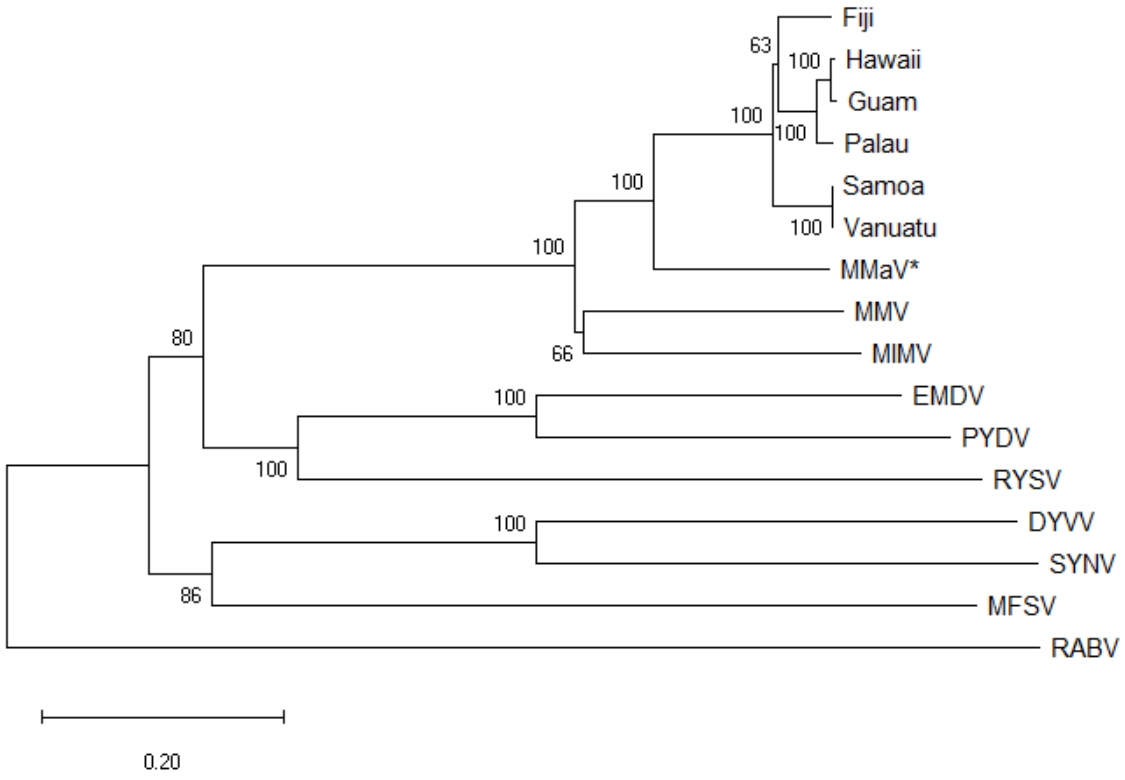

Fig. 2.4b. Phylogenetic tree generated using the neighbor-joining method for the L genes (as amino acid sequences) of the TaVCV isolates and other members of the genus *Nucleorhabdovirus*. Morogoro maize-associated virus (MMaV, GenBank accession number MK063878.2) is a putative nucleorhabdovirus that is the most closely related viral species to TaVCV, but is not yet formally recognized by the ICTV. 1,000 bootstraps were performed. *Rabies lyssavirus* (RABV) is used as the outgroup.

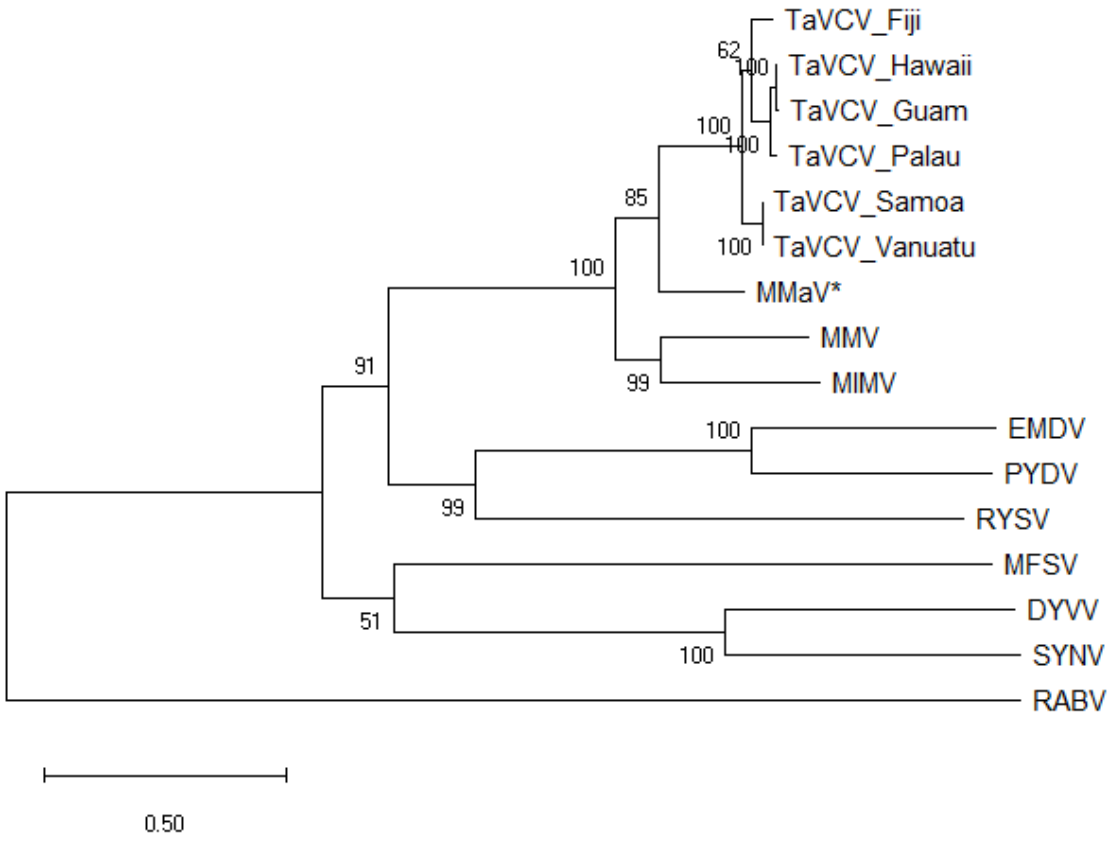

Fig. 2.5a. Phylogenetic tree generated using the maximum likelihood method for the whole viral proteome (as compiled amino acid sequences) of the TaVCV isolates and other members of the genus *Nucleorhabdovirus*. Morogoro maize-associated virus (MMaV, GenBank accession number MK063878.2) is a putative nucleorhabdovirus that is the most closely related viral species to TaVCV, but is not yet formally recognized by the ICTV. 1,000 bootstraps were performed. *Rabies lyssavirus* (RABV) is used as the outgroup.

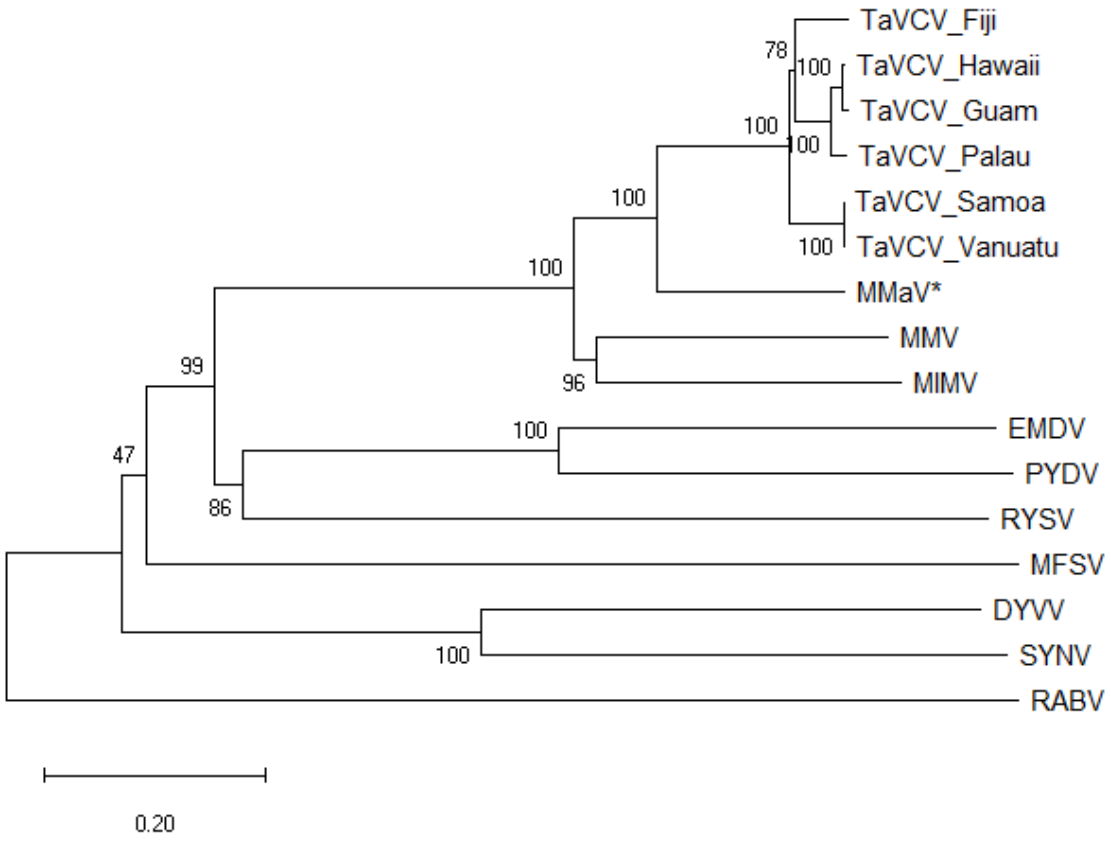

Fig. 2.5b. Phylogenetic tree generated using the neighbor-joining method for the whole viral proteome (as compiled amino acid sequences) of the TaVCV isolates and other members of the genus *Nucleorhabdovirus*. Morogoro maize-associated virus (MMaV, GenBank accession number MK063878.2) is a putative nucleorhabdovirus that is the most closely related viral species to TaVCV, but is not yet formally recognized by the ICTV. 1,000 bootstraps were performed. *Rabies lyssavirus* (RABV) is used as the outgroup.

CHAPTER 3: DISCOVERY AND MOLECULAR CHARACTERIZATION OF A PUTATIVE TARO TOTIVIRUS

Introduction

Totivirus is a genus of the family *Totiviridae*, which contains members characterized by icosahedral virions which are roughly 40 nm in diameter containing a double-stranded (ds)RNA genome that encodes at least two proteins on the positive-sense strand, a capsid or coat protein (CP) and RNA-dependent RNA polymerase (RdRp). A putative slippery site located toward the end but before the stop codon of the gene coding for the CP is the location of a rarely occurring -1 ribosomal frameshift which causes the expression of a CP+RdRp fusion protein (Brierley et al., 1992; Brierley, 1995). There are seven recognized members of the genus *Totivirus*, although other putative totiviruses have also been reported. Typically, members of the genus *Totivirus* have been known to infect fungi, though there have also been findings in which putative totiviruses or totivirus-like viruses have infected hosts other than fungi.

Some totiviruses or totivirus-like viruses were isolated from plants, which include Papaya meleira virus from papaya (Abreu et al., 2015), Black raspberry virus F from black raspberry (GenBank accession number NC_009890), Ribes virus F from gooseberry (GenBank accession number ACA61232), and an unnamed dsRNA species from black currant (Cox et al., 2000). Additionally, a recent publication by Guo et al. in 2016 features such a putative totivirus, tentatively named the Panax notoginseng virus A, with a complete genome submitted to GenBank. Plant-infecting putative totiviruses have yet to be recognized by the ICTV, but the lack of publications associated with some of these submissions challenges the recognition process. Any proposal for the recognition of new viruses requires satisfying the relevant viral family's demarcation criteria and must also be accompanied by a publication for those viruses.

Although Black raspberry virus F was in consideration for being recognized as a member of the family *Totiviridae* as it had sufficiently met the demarcation criteria with approximately 50% protein sequence identity to other currently recognized totiviruses, there were no publications available and thus its recognition could not be finalized. Despite the current circumstances regarding the recognition of plant-infecting totiviruses and totivirus-like viruses, the current publication for Panax notoginseng virus A demonstrates the potential of finding more of these viruses.

Here, we report the identification and characterization of a novel virus associated with taro discovered via high-throughput sequencing of a sample acquired from Samoa, which most likely represents a novel species of totivirus belonging to the genus *Totivirus*.

Materials and Methods

Double-Stranded (ds)RNA Extraction (Large-Scale)

The following method is based on the plant viral double-stranded RNA (dsRNA) protocol by Morris and Dodds (1979), Bar-Joseph et al. (1983) and Dodds et al. (1984). About 5 g of symptomatic leaf tissue from Hawaii or Samoa was ground into a powder in liquid nitrogen using a mortar and pestle, which was pre-cooled overnight in a -20 °C freezer. The powdered leaf tissue was then added to 200 mL of dsRNA extraction buffer (10X STE 18 mL, 10% SDS 30 mL, β-Mercaptoethanol 2 mL, dH_2O 72 mL, saturated phenol 40 mL, chloroform 40 mL; 10X STE = Tris-HCl 61.0 g, NaCl 58.0 g, EDTA 3.7 g, dH_2O to 1000 mL, pH 8.0), then stirred with a magnetic stir bar for 45-60 minutes at 4 °C. The solution was then transferred to a 250 mL bottle and centrifuged at 8,000 rpm for 10 minutes. The aqueous phase was transferred to a new bottle, then 0.2 volumes (with respect to the aqueous phase volume) of EtOH was added. 2 g of CF-11

cellulose powder was added to the solution, which was then gently shaken on an orbital shaker for 30 minutes at room temperature (RT). This solution with cellulose powder was added to a column and the liquid was allowed to flow through, then the column was washed with at least 100 mL of 1X STE containing 16.5% (v/v) EtOH. The liquid was then purged from the cellulose and the dsRNA was then eluted into a 50 mL centrifuge tube with three 10 mL aliquots of 1X STE, each of which was purged after each elution. 6 mL EtOH (0.2 volumes with respect to elution volume), then 1.5 g of CF-11 cellulose powder was added to the eluate and gently shaken on an orbital shaker overnight at RT. The solution with powder was then added to a column, the liquid was allowed to flow through and the column was then washed with at least 100 mL of 1X STE containing 16.5% (v/v) EtOH. The liquid was then purged from the cellulose, and the dsRNA was then eluted into a 15 mL centrifuge tube with three aliquots of 3 mL 1X STE, each of which was purged after each elution. The tubes were then spun in a centrifuge for 1 minute to pellet the cellulose, and the supernatant was then transferred to a 30 mL Corex centrifuge tube. 0.9 mL of 3 M sodium acetate (pH 5.2) was then added to the transferred solution, and the tube was filled as close to the top as possible with 95% EtOH (about 20 mL). The tube was sealed with Parafilm, inverted to mix the solution well and incubated overnight at -20 °C.

The next day, the tubes were centrifuged at 12,000 rpm for 30 minutes. The supernatant was then decanted, and the pellet was then resuspended in 500 µL of molecular-grade (nuclease-free) water. The dsRNA solution was then concentrated using an Amicon Ultra centrifugal filter (50 kDa molecular weight cutoff).

Preparation of cDNA Library for Next-Generation Sequencing

The dsRNA eluate was used as a template for reverse transcription. 1 µL dsRNA, 1 µL 10 µM Up-dN6 primer (5'-GCCGGAGCTCTGCAGAATTCNNNNNN-3'), 10 µL nuclease-free H_2O were mixed, incubated at 95 °C for 8-10 min, then immediately chilled on ice for at least 1 min and spun down by centrifugation. To this reaction, 4 µL 5x First-Strand Buffer, 2 µL 0.1 M dithiothreitol, 1 µL (40 U/µL) rRNAsin Ribonuclease Inhibitor and 1 µL SuperScript III Reverse Transcriptase (200 U/µL) were added. The reaction was incubated at 25 °C for 5-10 min, then 50 °C for 60 min, then inactivated by incubating at 98 °C for 2 min, followed by chilling on ice and a brief centrifugation step. 0.5 µL RNAse H (1.5 U/µL) was added and incubated at 37 °C for 30 min. 480 µL of nuclease-free water was then added to the reaction and purified and concentrated using an Amicon Ultra centrifugal filter (50 kDa molecular weight cutoff).

The eluate was mixed with an equal volume of 2x GoTaq Green Master Mix and incubated in a thermocycler with the following cycling conditions: 95 °C for 7 min, then 10 cycles of 95 °C for 1 min, 55 °C for 1 min and 72 °C for 1 min, followed by 72 °C for 7 min. 1 µL of the previous reaction, 2 µL 10 µM Up primer (5'-GCCGGAGCTCTGCAGAATTC-3'), 7 µL nuclease-free H_2O, 10 µL 2x GoTaq Green Master Mix were mixed and incubated in a thermocycler with the following cycling conditions: 95 °C for 7 min, then 35 cycles of 95 °C for 1 min, 55 °C for 1 min and 72 °C for 1 min, followed by 72 °C for 7 min. This reaction was then purified using an Amicon Ultra centrifugal filter (50 kDa molecular weight cutoff). Polymerase chain reaction (PCR) products which ranged from 300-1000 base pairs (bp) of length were then sequenced on the MiSeq platform for high-throughput sequencing. Sequencing data was then used to construct the genomes of viral sequences with the help of Galaxy version 19.05 and Geneious version 10.2.6.

Rapid Amplification of cDNA Ends (RACE)

Primers were designed based on the tentatively assembled viral genomes such that the terminal sequences can be generated by reverse transcription.

In a sterile microcentrifuge tube, 1 µL dsRNA, 1 µL 10 µM NeoTaTV_N primer (5'-TGATTGTCAGCCCAAGACCA-3') or NeoTaTV_C primer (5'-GCTGGTCCAAGATGTAACGGA-3') for 5'-RACE or 3'-RACE respectively, 10 µL nuclease-free H_2O were mixed, incubated at 95 °C for 8-10 min, then immediately chilled on ice for at least 1 min and spun down by centrifugation. To this reaction, 4 µL 5x First-Strand Buffer, 2 µL 0.1 M dithiothreitol, 1 µL (40 U/µL) rRNAsin Ribonuclease Inhibitor and 1 µL SuperScript III Reverse Transcriptase (200 U/µL) were added. The reaction was incubated at 50 °C for 60 min, then inactivated by incubating at 98 °C for 2 min, followed by chilling on ice and a brief centrifugation step, which was then purified by the QIAgen PCR Purification Kit.

The eluate was then used as a template for terminal deoxynucleotidyl transferase (TdT) tailing. 10 µL of the eluate containing cDNA, 5 µL 5x TdT buffer, 1.25 µL 100 µM dGTP (for 5'-RACE) or dATP (for 3'-RACE), 8.25 µL nuclease-free dH_2O and 0.5 µL TdT (15 U/µL) were mixed and incubated at 37 °C for 30 min, then inactivated by heating to 75 °C for 10 min. This reaction was also purified by the QIAgen PCR Purification Kit.

1 µL dGTP or dATP-tailed cDNA, 1 µL 10 µM Poly-dC_5_RACE primer for 5'-terminal dGTP-tailed cDNA (5'-TTACTAATATCCCCCCCCCCCC-3') or Poly-dT_3_RACE primer for 3'-terminal dATP-tailed cDNA (5'-GACCACGCGACGTGTCGAVTTTTTTTTTTTTTT-3') respectively, 7 µL nuclease-free dH_2O, 10 µL 2x GoTaq Green Master Mix was mixed, then incubated in a thermocycler at 95 °C for 5 min, then 52 °C (for 5'-terminus) or 37 °C (for 3'-terminus) for 2 min, then 72 °C for 40 min. 1 µL 10 µM terminal primer that was used for cDNA

synthesis was then added to the reaction, then the reaction was incubated in a thermocycler for 30 cycles of 95 °C for 1 min, 60 °C for 1 min, 72 °C for 3 min with a final extension step of 72 °C for 15 min. Each reaction was diluted at a 1:100 ratio in nuclease-free dH_2O for a half-nested PCR. This half-nested PCR used another primer designed to anneal further down the terminal sequence.

1 µL dGTP or dATP-tailed cDNA, 1 µL 10 µM Poly-dC_5_RACE primer for 5'-terminal dGTP-tailed cDNA (5'-TTACTAATATCCCCCCCCCCCC-3') or Poly-dT_3_RACE primer for 3'-terminal dATP-tailed cDNA (5'-GACCACGCGACGTGTCGAVTTTTTTTTTTTTTT-3'), 1 µL 10 µM TaTV_N primer (5'-GTCTAACGAAACTGTCCAT-3') or TaTV_C primer (5'-CGTTACATGTGTTGTTGTGA-3') for 5'-RACE or 3'-RACE respectively, 7 µL nuclease-free dH_2O, 10 µL 2x GoTaq Green Master Mix was mixed, then incubated in a thermocycler at 95 °C for 5 min, then 30 cycles of 95 °C for 1 min, 55 °C for 1 min, 72 °C for 3 min with a final extension step of 72 °C for 15 min. This reaction was run on an agarose gel and a band corresponding to the expected size was cut from the gel, extracted by a centrifugation step through filter paper at maximum speed (21,130 g) for 2 min.

0.3 µL of pGEM T-Easy vector, 3.7 µL gel eluate, 5 µL 2x Rapid Ligation Buffer and 1 µL T4 DNA Ligase (3 U/µL) were mixed and incubated overnight at RT. The following day, a tube containing chemically competent *E. coli* DH5α cells was thawed on ice for 10 min, then 2-5 µL of the ligation reaction was added to the tube of cells, flicked gently 4-6 times and continued incubation on ice for 60 min. The tube was then added to a water bath at exactly 42 °C and incubated for 30-45 sec before immediately placing the tubes back on the ice for 2 min. 450 µL of Super Optimal Broth (SOB) was then added to the tube and incubated at 37 °C for 45 min

with shaking (200-300 rpm). 250 µL was then plated on MacConkey Agar containing ampicillin antibiotics at a concentration of at least 100 µg/mL, then incubated overnight at 37 °C.

Bacteria colony PCR using T7 and SP6 primers was then performed for each white colony that grew on the agar, and colonies that amplified products at roughly the expected size were then grown in Luria-Bertani medium (LB) containing ampicillin at a concentration of at least 100 µg/mL overnight. The QIAgen Spin Miniprep Kit was used to purify the plasmid containing the insert of interest and the plasmid that was eluted from the kit was then sequenced.

Sequence Analysis and Phylogeny

MEGA-X (Kumar et al., 2018) was used for protein sequence alignment of L genes using the ClustalW algorithm. This alignment was then used for the generation of a phylogram with the neighbor-joining and maximum likelihood methods, which were each performed with 1,000 bootstrap replicates.

Primer name	Primer sequence (5'-3')
Up-dN6	GCCGGAGCTCTGCAGAATTCNNNNNN
Up	GCCGGAGCTCTGCAGAATTC
Poly-dC_5_RACE	TTACTAATATCCCCCCCCCCC
Poly-dT_3_RACE	GACCACGCGACGTGTCGAVTTTTTTTTTTTTTT
NeoTaTV_N	TGATTGTCAGCCCAAGACCA
NeoTaTV_C	GCTGGTCCAAGATGTAACGGA
TaTV_N	GTCTAACGAAACTGTCCAT
TaTV_C	CGTTACATGTGTTGTTGTGA

Table 7. List of primers used in this study. NeoTaTV_N and NeoTaTV_C are both primers used for the reverse transcription reaction and the first round of PCRs for their respective terminal RACE procedure. TaTV_N and TaTV_C are both primers used for the half-nested PCRs following the first round of PCRs to improve specificity that may have been an issue using only one primer set.

Results and Discussion

The taro virome remains an understudied aspect of its pathology, as most of the concern for taro is focused on the devastating alomae disease, caused by co-infection of CBDaV and TaBV, and the severe impact of TaVCV across the Pacific. Sanger sequencing, which can generate sequence reads of 500 to 1,000 bp, remains a relevant tool and plays a role in the sequencing of viruses and their genomes. Overlapping regions of primer pairs would often be the ideal strategy to sequence new viral genomes, but the discovery of new viruses was difficult when using this method. Some RNA viruses that have been sequenced in the past used an RNA purification method, including the method by Morris and Dodds (1979) for purifying dsRNA viruses and species of other RNA viruses in the process of replication. If the titer of a virus was high enough, the dsRNA eluate could be visualized on an agarose gel. The segments containing potential viral genomes would then be excised and sequenced with tagged random primers, creating a cDNA library containing a pool of viral sequences. This method was useful but was often challenging and required many unique sequences, which could be time-consuming if some of those sequences contributed little to no additional information. With the emergence of high-throughput sequencing (HTS) as a potential route for sequencing new viruses, much of this method is streamlined and only requires the steps of the experimental method up until generating

a cDNA library before preparing the sample for the HTS method. An added benefit of this is the ability to find viral sequences despite a low titer of a virus in plant materials used for the experiment. This method may not always result in full genomes, but if any gaps are present from missing sequences, there is always the potential to design primer sets to fill in the gaps of viral scaffolds. The terminal ends of viral sequences must also be confirmed by RACE as assemblies generated may contain extra sequence fragments that are not actually in the true sequence of the virus.

The complete sequence of the totivirus dsRNA genome is 4960 bp in length with a G/C content of 48.9%. Two open reading frames (ORFs), designated ORF1 and ORF2 from the 5' to 3' end, were found on the same strand. ORF1, in a +3 frame, starts from nucleotide (nt) 51 and stops at nt 2354 with a UAG stop codon. The protein coded by ORF1 has been calculated to be a molecular weight of 86.1 kDa. ORF2, in a +2 frame, starts from nt 2684 and stops at nt 4909 with a UGA stop codon. The protein coded by ORF2 has been calculated to be a molecular weight of 85.2 kDa. Both ORFs are separated by 329 nts, the 5' untranslated region consists of 50 nts, and the 3' untranslated region consists of 51 nts (Fig. 3.1). A putative slippery site was found within ORF1 which consists of a heptanucleotide sequence $_{2243}$GGGTTTT$_{2249}$ that, if a -1 frameshift occurred at this site, could generate a fusion protein of ORF1 and ORF2 that is 1619 amino acids long with a predicted molecular weight of 183.75 kDa (Fig. 3.1) (Yusop et al., 2019; Ghabrial, 2008).

The putative protein coded by ORF1 is most similar to the putative CP of Panax notoginseng virus A (GenBank accession number NC_029096.1) with a 49% amino acid sequence identity determined by LALIGN (https://embnet.vital-it.ch/software/LALIGN_form.html). CPs from other viruses with a significant similarity include

Pterostylis sanguinea totivirus A and Black raspberry virus F, which are both totiviruses. Some CPs from other totiviruses with a significant similarity include Saccharomyces cerevisiae virus L-A (ScVL-A), Tuber aestivum virus 1 (TaV1) and Scheffersomyces segobiensis virus L (SsVL), though the similarity with these viruses was restricted to the LA-virus coat domain (pfam09220), a conserved region found in all of these proteins.

A global protein sequence alignment conducted via LALIGN with ORF2 to the putative RdRp of Panax notoginseng virus A demonstrated that the two proteins had a 55% amino acid sequence identity. When ORF2 was searched against ScVL-A, TaV1, and SsVL, protein sequence identity ranged from 32-40%. The RdRp 4 domain (pfam02123) was shared between these sequences and found in ORF2. All of the eight conserved domains shared by all RdRps in totiviruses were also found in ORF2 (Bruenn, 1993), as shown in Fig. 3.2. Additionally, a global protein sequence alignment between the fusion protein of ORF1+ORF2 and the CP+RdRp fusion protein of Panax notoginseng virus A demonstrated a 54% amino acid sequence identity.

These characteristics of the ORFs strongly suggest that this dsRNA may be representative of a dsRNA virus belonging to the genus *Totivirus*, family *Totiviridae*, for which the name Taro-associated totivirus L (TaTV-L) was proposed. As expected, when a phylogenetic tree was generated using RdRp amino acid sequences from several select members of the family *Totiviridae*, TaTV-L formed a monophyletic clade together with other members of the genus *Totivirus* (Fig. 3.3a, b). The demarcation criteria for the family *Totiviridae* is 50% amino acid sequence identity, and the amino acid identities described earlier are close enough to the criteria that it would warrant the recognition of this species as a unique totivirus.

The viruses recognized by ICTV which belong to the genus *Totivirus* have all been noted to infect fungi (http://ictvonline.org/virusTaxonomy.asp). It is, therefore, possible that TaTV-L is

a virus that infects a fungus associated with *Colocasia esculenta*. On the contrary, there were no symptoms on the leaf sample used for the dsRNA extraction that indicated that there was an infection by a fungus.

Among the sequences gathered through HTS, sequences of a totivirus were found in the Samoan sample which marked the presence of a virus that had not yet been sequenced in GenBank, as the closest related virus was found to be Panax notoginseng virus A with a low protein identity. This factor alone made the sequencing of this virus potentially useful, but there are potential circumstances which complicate the issue of truly determining whether this is a bona fide plant virus or otherwise. The currently recognized species of the *Totivirus* genus have only fungal hosts. As fungal diseases have been recorded for taro, it is difficult to rule out the possibility that the totivirus infects a fungus associated with taro. As totiviruses are naturally dsRNA, a relatively high titer is also to be expected from a dsRNA extraction. With the current circumstances, it is difficult to speculate how the totivirus became associated with taro, as other isolates did not exhibit the symptoms of a totivirus. The symptoms that this totivirus might cause are also unclear, as interactions between totiviruses and plants have not been explored in depth. While the taro leaf sample used for the dsRNA extraction did not seem to exhibit any unique symptoms, the presence of this virus in the dsRNA eluate was confirmed by PCR. Gradually, more publications of totiviruses in plants are being produced.

Although the results of this study led to the discovery of only one undocumented virus, this serves as a proof of concept of the potential of HTS in the discovery of new viruses in the future. While this study covered the viromes of five regional isolates, there are other places that warrant investigation, and the reports of more unique viruses that have been found to infect taro in different places around the world raise a potential issue of the host range of different viruses.

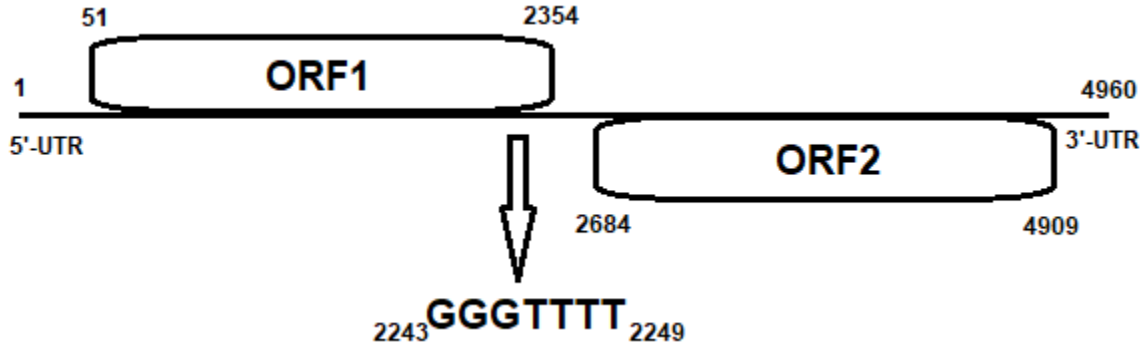

Fig. 3.1. Schematic representation of the Taro-associated totivirus L genome. A heptanucleotide sequence, the putative site of the -1 frameshift, marks a genetic feature belonging to members of the genus *Totivirus*. If this frameshift occurs, a fusion protein combining ORF1 and ORF2 may be rarely expressed. Note that this figure is not drawn to scale.

```
RdRp       1         2         3         4                5                 6        7       8
LRV1     LLGRG 59 WAANGS.HS 49 GKTRLLL 57 DYDDFNSQHT 46 TLMSGHRATSFINSVLNRAYI 11 HVGDDILM 33 EFLRV 9  YLAR
TvV1     LLGRG 58 WSRSGS.HY 45 GKERFIY 50 DYTDFNSQHT 43 TLPSGHRATTFINTVLNWCYT 11 CAGDDVIL 31 EFLRK 9  YPCR
ScVL-A   LMNRG 57 WVPGGSVHS 50 GKQRAIY 52 DYDDFNSQHS 52 TLLSGWRLTTFMNTVLNWAYM 15 HNGDDVMI 33 EFLRV 13 YLSR
ScVLBCLa LENGV 58 IMPGGSVHS 50 GKVRALY 51 DFDDFNSQHS 52 TLFSGWRLTTFFNTALNYCYL 13 HNGDDVFA 33 EFLRV 11 YLTR
UmVH1    LYGRG 66 WLVSGSSAG 61 GKARAIY 55 DYPDFNSMHT 63 GLYSGDRDTTLINTLLNIAYA 20 CHGDDIIT 34 EYLRI 10 CLAR
TaTV-L*  LVNRG 58 WVPTGSVHS 50 AKQRAIY 52 DFDNFNAQHS 54 TLLSGWRLTTFINTALNFIYF 15 HNGDDVLV 33 EFLRV 13 YLSR
         *         **        * *       *   **  *      * ** * *   *  **  *       ***       * **       *
GlV      LLGKV 65 WGTTGSGYI 41 TKVRAVI 55 DQSNFDRQPD 59 GLPSGWKWTALLGALINTQLL 16 VQGDDIAL 33 EFLRR 13 MMIK
```

Fig. 3.2. The eight conserved domains common to the family *Totiviridae*, including the *Leishmania RNA virus 1* (LRV1, genus *Leishmaniavirus*), *Trichomonas vaginalis virus 1* (TvV1, genus *Trichomonasvirus*), *Giardia lamblia virus* (GlV, genus *Giardiavirus*), and the putative totivirus TaTV-L. The numbers between each sequence fragment represent the number of amino acids between each domain. Asterisks underneath the protein sequences denote identical residues across all species, with a few notable exceptions in GlV. Adopted from Bruenn (1993).

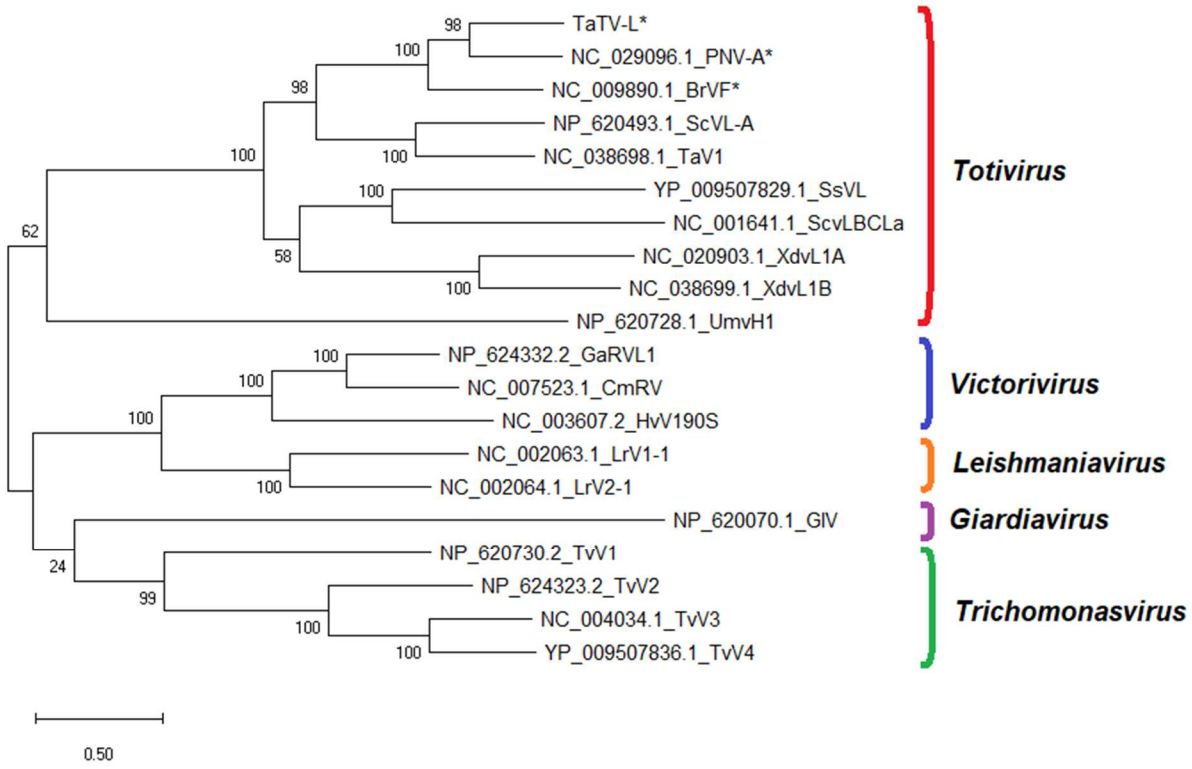

Fig. 3.3a. Phylogenetic tree generated with the maximum likelihood method. Asterisks (*) denote species used in the phylogenetic tree that are not yet officially recognized as members of the genus *Totivirus*. Taro-associated totivirus L groups together in a clade with other totiviruses with high bootstrap support (98%).

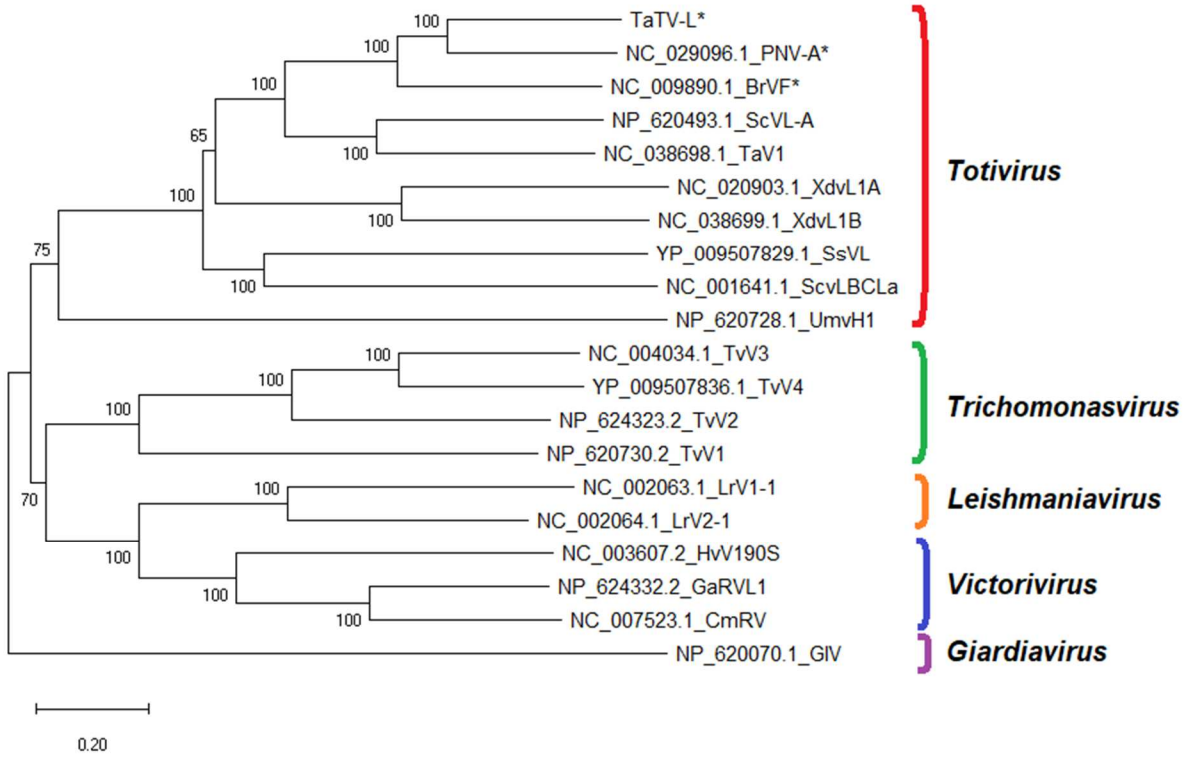

Fig. 3.3b. Phylogenetic tree generated with the maximum likelihood method. Asterisks (*) denote species used in the phylogenetic tree that are not yet officially recognized as members of the genus *Totivirus*. Taro-associated totivirus L groups together in a clade with other totiviruses with high bootstrap support (100%).

CHAPTER 4: CONCLUSIONS AND FUTURE STUDIES

TaVCV has a regional prevalence, and is becoming an increasing issue, especially for the state of Hawaii. As taro is a vegetatively propagated plant, systemic viruses such as TaVCV results in infected offspring, which makes this virus a challenge to remove once established, and plant therapy may be required to reduce the prevalence of the virus. TaVCV negatively impacts the yield of taro crops, and, in severe cases of infection, infected plants could die. Thus, it is very

problematic for taro cultivation, which can be severely damaged if the virus spreads to different countries. Gradually, the virus is being found in more places, and Hawaii (Long et al., 2014) has had a recent discovery. While the South Pacific is responsible for a small portion of the world's taro production, China and some countries in Africa consist of larger-scale taro cultivation. Regulations are in place that prohibit the movement of plants to other countries, but worldwide travel is now a regular occurrence, which may increase the risk of the virus spreading to places that have not yet been exposed. If TaVCV spreads to taro in countries with large-scale taro production, this would heavily impact taro cultivation as a whole. Therefore, more efforts must be made to reduce or eliminate this risk. Unfortunately, TaVCV and the taro virome remain understudied, despite the importance of this crop to both agriculture and society in the world.

This study has revealed the sequences of five isolates of TaVCV across the Pacific, as well as a novel taro-associated totivirus. Notably, Guam has also been found to have TaVCV in a taro sample used in this study, marking the first discovery of this virus at that location. All TaVCV isolates may have low genetic identity of at least 78%, but this fails to meet the demarcation criteria for the *Nucleorhabdovirus* genus which states that 50% nucleotide identity is required to denote a virus as a new species ("ICTV," 2019). Though ICTV may recognize some viruses as unique species despite having a slightly higher degree of identity than the criteria, the identity of these viruses is still too high. This high genetic diversity highlights a current challenge in PCR diagnostics, which are sensitive to nucleotide deviations and such a variability can disturb primer-template interactions to yield false negatives. Covering a wider range of genomic data can aid in the design of alternative PCR diagnostics which account for the nucleotide diversity among these isolates. A high protein identity of at least 89% also opens up a possibility for some antibody-based diagnostics.

Combined with other methods for nucleic acid extraction and isolation of viruses through either purification or isolation of dsRNA fractions, HTS is a very promising tool for the study of viruses whose sequences are unknown. While HTS has issues which include gaps introduced in scaffolds due to a lack of information, the ability to use random sequences to find new viruses reduces the amount of guesswork required to perform whole genome virus sequencing. This study has successfully demonstrated the utility of HTS by both sequencing isolates of TaVCV with high diversity as well as the sequencing of a virus not previously documented and serves as a potential framework to study viromes of plants, even for those other than taro.

APPENDIX: DEVELOPMENT OF AN ANTIBODY-BASED ASSAY FOR THE DETECTION OF TARO VEIN CHLOROSIS NUCLEORHABDOVIRUS (TAVCV)

Introduction

Some methods for detecting the presence of viruses in plant material include polymerase chain reaction (PCR) and enzyme-linked immunosorbent assay (ELISA). PCR is a viable option for viral diagnostics, but the high nucleotide variability among isolates of taro vein chlorosis nucleorhabdovirus (TaVCV) poses a challenge for the reliable detection of this virus. Low nucleotide identity does not necessarily correspond to low protein identity, as some codons will translate to the same amino acid. Silent mutations such as those contribute to a lower nucleotide identity but not a lower protein identity. Here, where high nucleotide variability of TaVCV makes the design of a robust PCR assay challenging, ELISA may be more reliable.

ELISA for the detection of viruses works by using antibodies that specifically target a viral protein featured prominently on its surface (Fig. A1). The development of an ELISA via hybridoma technology involves a workflow of synthesizing a recombinant protein to be expressed and purified, injecting a solution with the protein into an animal host to raise B-cells that have antibodies specific to the protein, then fusing B-cells into a murine myeloma cell line. This yields a fused cell which can proliferate for a long time and continue to produce protein-specific antibodies. Isolation of cell lines after the fusion yields a cell line producing monoclonal antibodies, which are antibodies that target a particular protein epitope. For convenience, this method is typically used for the development of an indirect (ID-)ELISA or a double antibody sandwich (DAS-)ELISA, so that conjugation of alkaline phosphatase or horseradish peroxidase does not need to be done for each new antibody. The antibodies could also be used for immunocapture reverse transcription (IC-RT-)PCR, which uses antibodies to coat the surface of

a PCR tube and selectively grab virus particles from a sample, which is then denatured by heat and used as a template for RT-PCR.

Here, we report the development of a monoclonal antibody hybridoma cell line for the detection of TaVCV through the synthesis of a nucleoprotein fragment from a Hawaiian isolate and the application of these antibodies via ELISA and IC-RT-PCR.

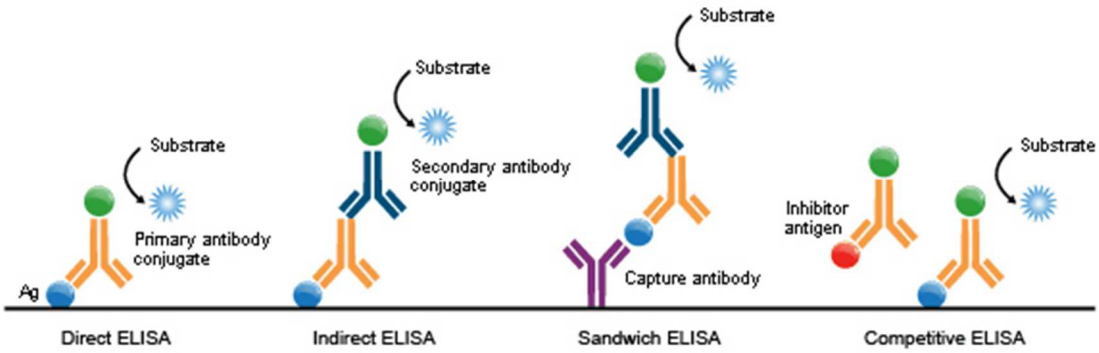

Fig. A1. The different types of ELISA used for detection assays. Adopted from https://upload.wikimedia.org/wikipedia/commons/3/3b/Elisa_tipus.gif

Materials and Methods

Development of a Plasmid Construct for the Expression of Nucleoproteins

RNA was extracted from taro leaves using the plant RNA isolation protocol for the NucleoSpin RNA Plus kit. The RNA eluate was used as a template for reverse transcription. 1 µL RNA, 1 µL 100 µM random hexamers, 10 µL nuclease-free H_2O were mixed, incubated at 95 °C for 8-10 min, then immediately chilled on ice for at least 1 min and spun down by centrifugation. To this reaction, 4 µL 5x First-Strand Buffer, 2 µL 0.1 M dithiothreitol, 1 µL (40 U/µL) rRNAsin Ribonuclease Inhibitor and 1 µL SuperScript III Reverse Transcriptase (200 U/µL) were added. The reaction was incubated at 25 °C for 5-10 min, then 50 °C for 60 min,

then inactivated by incubating at 98 °C for 2 min, followed by chilling on ice and a brief centrifugation step.

1 µL of the previous reaction, 1 µL 10 µM Cap2A(AsiSI) primer (5'-TTTGCGATCGCCATGGACGCCACTATAGCCTCCGACTGGG-3'), 1 µL 10 µM Cap2S(PmeI) primer (5'-TTTGTTTAAACTTATCATTGGTTGGATGTCCCTCCGC-3'), 7 µL nuclease-free H_2O, 10 µL 2x GoTaq Green Master Mix were mixed and incubated in a thermocycler with the following cycling conditions: 95 °C for 7 min, then 30 cycles of 95 °C for 30 sec, 55 °C for 45 sec and 72 °C for 1 min, followed by 72 °C for 10 min. These reactions were run on an agarose gel and a band corresponding to the expected size (1.1 kb) was cut from the gel, extracted by a centrifugation step through filter paper at maximum speed (21,130 g) for 2 min.

0.3 µL of pGEM T-Easy vector, 3.7 µL gel eluate, 5 µL 2x Rapid Ligation Buffer and 1 µL T4 DNA Ligase (3 U/µL) were mixed and incubated overnight at RT. The following day, a tube containing chemically competent *E. coli* DH5α cells was thawed on ice for 10 min, then 2-5 µL of the ligation reaction was added to the tube of cells, flicked gently 4-6 times and incubated on ice for 60 min. The tube was then added to a water bath at exactly 42 °C and incubated for 30-45 sec before immediately placing the tubes back on ice for 2 min. Super Optimal Broth (450 µL) was then added to the tube and incubated at 37 °C for 45 min with shaking (200-300 rpm). 250 µL was then plated on MacConkey Agar containing ampicillin antibiotics at a concentration of at least 100 µg/mL, then incubated overnight at 37 °C.

Bacteria colony PCR using T7 and SP6 primers was then performed for each white colony that grew on the agar, and colonies that amplified products at roughly the expected size were then grown in Luria-Bertani medium (LB) containing ampicillin at a concentration of at

least 100 µg/mL overnight. The QIAgen Spin Miniprep Kit was used to purify the plasmid containing the insert of interest and the plasmid that was eluted from the kit was then sequenced. The plasmids containing the PCR insert were then used for a restriction digest.

A volume containing 1 µg of pGEM T-Easy containing the PCR insert, 2 µL 10X Buffer B, 0.5 µL *Sfa*AI (*Asi*SI) (10 U/µL), 0.5 µL *Mss*I (*Pme*I) (5 U/µL), and a volume of nuclease-free water such that the final volume was 20 µL were mixed and incubated at 37 °C for 1 hour, then inactivated by incubating at 80 °C for 20 min. The restriction enzymes and 10X Buffer B were supplied by Thermo Scientific. The restriction digest was run on an agarose gel and a band corresponding to the expected size of the PCR insert (1.1 kb) was cut from the gel, extracted by the QIAquick Gel Extraction Kit. Another restriction digest was also done by replacing pGEM T-Easy with pFN6A vector.

A volume of double-digested pFN6A vector, a volume of double-digested PCR insert, 1 µL 10x T4 DNA Ligase Buffer and 1 µL T4 DNA Ligase (3 U/µL) were mixed such that the final volume was 10 µL with a molar ratio of 1:3 vector to insert and incubated overnight at RT. The following day, a tube containing chemically competent *E. coli* KRX cells was thawed on ice for 10 min, then 2-5 µL of the ligation reaction was added to the tube of cells, flicked gently 4-6 times and incubated on ice for 60 min. The tube was then added to a water bath at exactly 42 °C and incubated for 30-45 sec before immediately placing the tubes back on ice for 2 min. Super Optimal Broth (450 µL) was then added to the tube and incubated at 37 °C for 45 min with shaking (200-300 rpm). 250 µL was then plated on MacConkey Agar containing ampicillin antibiotics at a concentration of at least 100 µg/mL, then incubated overnight at 37 °C.

Bacteria colony PCR using modified T7 (5'-TAATACGACTCACTATAGG-3') and Cap2S(*Pme*I) primers was then performed for each colony that grew on the agar, and colonies

that amplified products at roughly the expected size were then grown in Luria-Bertani medium (LB) containing ampicillin at a concentration of at least 100 µg/mL overnight. The QIAgen Spin Miniprep Kit was used to purify the plasmid containing the insert of interest and the plasmid that was eluted from the kit was then sequenced. Colonies that contained the pFN6A plasmid with the PCR insert in frame with the $(HQ)_3$-tag were used for protein expression and purification.

Protein Expression and Purification

250 mL LB, 500 µL 100 µg/mL ampicillin, 1.25 mL 20% rhamnose, and 2.5 mL 20% glucose were mixed, inoculated with an *E. coli* KRX colony containing the pFN6A plasmid construct containing the PCR insert, then incubated at 37 °C for 2 days and shaken at 150 rpm. The culture is then centrifuged at 4,000 rpm for 20 minutes in an autoclaved 250 mL centrifuge bottle. The supernatant was removed, then the bacterial pellet was resuspended in 10 mL of Binding Buffer (100 mM HEPES pH 7.5, 1% Triton-X, 10 mM imidazole, 200 mM NaCl), after which 1.12 mL FastBreak solution (1,027 µL 10X FastBreak Reagent, 93 µL DNase I) was added and the solution was moved to a 50 mL conical tube. EDTA-free Pierce Protease Inhibitor Tablets (1 tablet per 10 mL) can be added to the Binding Buffer. This solution was freeze-thawed at least three times using a -80 °C freezer. 0.5 mL of 50% slurry of HisLink Resin was added to the solution and incubated at 4 °C for at least 30 minutes on an orbital shaker.

The conical tube was propped upright to let the resin sink to the bottom for at least 5 minutes, after which the supernatant was removed. The resin was resuspended in 5 mL of Wash Buffer (100 mM HEPES pH 7.5, 1% Triton-X, 10 mM imidazole, 1 M NaCl) and sunk to the bottom of the conical tube for at least 5 minutes, after which the supernatant was removed. EDTA-free Pierce Protease Inhibitor Tablets (1 tablet per 10 mL) can be added to the Wash Buffer. The wash step was repeated twice for a total of three washes. After this, wash buffer was

added to the resin to resuspend and transfer it to a spin column provided in the HisLink Spin Protein Purification System kit. The column was briefly centrifuged for 5 seconds and the flowthrough was discarded.

0.5 mL of Elution Buffer (100 mM HEPES pH 7.5, 100 mM imidazole) was added to the resin and the spin column was briefly centrifuged for 5 seconds. The eluate was transferred to a separate 1.5 mL microcentrifuge tube. The elution step was repeated twice to yield 1.5 mL of eluate containing the $(HQ)_3$-tagged protein. The eluate was run by sodium dodecyl sulfate-polyacrylamide gel electrophoresis (SDS-PAGE) to check for purity and size of the protein product.

Development of a Hybridoma Producing TaVCV-Specific Monoclonal Antibodies

In a 15 mL conical tube, 1 mL of solution containing 100 µg $(HQ)_3$-tagged protein was mixed with 1 mL of a 10% (w/v) solution of $KAl(SO_4)_2$ (alum) in distilled water, after which 10 drops (approximately 200 µL) of 1 M NaOH were added. This solution was mixed by vortexing, then left to incubate for 1 hour at RT. The solution was then centrifuged at 1,500 rpm for 5 minutes to pellet precipitated proteins, and the supernatant was removed. The pellet was resuspended in 1 mL phosphate-buffered saline (PBS) (137 mM NaCl, 2.7 mM KCl, 10 mM Na_2HPO_4, 1.8 mM KH_2PO_4; pH 7.4) and centrifuged once more at 1,500 rpm for 5 minutes, after which the supernatant was removed. The pellet was resuspended in PBS to a final volume of 825 µL. 250 µL of this solution was used to immunize each mouse via intraperitoneal injection. Injections were repeated every two weeks after the initial injection for a total of three injections.

All solutions used for this method were sterilized before use, and aseptic technique was used to prevent contamination. Spleens were harvested from each mouse and washed in GKN (NaCl 8 g, KCl 0.4 g, Na_2HPO_4 1.41 g, $NaH_2PO_4 \cdot H_2O$ 0.69 g, glucose 2 g, phenol red 0.01 g or

100 µL of 0.1 g/mL stock solution, dH_2O to 1 L; pH 7.4) in a Petri dish to remove blood or debris. After washing, the spleen was transferred to a second Petri dish containing 6-7 mL GKN, which was used to extract the splenocytes by using a 10 mL syringe with an 18 or 20 gauge needle to stick the spleen lengthwise and gently perfuse with GKN until the spleen appeared translucent to yield a single cell suspension. The Petri dish was canted on one side to settle large debris and the supernatant was transferred to a sterile 15 mL centrifuge tube, adding GKN for a final volume of 15 mL. A cell count was taken for the cell suspension and a volume containing 5 x 10^7 cells was transferred to a sterile 50 mL centrifuge tube. A culture of P3-X63-Ag8.653 myeloma cells was also prepared, a cell count was taken, the cells were washed and suspended in GKN, and a volume containing 1 x 10^7 cells was added to the 50 mL centrifuge tube containing the splenocytes. The volume was adjusted to 50 mL with GKN, then the cells were spun down at 400 g for 10 min at RT, after which the supernatant was decanted gently. The cells were loosened by hitting the bottom of the tube several times.

Splenocytes were fused together with P3-X63-Ag8.653 myeloma cells in solution by gently mixing the cell suspension and slowly adding 1 mL of polyethylene glycol (PEG) solution (melted PEG [ATCC, MW 1300-1600, sterile] 2 g, GKN 2 mL, DMSO 0.5 mL) with a 1 mL sterile pipette over 1 minute, with continued stirring for 90 seconds in a 37 °C water bath. Two aliquots of 1 mL GKN warmed to 37 °C were slowly added to the cell suspension each over 1 minute, then 7 mL GKN warmed to 37 °C was slowly added over 2-3 minutes. This was incubated at RT for 5 min, then 40 mL of GKN at RT was added to the cell suspension, then spun at 400 g for 10 min. The supernatant was decanted and the cell pellet was resuspended in 20 mL hypoxanthine-aminopterin-thymidine (HAT) media (hypoxanthine 0.1361 g, thymidine

0.0388 g, dH_2O to 100 mL, 1 mL aminopterin 100X stock solution; aminopterin 100X = aminopterin 1.76 mg, dH_2O added and NaOH added to dissolve, dH_2O to 100 mL).

The mixture was added to HAT media in a 96-well macrophage plate incubated 1-3 days in advance at 37 °C in 5% CO_2 to selectively proliferate successfully fused hybridomas. The cells were incubated at 37 °C for 1 to 2 weeks with 5% CO_2. Each well was checked periodically to find wells that contained successfully fused hybridomas. Hybridomas were weaned off HAT media by replacing half of the media with Dulbecco's Modified Eagle Medium supplemented with 10% fetal bovine serum (DMEM-10) every 2 to 3 days. Wells containing hybridomas were initially screened via indirect (ID-)ELISA to determine hybridomas that had antibody reactivity with TaVCV and the $(HQ)_3$-tagged protein used for immunizations. Cell count was determined for each well, then a single cell suspension was prepared to isolate monoclonal hybridomas, depositing cell concentrations of 5, 1, and 0.5 cells/well on a 96-well tissue culture plate. These were also screened via ID-ELISA for reactivity with TaVCV and the $(HQ)_3$-tagged protein.

ID-ELISA

For leaf samples, 0.1 g of leaf tissues (from sweet potato, healthy taro, or infected taro) were homogenized in 1 mL carbonate coating buffer (Na_2CO_3 1.59 g, $NaHCO_3$ 2.93 g, NaN_3 0.2 g, dH_2O to 1 L, pH 9.6), then centrifuged at 4,500 g for 2 min. For *E. coli*, an *E. coli* suspension of 0.1 OD in carbonate coating buffer was prepared. For purified proteins (the $(HQ)_3$-tagged protein used as antigen and another $(HQ)_3$-tagged protein p23 from HGSV-2), a suspension containing 10 µg/mL of protein in carbonate coating buffer was prepared. 100 µL of each of these solutions were plated on a 96-well microplate and incubated at 37 °C for 1-2 hours (or, alternatively, 4 °C overnight) and washed at least 3 times with PBS-T (10X PBS 100 mL, Tween-20 0.5 mL, dH_2O 900 mL; 10X PBS = NaCl 80.0 g, KCl 2.0 g, $Na_2HPO_4 \cdot 2H_2O$ 14.4 g,

KH_2PO_4 2.4 g, NaN_3 0.2 g, dH_2O to 1 L, pH 7.4). 200 µL of PBS-T containing 5% (w/v) non-fat dry milk was added to each well for blocking and incubated at 37 °C for 1-2 hours (or, alternatively, 4 °C overnight) and washed at least 3 times with PBS-T.

100 µL of hybridoma media or 1:1000 dilution of mouse sera was added to each well and incubated at 37 °C for 1-2 hours (or 4 °C overnight) and washed at least 3 times with PBS-T. After that, 100 µL of a 1:1000 dilution of a goat-anti-mouse IgG conjugated to alkaline phosphatase was added to each well, incubated at 37 °C for 1-2 hours (or 4 °C overnight) and washed at least 8 times with PBS-T. 100 µL of p-nitrophenyl phosphate (PNPP) solution (10 mg PNPP in 10 mL PNPP substrate buffer [$MgCl_2 \cdot 6H_2O$ 0.1 g, NaN_3 0.2 g, diethanolamine 97 mL, dH_2O to 1 L, pH 9.8]) was added to each well. OD readings were taken at 405 nm in 15-minute intervals after the application of PNPP solution, up to 60 minutes.

IC-RT-PCR

Hybridoma supernatant was concentrated using an Amicon Ultra centrifugal filter (50 kDa molecular weight cutoff). 1 µL of concentrated supernatant was added to 19 µL of carbonate coating buffer in a PCR tube, incubated at 37 °C for 2-3 hours, then washed at least 3 times with PBS-T. 0.1 g of leaf tissues were homogenized in 1 mL PBS-T, then centrifuged at 4,500 g for 2 min. 20 µL of leaf tissue supernatant was added to the PCR tube, incubated at 4 °C overnight, then washed at least 3 times with PBS-T, then at least 1 time with molecular-grade dH_2O. The RT-PCR was performed using SuperScript III One-Step RT-PCR System as follows. 1 µL 10 µM DCGF5 (5'-AGGGGYTGAGRCAAAAGGGGT-3'), 1 µL 10 µM DCGR5 (5'-CGCTCYTTCATACATGCSGCCTT-3'), 7.2 µL nuclease-free H_2O were added to the PCR tube, incubated at 95 °C for 8-10 min, then immediately chilled on ice for at least 1 min and centrifuged. To this reaction, 10 µL 2x Reaction Mix and 0.8 µL SuperScript III RT/Platinum

Taq Mix were added. The reaction was then incubated at 55 °C for 30 min, then 94 °C for 2 min, followed by 40 cycles of 94 °C for 15 sec, 55 °C for 30 sec, 68 °C for 1 min, then 68 °C for 5 min.

Results and Discussion

Detection assays are important for the health industry when human pathogens are concerned, and for crop cultivation when plant pathogens are concerned. The theory behind the development of ELISA and PCR assays have a sufficient foundation, but certain factors can complicate the use of these assays. The use of a PCR assay for TaVCV is hindered by high nucleotide diversity among its strains, so there is a greater potential utility for an ELISA.

When this work was being performed, little information about the genome of TaVCV was available at the time except for the genome of the Fijian isolate. However, a Fijian strain of TaVCV was unavailable at the time of developing the plasmid construct for the $(HQ)_3$-tagged TaVCV nucleoprotein, and a primer set designed to amplify the entire nucleoprotein was unsuccessful when screening through cDNA samples that were acquired from Hawaiian samples. Cap2A(AsiSI)/S(PmeI) was a primer set designed with restriction sites that yielded a successful amplification from a Kauai sample positive for TaVCV. The set was based on a previously established primer set Cap2A/B which was used for an RT-PCR assay before the development of the DCGF/R primers, targeting a segment of the nucleoprotein-coding gene. The development of the Cap2A/S primer set was to add a stop codon and restriction sites for the pFN6A plasmid construct. Thus, the $(HQ)_3$-tagged protein used in this chapter is a partial segment of the nucleocapsid rather than the complete nucleocapsid.

Notably, the protein eluate when checked by SDS-PAGE appeared to have a major protein band corresponding to a protein size of approximately 23 kDa (Fig. A2a). This is a

surprising difference in molecular weight to the theoretical molecular weight of 41 kDa. A few possibilities exist to account for this occurrence. The protein could have been cleaved by *E. coli* proteases during the process of expression and purification, the protein could be unstable and be cleaved as a result, or codons that are common to taro that may be rare to *E. coli* could be responsible for the incomplete expression of a protein. A band appearing at around 43 kDa in another SDS-PAGE (Fig. A2b) done for protein eluate extracted after a protein purification using the EDTA-free Pierce Protease Inhibitors implies that proteases may be partly responsible for the degradation of the protein, but a large amount of protein at approximately 23 kDa remained despite that, implying another reason may also be involved that does not involve proteases.

The initial screening (Table A1) revealed two wells, P1D5, and P2G5, which had significant reactivity against the protein and taro samples used. Three other wells with much weaker activity, P3A1, P4C7, and P4E6, were also maintained and subcloned in case some of the resulting subclones had a notable degree of reactivity downstream. Interestingly, negative controls using terminal bleeds consistently had higher reactivity against the taro sample that tested negative by RT-PCR. A subcloning attempt of P4E6 (Table A2) yielded two promising subclones, P4E6-B2 and P4E6-C2, both of which had high reactivity against TaVCV-positive taro in contrast to TaVCV-negative taro. While all subclones of P4E6-B2 had strong reactivity to TaVCV (Table A3), P4E6-B2.5 represents a subclone of P4E6-B2 that has the lowest cross-reactivity to *E. coli* KRX, sweet potato leaf, and $(HQ)_3$-tagged p23 protein. The IC-RT-PCR trial using P1D5-F4, P2G5, and P4E6-B2.5 hybridoma supernatants (Fig. A3) gives support to the viability of the P4E6-B2.5 as a potential monoclonal antibody for TaVCV diagnostic assays.

In ELISA trials using RT-PCR negative taro sampled from Kapiolani Community College, any antibody with reactivity to RT-PCR positive taro did not have as strong of a

reaction to the RT-PCR negative taro, though some activity was still present, indicating the possibility of a lower titer of TaVCV rather than being truly negative for the virus. There was some concern regarding the strong reactivity of the antibodies when the negative control was replaced by thermotherapy-treated taro samples. The samples treated by thermotherapy were negative in RT-PCR when tested with TaVCV detection primer sets, and the leaves that were used for ELISA appeared to be healthy. A strong reactivity against the RT-PCR negative sample raises the possibility that the antibody could target a protein native to taro, but this needs to be investigated further by inspecting the dsRNA content of these samples by high-throughput sequencing.

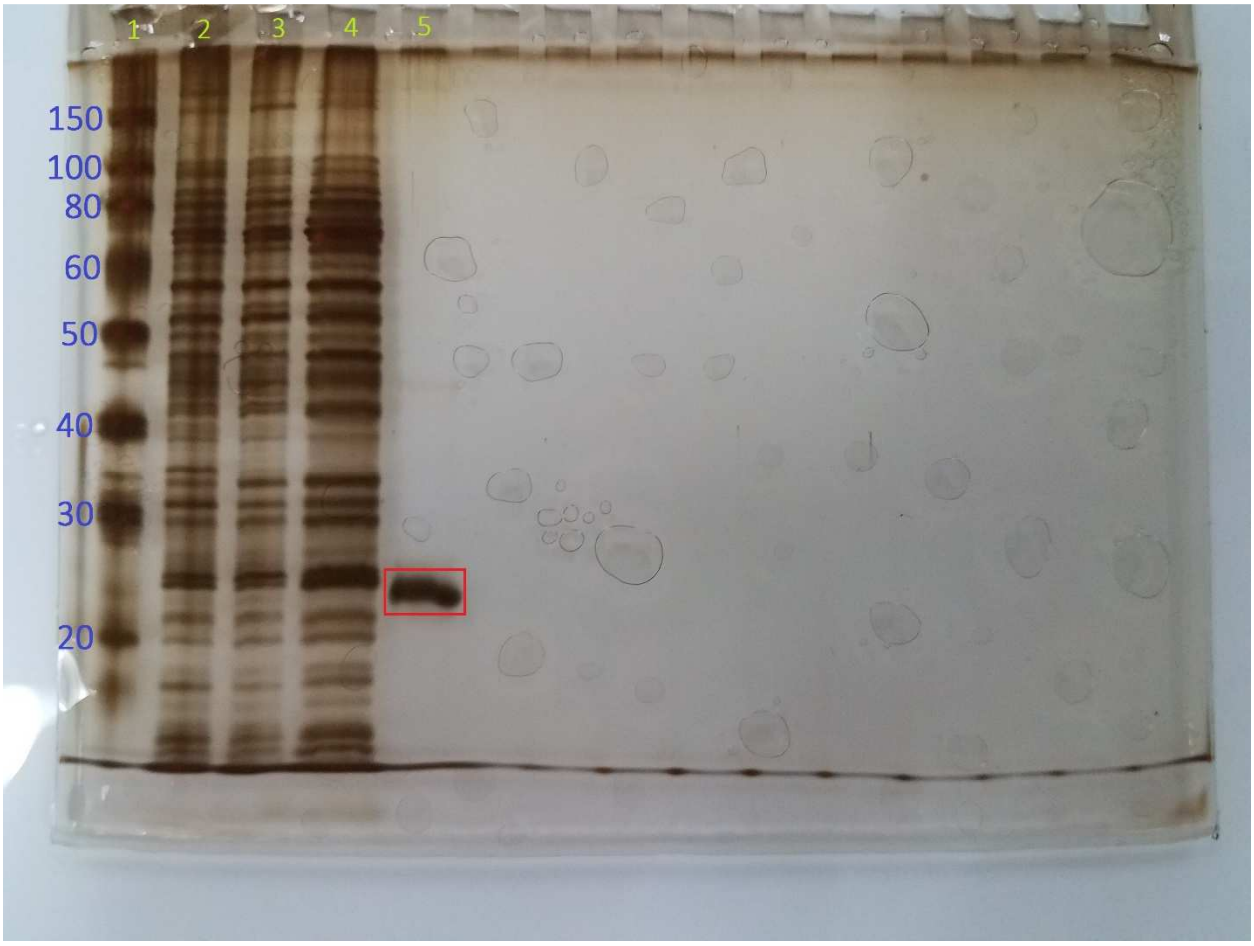

Fig. A2a. Silver Stain of a SDS-PAGE gel made using the Pierce Silver Stain Kit from Thermo Scientific. Lane assignments are as follows: SuperSignal Molecular Ladder with sizes provided in kDa (Lane 1), E. coli KRX lysate without construct (Lane 2), with construct and expressing (Lane 3), flowthrough (Lane 4) and $(HQ)_3$-tagged nucleoprotein (Lane 5). A distinct, pure band of 23 kDa is found in the nucleoprotein eluate, which was notably different from the expected 41 kDa molecular weight of the protein construct.

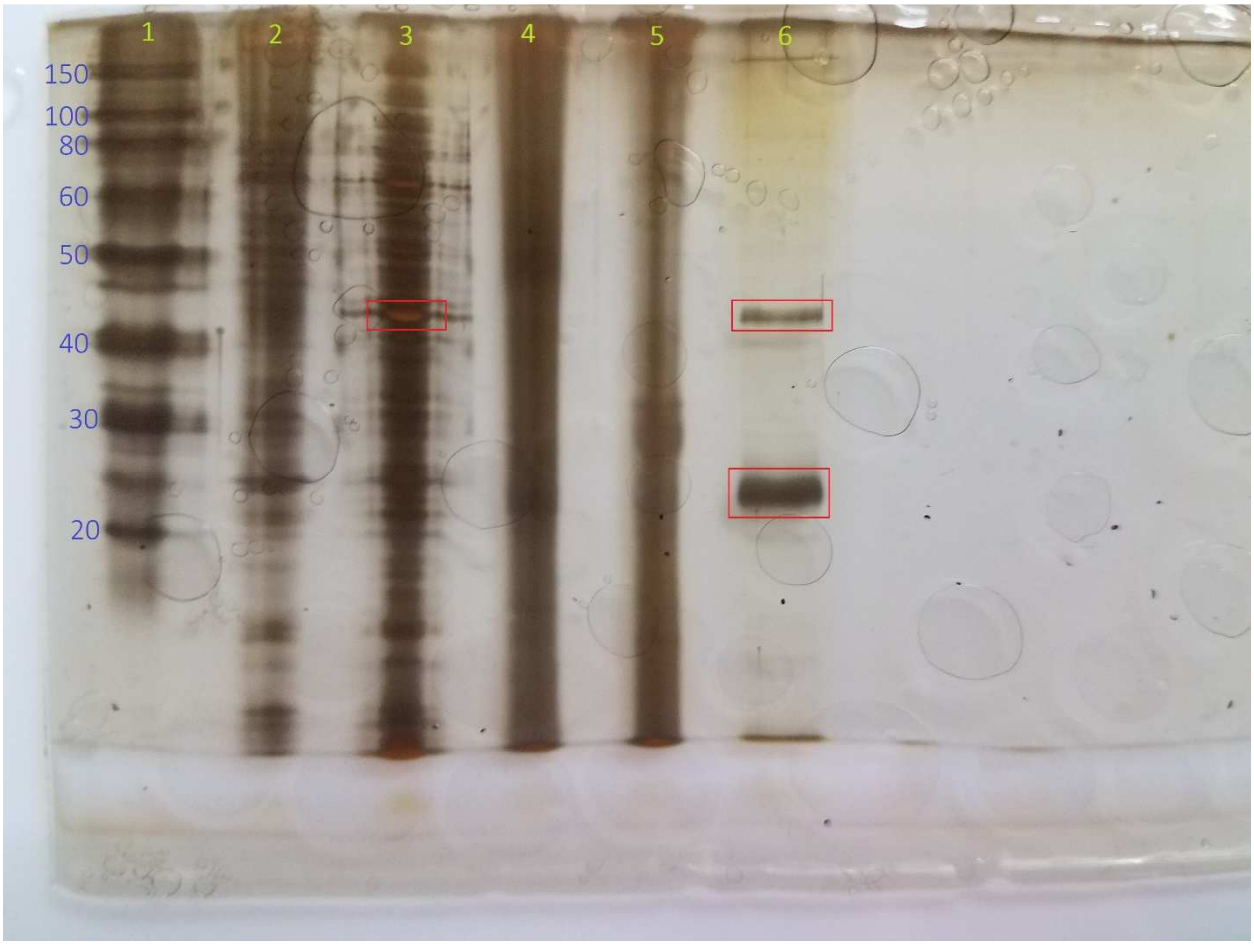

Fig. A2b. Silver Stain of a SDS-PAGE gel made using the Pierce Silver Stain Kit from Thermo Scientific. Lane assignments are as follows: SuperSignal Molecular Ladder with sizes provided in kDa (Lane 1), E. coli KRX lysate without construct (Lane 2), with construct and expressing (Lane 3), TaVCV-negative taro leaf (Lane 4), TaVCV-positive taro leaf (Lane 5), and $(HQ)_3$-

tagged nucleoprotein (Lane 6). The nucleoprotein was purified using a purification protocol that used EDTA-free Pierce Protease Inhibitor Tablets in the Binding and Wash Buffers. Distinct bands of 23 and 43 kDa are found in the nucleoprotein eluate, the latter of which was close to the expected 41 kDa molecular weight of the protein construct.

Condensed ID-ELISA notes (initial clones, all data taken at 30 min.)

	Taro (RT-PCR-)	Taro (RT-PCR+)	HQ-N
P1D5	0.178	0.269	0.257
P2G5	0.889	1.129	0.735
P3A1	0.121	0.147	0.102
P4C7	0.123	0.146	0.104
P4E6	0.172	0.257	0.101

*Plate 1, **Plate 3, ***Plate 4, ****Plate 5

Controls

Plate 1	Taro (RT-PCR-)	Taro (RT-PCR+)	HQ-N
Terminal bleed	0.4	0.227	0.55
Pre-immune	0.094	0.095	0.101

Plate 3	Taro (RT-PCR-)	Taro (RT-PCR+)	HQ-N
Terminal bleed	0.444	0.24	0.57
Pre-immune	0.096	0.104	0.099

Plate 4	Taro (RT-PCR-)	Taro (RT-PCR+)	HQ-N
Terminal bleed	0.461	0.268	0.762
Pre-immune	0.107	0.095	0.102

Plate 5	Taro (RT-PCR-)	Taro (RT-PCR+)	HQ-N
Terminal bleed	0.354	0.221	0.476
Pre-immune	0.093	0.092	0.103

Table A1. Initial screening of hybridomas by ID-ELISA. Data was taken at 30 min. P1D5 and P2G5 represent hybridoma cultures containing cells producing a high amount of antibody reactive with taro and the $(HQ)_3$-tagged nucleoprotein. P3A1, P4C7, and P4E6 represent

hybridoma cultures with some activity to taro (with a higher degree to TaVCV-positive taro) but very little activity to the $(HQ)_3$-tagged nucleoprotein. Here, the RT-PCR negative taro was sampled from Kapiolani Community College. A blood sample after the last injection was used as the positive control, while pre-immune serum was used as the negative control.

Condensed ID-ELISA notes (first cloning, all taken at 30 min.)

	E. coli KRX	Sweet potato	Taro (RT-PCR-)	Taro (RT-PCR+)	HQ-p23	HQ-N
P1D5-C1*	1.484	1.159	1.241	1.593	0.985	1.18
P1D5-F4*	2.01	1.771	1.543	2.152	1.665	1.615
P2G5-B10*	0.307	0.31	0.237	0.254	0.295	0.318
P3A1-F5**	0.227	0.172	0.145	0.211	0.186	0.221
P4C7-C7**	0.192	0.232	0.211	0.316	0.377	0.276
P4C7-C9**	0.343	0.33	0.327	0.401	0.309	0.361
P4E6-B2***	0.998	0.427	0.629	0.881	0.276	0.354
P4E6-C2****	0.92	0.543	0.695	1.217	0.593	0.631

*Plate 1, **Plate 2, ***Plate 3, ****Plate 4

Controls

Plate 1	E. coli KRX	Sweet potato	Taro (RT-PCR-)	Taro (RT-PCR+)	HQ-p23	HQ-N
Terminal bleed	0.475	0.268	0.383	0.327	0.382	0.505
Pre-immune	0.269	0.191	0.171	0.182	0.219	0.212

Plate 2	E. coli KRX	Sweet potato	Taro (RT-PCR-)	Taro (RT-PCR+)	HQ-p23	HQ-N
Terminal bleed	0.434	0.291	0.345	0.336	0.494	0.832
Pre-immune	0.177	0.142	0.135	0.133	0.182	0.277

Plate 3	E. coli KRX	Sweet potato	Taro (RT-PCR-)	Taro (RT-PCR+)	HQ-p23	HQ-N
Terminal bleed	0.387	0.253	0.352	0.269	0.585	0.668
Pre-immune	0.2	0.235	0.205	0.166	0.251	0.383

Plate 4	E. coli KRX	Sweet potato	Taro (RT-PCR-)	Taro (RT-PCR+)	HQ-p23	HQ-N
Terminal bleed	0.367	0.264	0.372	0.269	0.322	0.949
Pre-immune	0.161	0.18	0.208	0.307	0.192	0.267

Table A2. Screening by ID-ELISA of the hybridomas isolated in the first subcloning. Data was taken at 30 min. The subclones of P1D5 and P4E6 represented a culture of hybridomas with antibody reactivity to the RT-PCR positive taro much more compared to the RT-PCR negative taro. Here, the RT-PCR negative taro was sampled from Kapiolani Community College. A blood

sample after the last injection was used as the positive control, while pre-immune serum was used as the negative control.

	KRX	SP	TaVCV-	TaVCV+	HQ-p23	HQ-N	KRX	SP	TaVCV-	TaVCV+	HQ-p23	HQ-N	
P1D5-F4.1	0.276	0.402	0.466	0.66	0.319	0.294	0.39	0.36	0.294	0.345	0.363	0.527	P4C7-C7.1
2	0.469	0.485	0.617	0.713	0.373	0.386	0.36	0.306	0.377	0.378	0.325	0.394	2
3	0.437	0.354	0.284	0.304	0.382	0.245	0.306	0.294	0.276	0.316	0.308	0.309	3
4	0.353	0.417	0.556	0.729	0.459	0.394	0.411	0.428	0.391	0.353	0.354	0.508	4
5	0.525	0.564	0.72	0.745	0.477	0.408	0.526	0.45	0.449	0.442	0.421	0.466	5
P2G5-B10.1	0.464	0.63	0.58	0.65	0.457	0.597	0.371	0.381	0.354	0.316	0.36	0.281	6
negative	0.426	0.414	0.414	0.443	0.579	0.454	0.375	0.418	0.447	0.382	0.252	0.228	7
positive	0.285	0.503	0.42	0.483	0.447	0.733	0.491	0.458	0.45	0.38	0.245	0.295	8

	KRX	SP	TaVCV-	TaVCV+	HQ-p23	HQ-N	KRX	SP	TaVCV-	TaVCV+	HQ-p23	HQ-N	
P4C7-C9.1	0.3	0.294	0.371	0.431	0.285	0.26	0.328	0.443	0.473	0.836	0.395	0.338	P4E6-B2.1
2	0.258	0.237	0.324	0.339	0.259	0.252	0.328	0.426	0.507	0.995	0.356	0.298	2
3	0.249	0.279	0.287	0.32	0.273	0.272	0.319	0.37	0.534	0.945	0.335	0.333	3
4	0.26	0.268	0.332	0.367	0.268	0.261	0.312	0.302	0.328	0.548	0.298	0.312	4
5	0.235	0.281	0.289	0.343	0.257	0.275	0.282	0.294	0.285	0.477	0.258	0.313	5
P4E6-C2.1	0.286	0.333	0.383	0.538	0.294	0.279	0.366	0.445	0.577	1.216	0.336	0.278	6
2	0.265	0.304	0.306	0.377	0.268	0.256	0.248	0.257	0.229	0.235	0.242	0.255	negative
3	0.324	0.371	0.333	0.337	0.315	0.297	0.344	0.281	0.294	0.308	0.32	1.452	positive

Table A3. Screening by ID-ELISA of the hybridomas isolated in the second subcloning. Data was taken at 30 min. The P4E6-B2 subclones each had reactivity to RT-PCR positive taro, though little reactivity was noted with $(HQ)_3$-tagged nucleoprotein. While P4E6-B2.5 represented a hybridoma culture with the least reactivity to RT-PCR positive taro, it also represented the culture with the least cross-reactivity to other samples used in this trial. Here, the RT-PCR negative taro was sampled from Kapiolani Community College. A blood sample after the last injection was used as the positive control. As limited amounts of pre-immune serum was available at the time, dH_2O was used as the negative control.

	KRX	SP	TaVCV-	TaVCV+	p23	N	KRX	SP	TaVCV-	TaVCV+	p23	N	
P1D5	0.07	0.084	0.099	0.086	0.071	0.072	0.247	0.575	1.108	0.65	0.194	0.172	P1D5-C1
dup	0.071	0.082	0.091	0.083	0.076	0.071	0.201	0.534	1.034	0.642	0.131	0.158	dup
trip	0.071	0.082	0.092	0.083	0.07	0.071	0.212	0.519	1.022	0.612	0.169	0.139	trip
P2G5	0.068	0.074	0.077	0.077	0.068	0.069	0.191	0.516	1.04	0.587	0.138	0.139	P1D5-F4
dup	0.068	0.073	0.106	0.081	0.067	0.069	0.21	0.5	0.967	0.537	0.153	0.154	dup
trip	0.077	0.078	0.081	0.081	0.068	0.07	0.179	0.505	0.949	0.549	0.137	0.131	trip
P4E6-B2.5	0.378	0.405	1.918	0.831	0.314	0.34	0.067	0.067	0.069	0.068	0.068	0.067	negative
dup	0.436	0.489	2.059	0.884	0.316	0.375	0.137	0.41	0.127	0.229	1.748	0.188	positive

Table A4. Screening by ID-ELISA of various hybridoma cell lines raised throughout the course of the experiments. Data was taken at 30 min. Here, the RT-PCR negative taro was a leaf sample

from a taro plant that has undergone thermotherapy to eliminate TaVCV. Surprisingly, the RT-PCR negative taro had very high reactivity with some of the hybridoma cultures, especially P4E6-B2.5. A blood sample after the last injection was used as the positive control. As limited amounts of pre-immune serum was available at the time, dH_2O was used as the negative control.

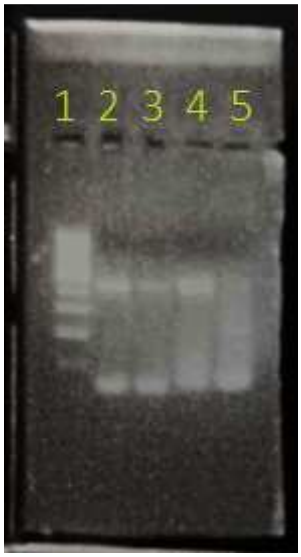

Fig. A3. Results of IC-RT-PCR using concentrated hybridoma supernatant, RT-PCR positive taro leaf lysate, and DCGF/R5 primer set. Lane assignments are as follows: GeneRuler 100 bp (Lane 1), P1D5-F4 supernatant (Lane 2), P2G5 supernatant (Lane 3), P4E6-B2.5 supernatant (Lane 4), carbonate coating buffer as negative control (Lane 5). P4E6-B2.5 appears to be the most reactive to TaVCV among the supernatants tested in this trial.

LITERATURE CITED

Abreu, E. F. M., Daltro, C. B., Nogueira, E. O. P. L., Andrade, E. C., Aragão, F. J. L. (2015). Sequence and genome organization of papaya meleira virus infecting papaya in Brazil. *Arch Virol*, *160*(12), 3143-3147. doi: 10.1007/s00705-015-2605-x.

Alcantara, R. M., Hurtada, W. A., & Dizon, E. I. (2013). The Nutritional Value and Phytochemical Components of Taro [Colocasia esculenta (L.) Schott] Powder and its Selected Processed Foods. *Journal of Nutrition & Food Science*, *3*(3), 1–7.

Alercia, A. (2013). Nutritious Underutilized Species - Taro (Colocasia esculenta L.). Fact Sheet, Rome: Bioversity International, Via dei Tre Denari 472/a, 00057 Maccarese (Fiumicino). Retrieved from http://www.bioversityinternational.org/elibrary/publications/detail/nutritious-underutilized-species-taro/

Ammar, M. S., Hegazy, A. E., & Bedeir, S. H. (2009). Using of Taro Flour as Partial Substitute of Wheat Flour in Bread Making. *World Journal of Dairy & Food Sciences*, 4(2), 94–99.

Brown, A. C., & Valiere, A. (2004). The Medicinal Uses of Poi. *Nutrition in Clinical Care*, *7*(2), 69–74.

Arakaki, A. (1993). Relationship between Nematode Populations and Corm Rot in “Bun Long” Taro Production. *Research Extension Series - Hawaii Institute of Tropical Agriculture and Human Resources*, 71–72.

Asche, M., Wilson, M. R. (1989). The three taro planthoppers: species recognition in Tarophagus (Hemiptera: Delphacidae). *Bulletin of Entomological Research*, *79*(2), 285–298. http://doi.org/10.1017/S0007485300018277

Babaie, G. H., & Izadpanah, K. (2003). Vector Transmission of Eggplant Mottled Dwarf Virus

in Iran. *Journal of Phytopathology*, *151*(11-12), 679–682.

Behncken, G. M. (1973). Evidence of multiplication of sowthistle yellow vein virus in an inefficient aphid vector, Macrosiphum euphorbiae. *Virology*, *53*(2), 405–412. http://doi.org/10.1016/0042-6822(73)90220-1

Bishop, R. V. (2013, December). The mother of our breath. Retrieved September 28, 2019, from https://www.ileia.org/2013/12/19/the-mother-of-our-breath/

Black, L. M. (1943). Genetic Variation in the Clover Leafhopper's ability to transmit Potato Yellow Dwarf Virus. *Genetics*, *28*(3), 200–209.

Bridge, J., Mortimer, J. J., & Jackson, G. V. H. (1983). Hirschmanniella miticausa n. sp. (Nematoda: Pratylenchidae) and its pathogenicity on taro (Colocasia esculenta). *Revue Nematol*, *6*(2), 285–290.

Brierley, I., Jenner, A. J., & Inglis, S. C. (1992). Mutational analysis of the "slippery-sequence" component of a coronavirus ribosomal frameshifting signal. *J Mol Biol, 227*(2), 463–479.

Brierley, I. (1995). Ribosomal frameshifting on viral RNAs. *J Gen Virol, 76*(9), 1885–1892.

Brooks, F. E. (2005). Taro leaf blight. http://doi.org/DOI:10.1094/PHI-I-2005-0531-01

Brooks, F. E. (2008). Detached-leaf bioassay for evaluating taro resistance to Phytophthora colocasiae. *Plant Disease*, *92*(1), 126–131.

Brown, F. (1987). The Family Rhabdoviridae - General Description and Taxonomy. In R. R. Wagner (Ed.), *The Rhabdoviruses, Part of the series The Viruses* (pp. 1–8). New York: Plenum.

Bruenn, J. A. A closely related group of RNA-dependent RNA polymerases from double-stranded RNA viruses. *Nucl Acids Res*, *21*(24), 5667-5669.

Brunt, A. A., Crabtree, K., Dallwitz, M. J., Gibbs, A. J., Watson, L., & Zurcher, E. J. (eds. .

(1996). Plant Viruses Online: Descriptions and Lists from the VIDE Database. Version: 20th. Retrieved June 22, 2019, from http://biology.anu.edu.au/Groups/MES/vide/

Carmichael, A., Harding, R., Jackson, G., Kumar, S., Lal, S. N., Masamdu, R., … Clarke, A. R. (2008). *Taro Pest - An illustrated guide to pests and diseases of taro in the South Pacific. ACIAR MONOGRAPH SERIES.* Canberra: Australian Centre for International Agricultural Research (ACIAR).

Cho, J. J., Yamakawa, R. A., & Hollyer, J. (2007, February). Hawaiian Kalo, Past and Future. Sustainable Agriculture. Cooperative Extension Service Publication, Honolulu: University of Hawaii - College of Tropical Agriculture and Human Resources. Retrieved from http://www.ctahr.hawaii.edu/oc/freepubs/pdf/SA-1.pdf

Christie, S. R., Christie, R. G., & Edwardson, J. R. (1974). Transmission of a Bacilliform Virus of Sowthistle and Bidens pilosa. *Phytopathology*, *64*(6), 840–845. http://doi.org/10.1094/Phyto-64-840

Cox, S. D., Mayo, M. A., & Jones, A. T. (2000). The Occurrence of dsRNA Species in Apparently Healthy and Virus-infected Ribes Cultivars, and Evidence That One Such Species Originates from a Member of the Virus Family Totiviridae. *European Journal of Plant Pathology*, *106*(4), 353-364.

CTAHR and Taro. (2009). Background Paper, Honolulu: College of Tropical Agriculture and Human Resources. Retrieved from http://www.ctahr.hawaii.edu/oc/freepubs/pdf/CTAHR_and_taro.pdf

Deo, P. C., Tyagi, A. P., Taylor, M., Becker, D. K., & Harding, R. M. (2009). Improving taro (Colocasia esculenta var. esculenta) production using biotechnological approaches. *South Pacific Journal of Natural Science*, *27*(1), 6–13. Retrieved from

http://eprints.qut.edu.au/29273/1/29273.pdf

Duffus, J. E. (1963). Possible multiplication in the aphid vector of sowthistle yellow vein virus, a virus with an extremely long insect latent period. *Virology*, *21*(2), 194–202. http://doi.org/10.1016/0042-6822(63)90257-5

Ghabrial, S. A. (2008). Totiviruses. In: Mahy BWJ, Van Regenmortel MHV (eds) *Encyclopedia of virology*. Elsevier, San Diego, pp 163–174.

Gollifer, D. E., Jackson, G. V. H., Dabek, A. J. and, & Plumb, R. T. (1978). Incidence, and effects on yield, of virus diseases of taro (Colocasia esculenta) in the Solomon Islands. *Annals of Applied Biology*, *88*(1), 131–135. http://doi.org/10.1111/j.1744-7348.1978.tb00687.x

Gollifer, D. E., Jackson, G. V. H., Dabek, A. J., Plumb, R. T., & May, Y. Y. (1977). The Occurrence and Transmission of Viruses of Edible Aroids in the Solomon Islands and the Southwest Pacific. *PANS*, *23*(2), 171–177. http://doi.org/10.1080/09670877709412425

Gomes, A. (2012, December). Revenue from crops surges 7% to top $700M. Star Advertiser. Honolulu. Retrieved from http://www.staradvertiser.com/business/20121223_Revenue__from_crops_surges_7__to_to p_700M.html?id=184585611

Goodin, M. M., Dietzgen, R. G., Schichnes, D., Ruzin, S., & Jackson, A. O. (2002). pGD vectors: versatile tools for the expression of green and red fluorescent protein fusions in agroinfiltrated plant leaves. *The Plant Journal*, *31*(3), 375–383.

Greenwell, A. B. H. (1947). Taro: With Special Reference to Its Culture and Uses in Hawaii. *Economic Botany*, *1*(3), 276–289.

Guo, L., Yang, X., Wu, W., Tan, G., Fang, S., Zhang, S., Li, F. (2016). Identification and

molecular characterization of Panax notoginseng virus A, which may represent an undescribed novel species of the genus Totivirus, family Totiviridae. *Arch Virol*, *161*(3), 731-734.

Healy, D. M., Banyard, A. C., & Fooks, A. R. (2013). *Rhabdoviruses. In eLS.* Chichester: John Wiley & Sons Ltd. http://doi.org/10.1002/9780470015902.a0001085.pub3

Higgins, C. M., Bejerman, N., Li, M., James, A. P., Dietzgen, R. G., Pearson, M. N., … Harding, R. M. (2016a). Complete genome sequence of Colocasia bobone disease-associated virus, a putative cytorhabdovirus infecting taro. *Archives of Virology, 161*(3), 745–748. http://doi.org/10.1007/s00705-015-2713-7

Higgins, C. M., Bejerman, N., Li, M., James, A. P., Dietzgen, R. G., Pearson, M. N., … Harding, R. M. (2016b). Erratum to: Complete genome sequence of Colocasia bobone disease-associated virus, a putative cytorhabdovirus infecting taro. *Archives of Virology, 161*(10), 2951–2952. http://doi.org/10.1007/s00705-016-2995-4

Hollyer, J., Paull, R., & Huang, A. (2000). Processing Taro Chips. *Food Manufacturing and Technology*, *1*, 1–2.

Huang, Y. W., Geng, Y. F., Ying, X. B., Ying, X., & Fang, R. X. (2005). Identification of a Movement Protein of Rice Yellow Stunt Rhabdovirus. *Journal of Virology*, *79*(4), 2108–2114. http://doi.org/10.1128/JVI.79.4.2108-2114.2005

Hunt, D. M., Smith, E. F. and Buckley, D.W. (1984). Aberrant polyadenylation by a vesicular stomatitis virus mutant is due to an altered L protein. *Journal of Virology*, *52*(2), 515-521.

Hunter, D., Pouono, K., & Semisi, S. (1998). The Impact of Taro Leaf Blight in the Pacific Islands with special reference to Samoa. *J. S. Pac. Agr.*, *5*, 44–56.

International Committee on Taxonomy of Viruses. (2019). http://talk.ictvonline.org/taxonomy/

Ivancic, A., Liwqula, R., Levela, H., Saelea, J., & Wagatora, D. (1993). *Genetic Resistance to Alomae-Bobone Virus Complex The Lethal Disease of Taro (Colocasia esculenta (L.) Schott)*. Honolulu.

Jacobs, R. (2011). Kalo Is More Than a Native Hawaiian Plant—It's an Ancestor to Hawaiian Culture. Retrieved from http://indiancountrytodaymedianetwork.com/2011/11/21/kalomore-native-hawaiian-plant-its-ancestor-hawaiian-culture-63402

Jackson A. O., Dietzgen R. G., Goodin M. M., Bragg J. N., & Deng M. (2005). Biology of Plant Rhabdoviruses. *Annual Review of Phytopathology*, *43*, 623–660. http://doi.org/10.1146/annurev.phyto.43.011205.141136

James, M., Kenten, R. H., & Woods, R. D. (1973). Virus-like particles associated with two diseases of Colocasia esculenta (L.) Schott in the British Solomon Islands. *Journal of General Virology*, *21*, 145–153.

Jane, J., Shen, L., Chen, J., Lim, S., Kasemsuwan, T., & Nip, W. K. (1992). Physical and Chemical Studies of Taro Starches and Flours. *Cereal Chemistry*, *69*(5), 528–535.

Kazmi, S. A., Yang, Z., Hong, N., Wang, G., & Wang, Y. (2015). Characterization by Small RNA Sequencing of Taro Bacilliform CH Virus (TaBCHV), a Novel Badnavirus. *PLoS One*, *10*(7), 1–13. http://doi.org/10.1371/journal.pone.0134147

Kondo, H., Maeda, T., Shirako, Y., & Tamada, T. (2006). Orchid fleck virus is a rhabdovirus with an unusual bipartite genome. *Journal of General Virology*, *87*(8), 2413–2421. http://doi.org/10.1099/vir.0.81811-0

Kosugi, S., Hasebe, M., Tomita, M., Yanagawa, H. (2009). Systematic identification of yeast cell

cycle-dependent nucleocytoplasmic shuttling proteins by prediction of composite motifs. *Proc Natl Acad Sci USA*, *106*, 10171–10176.

Kreike, C. M., Van Eck, H. J., & Lebot, V. (2004). Genetic diversity of taro, Colocasia esculenta (L.) Schott, in Southeast Asia and the Pacific. TAG. Theoretical and Applied Genetics. *Theoretische Und Angewandte Genetik*, *109*(4), 761–768. http://doi.org/10.1007/s00122-004-1691-z

Kumar, S., Stecher, G., Li, M., Knyaz, C., and Tamura, K. (2018). MEGA X: Molecular Evolutionary Genetics Analysis across computing platforms. *Molecular Biology and Evolution*, *35*(6), 1547-1549.

Kuruvilla, K. M., & Singh, A. (1981). Karyotypic and electrophoretic studies on taro and its origin. *Euphytica*, *30*(2), 405–413.

la Cour, T., Kiemer, L., Mølgaard, A., Gupta, R., Skriver, K., Brunak, S. (2004). Analysis and prediction of leucine-rich nuclear export signals. *Protein Eng Des Sel*, *17*(6), 527–536.

Lal, S., Moxon, J., Autrar, M., Milner, R. J., Hunter, D., Hazelman, S., … Vasuidreketi, T. (2008). *Taro Beetle Management in Papua New Guinea and Fiji: Final Project Report.* Suva.

Lebot, V., & Aradhya, K. M. (1991). Isozyme variation in taro (Colocasia esculenta (L.) Schott) from Asia and Oceania. Euphytica, *56*(1), 55–66.

Lee, W. (1999). Taro (Colocasia esculenta). Retrieved from http://www.ethnoleaflets.com/leaflets/taro.htm

Levin, P. (2006). *Statewide Strategic Control Plan for Apple Snail (Pomacea canaliculata) in Hawai'i.* Honolulu.

Liloqula, R., Saelea, J., & Levela, H. (1993). Traditional Taro Cultivation in the Solomon

Islands. In L. Ferentinos (Ed.), *Sustainable Taro Culture for the Pacific Conference; 1992, September 24-25* (pp. 125–131). Honolulu: University of Hawaii.

Long, M. H., Ayin, C., Li, R., Hu, J. S., & Melzer, M. J. (2014). First Report of Taro Vein Chlorosis Virus Infecting Taro (Colocasia esculenta) in the United States. *Plant Disease*, *98*(8), 1160. http://doi.org/10.1094/PDIS-12-13-1277-PDN

Long, M. H., Gosai, R. C., & Melzer, M. J. (2016). Taro Vein Chlorosis. Retrieved from https://www.ctahr.hawaii.edu/oc/freepubs/pdf/PD-111.pdf

Macanawai, A. R., Ebenebe, A. A., Hunter, D., Devitt, L. C., Hafner, G. J., & Harding, R. M. (2005). Investigations into the seed and mealybug transmission of Taro bacilliform virus. *Australasian Plant Pathology*, *34*(1), 73–76. http://doi.org/10.1071/AP04084

Manikonda, P., Srinivas, K. P., Reddy, C. V. S., Ramesh, B., Navodayam, K., Krishnaprasadji, J., Ratan, P. B., Sreenivasulu, P. (2011). Konjac mosaic virus Naturally Infecting Three Aroid Plant Species in Andhra Pradesh, India. *Journal of Phytopathology, 159*(2), 133-135. http://doi.org/10.1111/j.1439-0434.2010.01720.x

Martin, D. A. (2004). *Hawaii Taro.* Honolulu. Retrieved from http://www.nass.usda.gov/Statistics_by_State/Hawaii/Publications/Archive/xtar03.pdf

Matthews, P. J. (1995). Aroids and the Austronesians. *Tropics*, *4*(2), 105–126. http://doi.org/10.3759/tropics.4.105

Matthews, P. J. (2004). Genetic Diversity in Taro, and the Preservation of Culinary Knowledge. *Ethnobotany Research and Applications*, *2*, 55–71.

McGregor, A., Afeaki, P., Hamilton, A., Hollyer, J., Masamdu, R., & Nalder, K. (2011). Pacific Island Taro Market Access Scoping Study. Suva, Fiji.

Min, B. E., Martin, K., Wang, R., Tafelmeyer, P., Bridges, M., & Goodin, M. (2010). A Host-

Factor Interaction and Localization Map for a Plant-Adapted Rhabdovirus Implicates Cytoplasm-Tethered Transcription Activators in Cell-to-Cell Movement. *Molecular Plant-Microbe Interactions*, *23*(11), 1420-1432.

Moore, L. M., & Lawrence, J. H. (2003). Plant Guide - Taro. Plant Guide, United States Department of Agriculture - Natural Resources Conservation Service. Retrieved from http://plants.usda.gov/plantguide/pdf/cs_coes.pdf

Morris, T. J., Dodds, J. A. (1979). Isolation and analysis of double-stranded RNA from virus-infected plant and fungal tissue. *Phytopathology*, *69*, 854–858.

Nelson, S., Brooks, F., & Teves, G. (2011). Taro Leaf Blight in Hawai‘i. *Plant Disease*, *71*, 1–14.

Onwueme, I. (1999). Taro Cultivation in Asia and the Pacific. Publication, Bangkok, Thailand: Food and Agriculture Organization of the United Nations, Regional Office for Asia and the Pacific.

Ooka, J. J. (1990). Taro Diseases. *Research Extension series - Hawaii Institute of Tropical Agriculture and Human Resources*. Honolulu. Retrieved from http://www.ctahr.hawaii.edu/oc/freepubs/pdf/RES-114-11.pdf

Parris, G. K. (1941). DISEASES OF TARO IN HAWAII AND THEIR CONTROL - With Notes on Field Production. *Hawaii Agricultural Experiment Station of the University of Hawaii Circular*, *18*, 9–28. Retrieved from http://www.ctahr.hawaii.edu/oc/freepubs/pdf/C2-18.pdf

Payne, J. H., Ley, G. J., & Akau, G. (1941). Processing and Chemical Investigations of Taro (Bulletin 86). Honolulu: Hawaii Agricultural Experiment Station - University of Hawaii.

Pearson, M. ., Jackson, G. V. H., Saelea, J., & Morar, S. G. (1999). Evidence for two

rhabdoviruses in taro (Colocasia esculenta) in the Pacific region. *Australasian Plant Pathology*, *28*(3), 248–253. http://doi.org/10.1071/AP99040

Plucknett, D. L. (1983). Taxonomy of the Genus Colocasia. In J.-K. Wang & S. Higa (Eds.), *Taro: A Review of Colocasia esculenta and its Potentials* (pp. 14–19). Honolulu: University of Hawaii Press.

Pole, F. S. (1993). Continuing Role of Aroids in the Root Crop-Based Cropping System of Tonga. In L. Ferentinos (Ed.), *Sustainable Taro Culture for the Pacific Conference; 1992, 165 September 24-25* (pp. 11–14). Honolulu: University of Hawaii.

Potgieter, M. (1940). Taro (Colocasia esculenta) as a food. *Journal of the American Dietetic Association*, *16*, 536–540.

Primo, A. (1993). Colocasia Taro on Pohnpei Island. In L. Ferentinos (Ed.), *Sustainable Taro Culture for the Pacific Conference; 1992, September 24-25* (pp. 6–7). Honolulu: University of Hawaii.

Pringle, C. R. (1991). The order Mononegavirales. *Archives of Virology*. 117(1–2): 137–40.

Purseglove, J. W. (1973). Tropical Crops: Monocotyledons Vols. 1 and 2. *Experimental Agriculture*, *9*(3), 287.

Rao, V. R., Hunter, D., Eyzaguirre, P. B., & Matthews, P. J. (2010). Ethnobotany and global diversity of taro. In V. R. Rao, P. J. Matthews, P. B. Eyzaguirre, & D. Hunter (Eds.), *The Global Diversity of Taro Ethnobotany and Conservation* (pp. 1–6). Rome: Bioversity International.

Read, D. A., Featherston, J., Rees, D. J. G., Thompson, G. D., Roberts, R., Flett, … Mbega, E. R.

(2019). Molecular characterization of Morogoro maize-associated virus, a nucleorhabdovirus detected in maize (Zea mays) in Tanzania. *Archives of Virology*, *164*(6), 1711-1715.

Redinbaugh, M. G., & Hogenhout, S. A. (2005). Plant rhabdoviruses. *Curr Top Microbiol Immunol.*, *292*, 143–163.

Redinbaugh, M. G., Seifers, D. L., Meulia, T., Abt, J. J., Anderson, R. J., Styer, W. E., … Hogenhout, S. A. (2002). Maize fine streak virus, a New Leafhopper-Transmitted Rhabdovirus. *Phytopathology*, *92*, 1167–1174.

Revill, P. A., Jackson, G. V. H., Hafner, G. J., Yang, I., Maino, M. K., Dowling, M. L., … Harding, R. M. (2005). Incidence and distribution of viruses of Taro (Colocasia esculenta) in Pacific Island countries. *Australasian Plant Pathology*, *34*(3), 327–331. http://doi.org/10.1071/AP05032

Revill, P., Trinh, X., Dale, J., & Harding, R. (2005a). Taro vein chlorosis virus: characterization and variability of a new nucleorhabdovirus. *Journal of General Virology*, *86*(2), 491–499. http://doi.org/10.1099/vir.0.80591-0

Richardson, J., & Sylvester, E. S. (1968). Further evidence of multiplication of sowthistle yellow vein virus in its aphid vector, Hyperomyzus lactucae. *Virology*, *35*(3), 347–355.

Sami, R. (2011). What's holding Pacific Island taro exports back? Retrieved September 11, 2019, from http://www.spc.int/lrd/fact/press-releases/whats-holding-pacific-island-taro-exports-back

Sato, D. M., Hara, A. H., Mau, R. F. L., Tsuda, D. M., & Hamasaki, T. (1997). Taro Root Aphid. *Insect Pests*, 1–2.

Scholthof, K. B., Hillman, B. I., Modrell, B., Heaton, L. A., & Jackson, A. O. (1994).

Characterization and detection of sc4: a sixth gene encoded by sonchus yellow net virus. *Virology*, *204*(1), 279–288.

Singh, D., Jackson, G., Hunter, D., Fullerton, R., Lebot, V., Taylor, M., … Tyson, J. (2012). Taro Leaf Blight—A Threat to Food Security. *Agriculture*, *2*, 182–203. http://doi.org/10.3390/agriculture2030182

Sipes, B. S., & Arakaki, A. S. (1997). Root-knot Nematode Management in Dryland Taro with Tropical Cover Crops. *Journal of Nematology*, *29*(4S), 721–724.

Sivan, P., & Liyanage, A. de S. (1993). Breeding and Evaluation of Taro (Colocasia esculenta) for the South Pacific Region. In L. Ferentinos (Ed.), *Sustainable Taro Culture for the Pacific Conference; 1992, September 24-25* (pp. 1–5). Honolulu: University of Hawaii.

Sivaprasad, Y., Bhaskara Reddy, B. V., Naresh Kumar, C. V. M., Raja Reddy, K., & Sai Gopal, D. V. R. (2011). First report of Groundnut Bud Necrosis Virus infecting Taro (Colocasia esculenta). *Australasian Plant Disease Notes*, *6*(1), 30–32.

Taotua, F. (1993). Taro Cultivators in Samoa. In L. Ferentinos (Ed.), *Sustainable Taro Culture for the Pacific Conference; 1992, September 24-25* (pp. 101–102). Honolulu: University of Hawaii.

Temesgen, M., & Retta, N. (2015). Nutritional Potential, Health and Food Security Benefits of Taro Colocasia Esculenta (L.): A Review. *Food Science and Quality Management*, *36*, 23–30.

Todd, J. C., Ammar, E. D., Redinbaugh, M. G., Hoy, C., & Hogenhout, S. A. (2010). Plant Host Range and Leafhopper Transmission of Maize fine streak virus. *Phytopathology*, *100*, 1138–1145.

Torigoe, H., Fukunaga, M., & Muta, T. (2002). Control of stunting and wilting of taro, Colocasia

esculenta, 3: Effect of organic matter on the root-lesion nematode, Pratylenchus coffeae, on tar. Retrieved September 7, 2019, from http://agris.fao.org/agrissearch/search.do?recordID=JP2003000414

Trujillo, E. E., Menezes, T. D., Cavaletto, C. G., Shimabuku, R., & Fukuda, S. K. (2002). Promising New Taro Cultivars with Resistance to Taro Leaf Blight: ‘Pa“lehua”, ‘Pa“akala”, and “Pauakea.” *New Plants for Hawaii*, *7*, 1–4.

Uchida, J., Levin, P., Miyasaka, S., Teves, G., Hollyer, J., Nelson, S., & Ooka, J. (2008). Taro Mauka to Makai. A Taro Production and Business Guide for Hawaii Growers. (D. Evans, Ed.) (Second). College of Tropical Agriculture and Human Resources, University of Hawaii.

USDA Crop Production 2018 Summary. (2019). Retrieved from https://www.nass.usda.gov/Publications/Todays_Reports/reports/cropan19.pdf

USDA Crop Values 2018 Summary. (2019). Retrieved from https://downloads.usda.library.cornell.edu/usda-esmis/files/k35694332/g445cn37b/8910k2787/cpvl0419.pdf

Vilsoni, F. (1993). Sustainable Taro Culture: Fiji Situation. In L. Ferentinos (Ed.), *Sustainable Taro Culture for the Pacific Conference; 1992, September 24-25* (pp. 84–87). Honolulu: University of Hawaii.

Walker, P. J., Benmansour, A., Dietzgen, R., & et al. (2000). *Family Rhabdoviridae. In Virus Taxonomy and Nomenclature of Viruses. Seventh Report of the International Committee on Taxonomy of Viruses.* San Diego.

Walker, P. J., Firth, C., Widen, S. G., Blasdell, K. R., Guzman, H., Wood, T. G., & et al. (2015).

Evolution of Genome Size and Complexity in the Rhabdoviridae. *PLoS Pathog*, *11*(2), 1–25. http://doi.org/10.1371/journal.ppat.1004664

Wang, Y. F., Wang, G. P., Wang, L. P. & Hong, N. (2014). First Report of Cucumber mosaic virus in Taro Plants in China. *Plant Disease*, *98*(4), 574. https://doi.org/10.1094/PDIS-09-13-0916-PDN

Watson, J. T., Jones, R. C., Siston, A. M., Diaz, P. S., Gerber, S. I., Crowe, J. B. & Satzger, R. D. (2005). Outbreak of Food-borne Illness Associated with Plant Material Containing Raphides. *Clinical Toxicology*, *43*(1), 17-21. https://doi.org/10.1081/CLT-44721

Whitney, L. D., Bowers, F. A. I., & Takahashi, M. (1939). Taro Varieties in Hawaii. Hawaii Agricultural Experiment Station of the University of Hawaii (Vol. 84). Honolulu.

Yang, I. C., Hafner, G. J., Dale, J. L., & Harding, R. M. (2003). Genomic characterisation of taro bacilliform virus. *Archives of Virology*, *148*(5), 937–49.

Yusop, M. S. M., Saad, M. F. M., Talip, N., Baharum, S. N., Bunawan, H. (2019). A review on viruses infecting taro (*Colocasia esculenta* (L.) Schott). *Pathogens*, *8*(2), 56. doi:10.3390/pathogens8020056.